

UNCLASSIFIED

AD NUMBER
ADB043281
NEW LIMITATION CHANGE
TO Approved for public release, distribution unlimited
FROM Distribution authorized to U.S. Gov't. agencies only; Administrative/Operational Use; Sep 1979. Other requests shall be referred to Air Force Materials Lab., Wright-Patterson AFB, OH 45433.
AUTHORITY
AFWAL ltr, 3 Aug 1983

THIS PAGE IS UNCLASSIFIED

AFML-TR-79-4134

ADB043281

POLYMERIC MATERIALS FOR ADVANCED AIRCRAFT AND AEROSPACE VEHICLES

*UNIVERSITY OF DAYTON
RESEARCH INSTITUTE
DAYTON, OHIO 45469*

SEPTEMBER 1979

TECHNICAL REPORT AFML-TR-79-4134

Final Report for the period 15 June 1978 through 14 June 1979

Distribution limited to U. S. Government agencies only (Test Evaluation); applicable August 1979. Other requests for this document must be referred to the Air Force Materials Laboratory (AFML/MBP), Wright-Patterson Air Force Base, Ohio 45433.

AIR FORCE MATERIALS LABORATORY
AIR FORCE WRIGHT AERONAUTICAL LABORATORIES
AIR FORCE SYSTEMS COMMAND
WRIGHT-PATTERSON AIR FORCE BASE, OHIO 45433

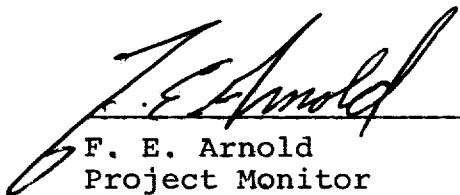
BEST AVAILABLE COPY

20040224046


NOTICE

When Government drawings, specifications, or other data are used for any purpose other than in connection with a definitely related Government procurement operation, the United States Government thereby incurs no responsibility nor any obligation whatsoever; and the fact that the said drawings, specifications, or other data, is not to be regarded by implication or otherwise as in any manner licensing the holder or any other person or corporation, or conveying any rights or permission to manufacture, use, or sell any patented invention that may in any way be related thereto.

This technical report has been reviewed and is approved for publication.




F. E. Arnold
Project Monitor



R. L. Van Deusen, Chief
Polymer Branch
Nonmetallic Materials Division

FOR THE COMMANDER



J. M. Kelble, Chief
Nonmetallic Materials Division

If your address has changed, if you wish to be removed from our mailing list, or if the addressee is no longer employed by your organization please notify AFML/MBP, W-PAFB, OH 45433 to help us maintain a current mailing list.

Copies of this report should not be returned unless return is required by security considerations, contractual obligations, or notice on specific documents.

Unclassified

SECURITY CLASSIFICATION OF THIS PAGE (When Data Entered)

REPORT DOCUMENTATION PAGE		READ INSTRUCTIONS BEFORE COMPLETING FORM
1. REPORT NUMBER AFML-TR-79-4134	2. GOVT ACCESSION NO.	3. RECIPIENT'S CATALOG NUMBER
4. TITLE (and Subtitle) Polymeric Materials for Advanced Aircraft and Aerospace Vehicles		5. TYPE OF REPORT & PERIOD COVERED Interim Technical Report 15 June 1978 - 14 June 79
		6. PERFORMING ORG. REPORT NUMBER UDR-TM-79-14
7. AUTHOR(s) Donald R. Wiff		8. CONTRACT OR GRANT NUMBER(s) F33615-78-C-5126
9. PERFORMING ORGANIZATION NAME AND ADDRESS University of Dayton Research Institute 300 College Park Dayton, OH 45469		10. PROGRAM ELEMENT, PROJECT, TASK AREA & WORK UNIT NUMBERS 62102F/2419/84 24190415 61102F/2303/Q3 2303Q307
11. CONTROLLING OFFICE NAME AND ADDRESS Air Force Materials Laboratory, Air Force Wright Aeronautical Laboratories, Wright-Patterson Air Force Base, OH 45433		12. REPORT DATE September 1979
14. MONITORING AGENCY NAME & ADDRESS (if different from Controlling Office)		13. NUMBER OF PAGES 106
		15. SECURITY CLASS. (of this report)
15a. DECLASSIFICATION/DOWNGRADING SCHEDULE		
16. DISTRIBUTION STATEMENT (of this Report) Distribution limited to U. S. Gov't agencies only (test evaluation); applicable August 1979. Other requests for this document must be referred to the Air Force Materials Laboratory (AFML/MBP), Wright Patterson AFB, OH 45433.		
17. DISTRIBUTION STATEMENT (of the abstract entered in Block 20, if different from Report)		
18. SUPPLEMENTARY NOTES		
19. KEY WORDS (Continue on reverse side if necessary and identify by block number) <div style="display: flex; justify-content: space-between;"> <div> polysiloxanes acetylene terminated polymers aromatic heterocyclic polymers composites structural resins </div> <div> ordered polymers rigid-rod polymers kinetics processing morphology </div> <div> x-ray diffraction polefigures dynamic imaging synthesis mechanical properties single crystal studies (cont.) </div> </div>		
20. ABSTRACT (Continue on reverse side if necessary and identify by block number) <p>The synthesis, kinetics and mechanical properties of unique resin systems for use in structural composites is reported. The general class of resins studied is acetylene terminated oligomers, designated ATX. Applying an ideal processing window analysis technique expedites the processing of materials for mechanical testing. A new method for determining a real processing window has been perfected and applied to systems having very fast cure reaction times. Mechanical relaxation spectra determination to better correlate material</p> <p align="right">continued-</p>		

Unclassified

SECURITY CLASSIFICATION OF THIS PAGE(When Data Entered)

20. Abstract (Cont.)

structure with mechanical properties is considered.

An extension of composite concepts - blending a rigid rod polymer with its flexible coil analog - has yielded molecular composites with excellent properties. The preliminary synthesis, morphology, and mechanical properties of the pure rigid rod polymeric material (films and fibers) and the molecular composites (cast and precipitated films) are presented.

19. Key Words (Cont.)

cross linked polymers
molecular composites
ill-posed problems
relaxation spectra

UNCLASSIFIED

SECURITY CLASSIFICATION OF THIS PAGE(When Data Entered)

FOREWORD

This annual report was prepared by the University of Dayton Research Institute, Dayton, Ohio under United States Air Force Contract F33615-78-C-5126. The work was administered under the direction of the Nonmetallic Materials Division, Air Force Materials Laboratory, Wright-Patterson Air Force Base, Ohio.

This report covers work conducted from 15 June 1978 to 14 June 1979 in the exploratory development of polymeric materials for advanced aircraft and aerospace vehicles.

TABLE OF CONTENTS

SECTION		PAGE
I	RESINS	1
1.	INTRODUCTION	1
2.	EXPERIMENTAL AND RESULTS	3
A.	Acetylene Terminated Systems Synthesis	3
B.	Inter and Intramolecular Cycloaddition Synthesis	12
	(1) SBQ Monomers	12
C.	T _g Predictions	20
D.	Kinetic Analysis	21
	(1) Theory	21
	(2) Results from Kinetic and Cure Computer Programs	23
E.	Rheometrics Mechanical Spectrometer	23
	(1) Instrumentation	23
	(2) Radel	23
	(3) Torsion Impregnated Cloth Analysis (TICA)	23
	(4) Epoxy	47
	(5) Intramolecular Cyclization (IMC) System	47
F.	Inferring Relaxation Spectra	47
G.	Characterization by Thermal Methods	50
H.	Solution Thermodynamics	55
	(1) Intrinsic Viscosity	55
	(2) Radel Fractionation	56
	(3) Number Average Molecular Weight	57
II	ORDERED POLYMERS	58
1.	INTRODUCTION	58
2.	EXPERIMENTAL AND RESULTS	59

TABLE OF CONTENTS (Concluded)

SECTION	PAGE
A. Articulated PBO and Model Compound Synthesis	59
B. Articulated PBO - Film Casting and Mechanical Properties	62
C. Molecular Composites (Blends)	62
(1) Cast Films Preparation	62
(2) Precipitated Films - Preparation and Mechanical Properties	65
(3) Polymer Reclamation	66
D. Morphology	66
(1) Model Compound Studies Via XRD	66
(2) Texture Analysis	68
(3) Pole Figure Analysis	80
(4) Dynamic Imaging	85
III POLYSACS	88
1. INTRODUCTION	88
2. EXPERIMENTAL AND RESULTS	88
A. Synthesis	88
B. Thermal Analysis	97
IV CONCLUSIONS	98
REFERENCES	100

LIST OF ILLUSTRATIONS

FIGURE		PAGE
1	Mechanism of SBQ Synthesis	14
2	Synthesis Scheme of BA DABA BA	18
3	Synthesis Scheme of BA DAB BA	19
4	Ideal Processing Window for A-BA (BATQ M-11) $n=1.40$	25
5	Ideal Processing Window for A-BA (BATQ M=11) $n=0.00$	26
6	Ideal Processing Window for BATQ N=0 $n=1.34$	27
7	Ideal Processing Window for BATQ N=0 $n=0.00$	28
8	Ideal Processing Window for FLH-5-99 $n=1.27$	29
9	Ideal Processing Window for FLH-5-99 $n=0.00$	30
10	Ideal Processing Window for BA-DAB-BA $n=0.23$	31
11	Ideal Processing Window for BA-DAB-BA $n=0.00$	32
12	Ideal Processing Window for BA-DABA-BA $n=0.64$	33
13	Ideal Processing Window for BA-DABA-BA $n=0.00$	34
14	Ideal Processing Window for PATS X-27 $n=1.21$	35
15	Ideal Processing Window for PATS X-27 $n=0.00$	36
16	Ideal Processing Window for GD-37 Run-2 Cut 3 $n=0.55$	37
17	Ideal Processing Window for GD-37 Run-2 Cut 3 $n=0.00$	38
18	Ideal Processing Window for ATQ-BN-17B $n=0.86$	39
19	Ideal Processing Window for ATQ-BN-17B $n=0.00$	40
20	Ideal Processing Window for ATQ-BN-17A $n=0.69$	41
21	Ideal Processing Window for ATQ-BN-17A $n=0.00$	42
22	Ideal Processing Window for AA-BA-BN-13A $n=0.64$	43
23	Ideal Processing Window for AA-BA-BN-13A $n=0.00$	44
24	Ideal Processing Window for BA-DAB-BA (FHL-335-160-1) $n=0.00$	45

LIST OF ILLUSTRATIONS (Concluded)

FIGURE		PAGE
25	Ideal Processing Window for BA-DAB-BA (FLH-335-160-1) $n=0.34$	46
26	A Typical Relaxation Spectrum Which May Be Inferred when Insufficient Numerical Analysis Techniques Are Used	49
27	Molecular Packing Scheme for the Trans-PBO Model Compound	69
28	Comparison of D-Spacings Present in WAXS Photographs of ABPBI/PBT Blends for Edge Specimen View	71
29	Comparison of D-Spacings Present in WAXS Photographs of ABPBI/PDIAB Blends for Flat View of the Specimen	72
30	Comparison of D-Spacings Present in WAXS Photographs of ABPBI/PDIAB Blends for Edge View of the Specimen	73
31	SAXS Results of 80/20 (ABPBI/PBT) Taken on the ORNL Ten Meter System	75
32	An Intensity Scan Along the AA' Path Shown on the Contour Plot in Figure 31	76
33	WAXS Photograph of PBT 46 Fiber	77
34	SAXS Photograph of PBT 46 Fiber Using the 29 cm Setting in a Statton Camera	77
35	Schematic Showing the Geometrical Polefigure Plotting of a Point P', the Projection of the Pole P and the Flat Film XRD Spot S	81
36	Identification of Various Directions and Angles in Relation to a Specimen	82
37	A Measured Polefigure of a PBO Heat-Treated Fiber (Celanese 26085-25-1)	84
38	Photograph of the Dynamic Imaging of X-ray Diffraction Pattern System	86

LIST OF TABLES

TABLE		PAGE
1	Summary of Reactant Structures Used in SBQ Synthesis	15
2	Kinetic Analysis Data of Acetylene Terminated Systems	24
3	Intrinsic Viscosity	55
4	Radel Fractions	57
5	Number Average Molecular Weight	57
6	Synthesized Articulated PBO Monomers and Model Compounds	60
7	Synthesized Copolymer Data	61
8	Mechanical Data of Articulated PBO Polymers	62
9	Polymer Blends	64
10	Mechanical Properties of AB-PBI/PBT Blends	64
11	Mechanical Properties of Selected Precipitated Blend Films	67
12	Results of PBT #33, 38, 38H1 Fiber Morphology Study	78
13	Characteristics of the X-ray Diffraction Patterns of PBT 26554-9-5 (as Spun) and PBT #46 Fibers	79

SECTION I

RESINS

1. INTRODUCTION

This report discusses, in part, the synthesis, preparation, and purification of intermediates and monomers used by Air Force Materials Laboratory (AFML) Polymer Branch scientists for further polymerizations. These resin systems are acetylene terminated monomers or oligomers of homopolymer resins currently being investigated by applications engineers for use in advanced composite programs. The general class of these acetylene terminated systems is designated ATX, with special designations for various homopolymer backbone structures, e.g., acetylene terminated quinoxaline, ATQ; acetylene terminated sulfone, ATS; etc. Other intermediates have been prepared for investigation of intra molecular cycloaddition (IMC) studies. These new materials are expected to have low processing temperatures due to the oligomeric nature of the starting materials and a final resin which is a hard resilient material due to the increased molecular weight and the accompanied crosslinking.

To aid the synthesis part of the program, a semi-empirical method of predicting glass transition temperature, T_g , of various amorphous homopolymers and copolymers has been devised. This technique will be discussed in the body of the report. We hope in the future to extend this to include crosslinked systems.

The study of cure kinetics of ATX systems leading to reaction kinetics parameters along with "ideal" and "real" processing window analyses has been continued. Improvement in instrumental precision and upgrading of a fully automated cure kinetics analysis procedure have been achieved. Specimen preparation procedures involved with impregnating glass fiber cloth with the uncured polymer have been established. These specimens are being used in the torsion impregnated cloth analysis (TICA).

The data on these specimens are obtained from a Rheometrics Mechanical Spectrometer. These data are used for constructing a "real" processing window.

Once an "ideal" or better yet a "real" processing window has been obtained, dogbone test specimens can be routinely prepared by varying cure conditions within this processing window. The capability exists to then test these for mechanical properties (modulus, tensile strength, and failure envelope or Smith Plot).

In order to glean as much information as possible from 5-gram (.176 oz) size batches of polymer provided by research chemists in AFML Polymer Branch, physical property measurement techniques have been adjusted to these small quantities. One of the procedures impacting this restriction is the above processing window technique. There is not enough material available to blindly begin processing on a trial and error basis. Another unique technique being pursued is to be able to perform one type or set of mechanical measurements and predict other mechanical properties within understandable bounds. The approach is to infer a reliable relaxation spectrum and from this, using linear viscoelastic equations, predict other rheological properties. This process was begun under our preceding contract, but is expected to be made fully operational during the present three year contract. Characterization of milligram size polymer samples is being accomplished under the present contract by routine differential scanning calorimetry (DSC), isothermal aging, and dynamic mechanical analysis (TMA). Results of these investigations applied to various reactive plasticizer resins serve as guides to the polymer synthesis scientists during their various polymerization reactions.

Fractionation by the solvent-non-solvent technique has been applied to the homopolymer polysulfone (PS). The fractionation was verified by liquid chromatography (LC), vapor phase osmometry (VPO), viscosity measurements, and ultracentrifugation

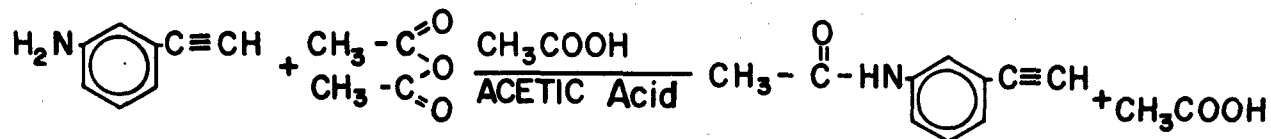
which yielded molecular weight distributions (MWD). Correlation of these measurements yielding MWD's and molecular weights (MW) with mechanical properties of specimens prepared from the respective PS fractions should soon be forthcoming.

2. EXPERIMENTAL AND RESULTS

A. Acetylene Terminated Systems Synthesis (J. Gamble)

The synthesis of 3-acetamidophenylacetylene) was the first product in a series of various character reactions to be performed at a later date.

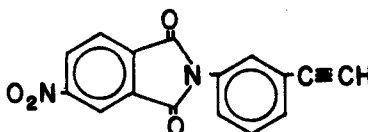
SYNTHESIS:



PERCENT YIELD: 62%

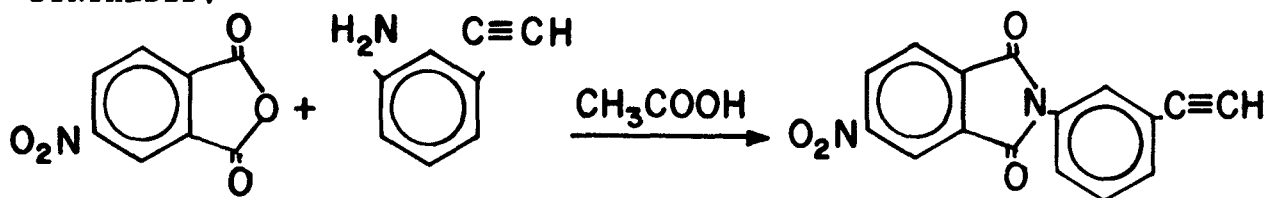
This reaction was performed on three separate occasions to synthesize the necessary amount of final product.

Impure starting material (aminophenylacetylene) was used and consequently the yield was lowered. (Excess activated charcoal was used to remove the impurities.)

The synthesis of  was the

first product in a character reaction (shown on the following page) to improve the processing properties of the compound, Therimide.

SYNTHESIS:

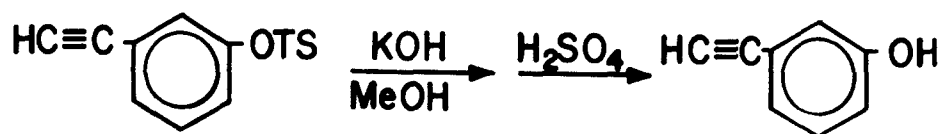


PERCENT YIELD: 75%

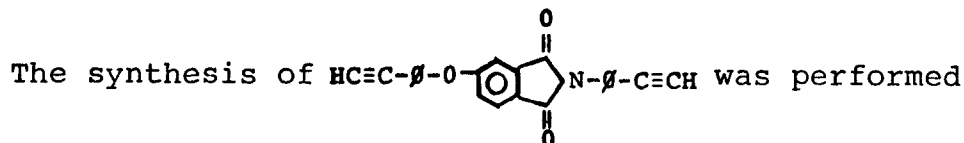
This reaction was performed on two separate occasions to synthesize the necessary amount of final product.

The compound (3-ethynylphenol) was the precursor to many character reactions, consequently it was performed on many occasions as demand dictated.

SYNTHESIS:

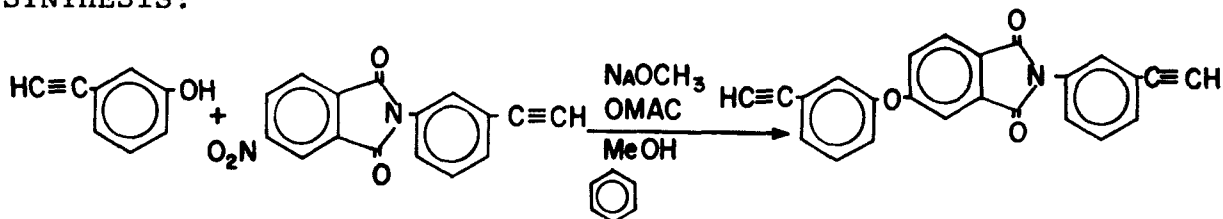


PERCENT YIELD: 85%



in order to produce 12 grams (.423 oz) of final product; 10 grams (.353 oz) to be sent to SRI International (Stanford Research Institute) for moisture analysis, and 2 grams (.071 oz) to be kept for future reference.

SYNTHESIS:



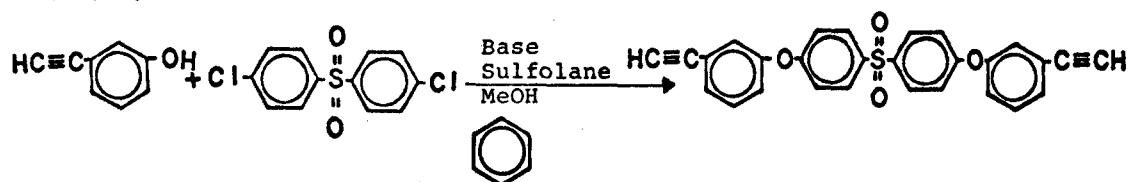
PERCENT YIELD: 74%

Because of a faulty oven, the 10 grams (.353 oz) of sample to be sent to SRI was destroyed. (The sample was given to another experimenter for heat treating.) The reaction was run again to obtain another 10 grams (.353 oz).

The synthesis of $\text{HC}\equiv\text{C}-\text{C}_6\text{H}_4-\text{O}-\text{S}(\text{O})_2-\text{C}_6\text{H}_4-\text{O}-\text{C}_6\text{H}_4-\text{C}\equiv\text{CH}$ was performed

to test this compound's compatability with Radel, a commercially available product, as a possible thermo-plasticizer to increase the processing properties of the Radel itself.

SYNTHESIS:

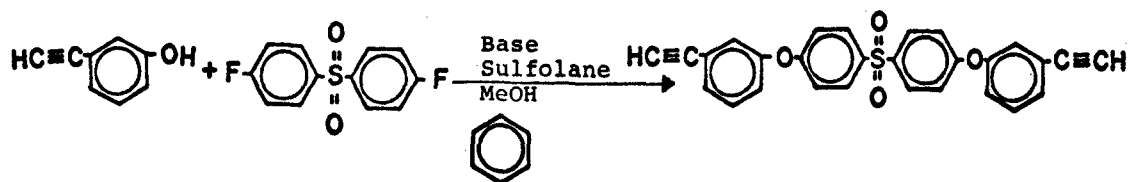


PERCENT YIELD: Unknown, the percent yield was not calculated because the product was thought to have dimerized, (as was later indicated by an IR spectra).

The synthesis of $\text{HC}\equiv\text{C}-\text{C}_6\text{H}_4-\text{O}-\text{S}(\text{O})_2-\text{C}_6\text{H}_4-\text{O}-\text{C}_6\text{H}_4-\text{C}\equiv\text{CH}$ was performed

again utilizing another novel mechanism different from the one used above in order to gain a higher yield and purer final product.

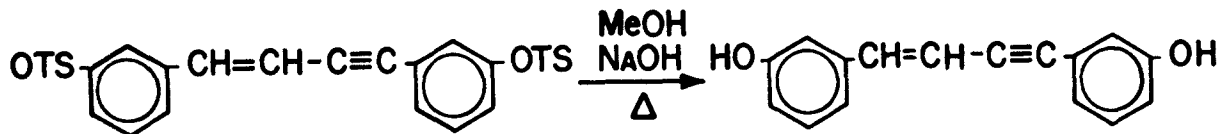
SYNTHESIS:



PERCENT YIELD: 71%

The synthesis of (E)-3,3'-(1-Buten-3-ynylene) diphenol was the first product in a series of various character reactions to be performed later.

SYNTHESIS:



PERCENT YIELD: 10%

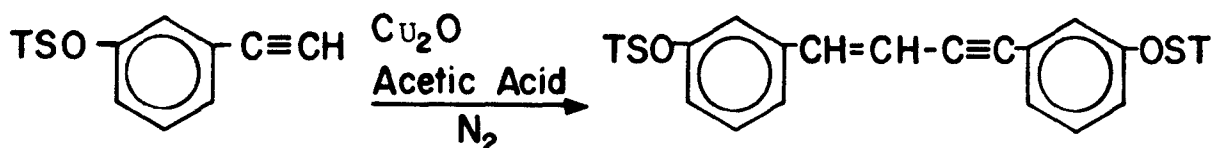
The reason for such low yield was thought to be attributed to the type of base used. This reaction was performed again utilizing a different base more soluble in alcohol to try and increase the yield.

The reaction was again performed on three separate occasions and again the product polymerized. To correct this problem the starting product (bis-tosolated eynene) was made and then de-tosolated to give a 40.7% yield. It was determined by this series of reactions that the tosolated material purchased from MRI (Midwest Research Institute) was bad and would need to be subsequently synthesized in this laboratory.

The synthesis of $\text{TSO}-\text{C}_6\text{H}_4-\text{CH}=\text{CH}-\text{C}\equiv\text{C}-\text{C}_6\text{H}_4-\text{OST}$ was

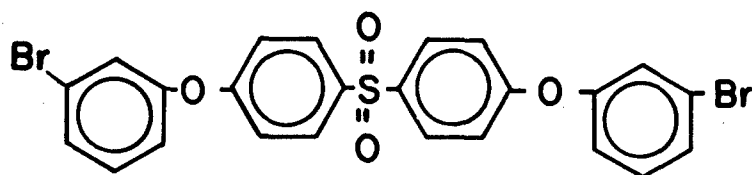
performed to replace the product received from MRI which was previously found to be impure.

SYNTHESIS:

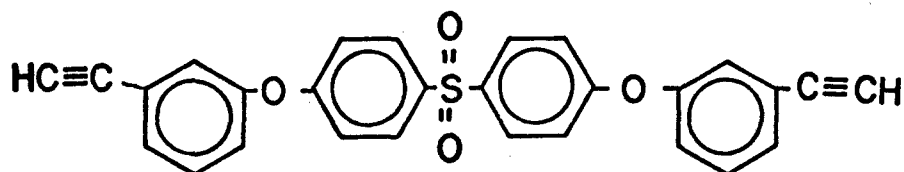


PERCENT YIELD: 73%

The product

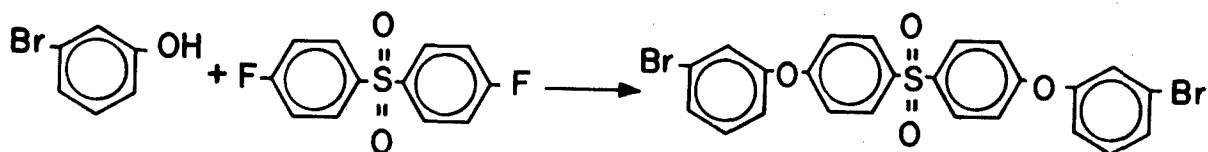


was the precursor in a series of character reactions designed to synthesize the product, ATS,



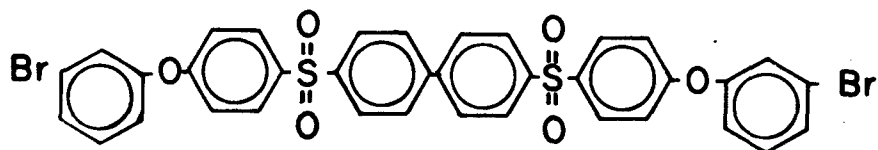
via a novel mechanism different from the procedures utilized on on page 5.

SYNTHESIS:



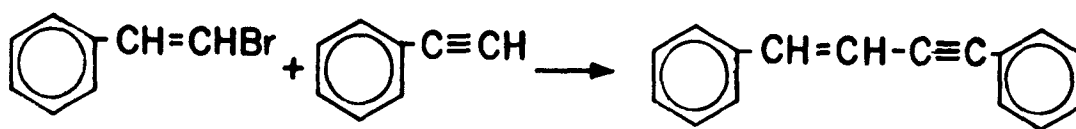
PERCENT YIELD: 71%

The reason for the low percentage yield was due to the formation of a bi-product thought to be:



The synthesis of this eynene was the first product in a series of IMC character reactions.

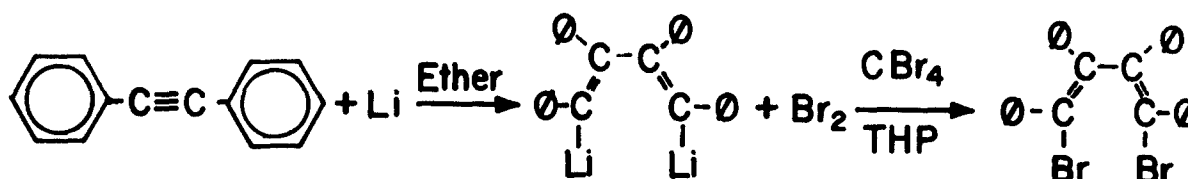
SYNTHESIS:



PERCENT YIELD: 53%

The synthesis of this compound was an attempt at a new novel IMC system.

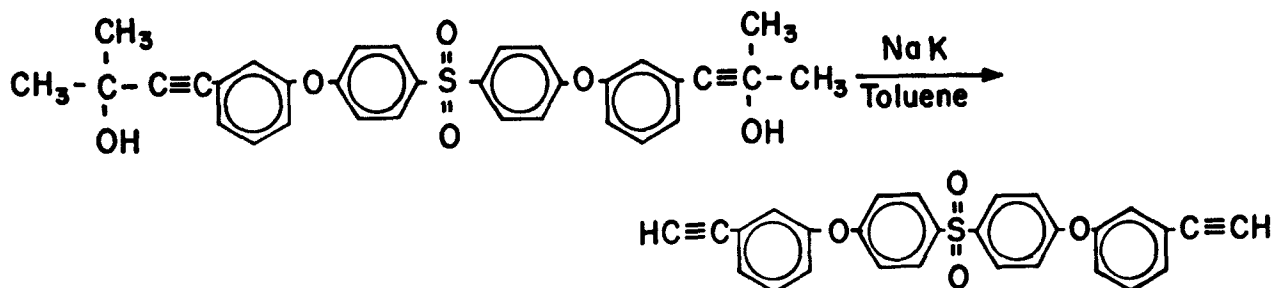
SYNTHESIS:



PERCENT YIELD: 52%

The synthesis of this compound, ATS, was an attempt at an approach that would be cost effective compared to other routes currently performed. (Reference page 5.)

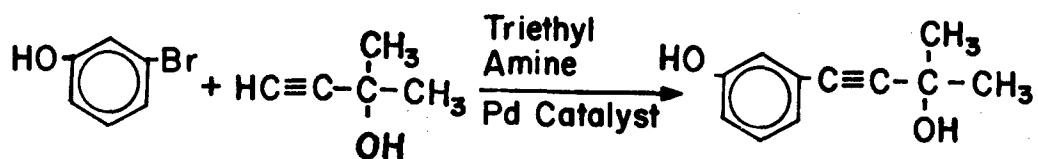
SYNTHESIS:



PERCENT YIELD: Unknown, too many isomeric products were obtained so this mechanism was discarded.

Again the synthesis of this compound was the first step in the synthesis of ATS as was shown on page 7. This was again a try at cost effective synthesis via a new synthetic route.

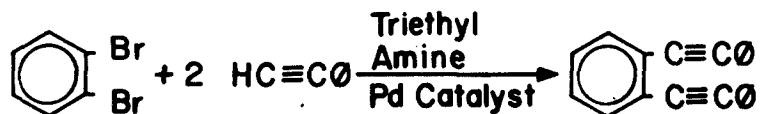
SYNTHESIS:



This reaction was not applicable due to the fact that too many isomeric bi-products were formed and that purification would prove too costly for production.

The synthesis of this compound was another look at a possible route to a new IMC system.

SYNTHESIS:



PERCENT YIELD: 25%

Because the above material vaporized in the DSC, the molecular weight was attempted to be increased by a new procedure. Under all cases tested though, the reaction failed.

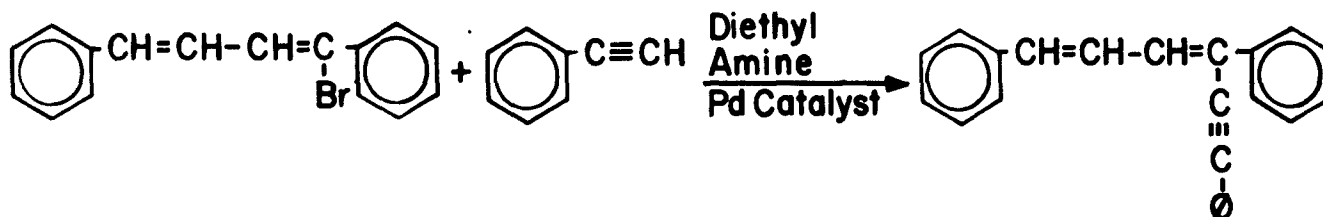
SYNTHESIS:



Reaction failed.

This is another attempt at an IMC system comparable to those explored in previous projects. (Reference pages 8 and 9.)

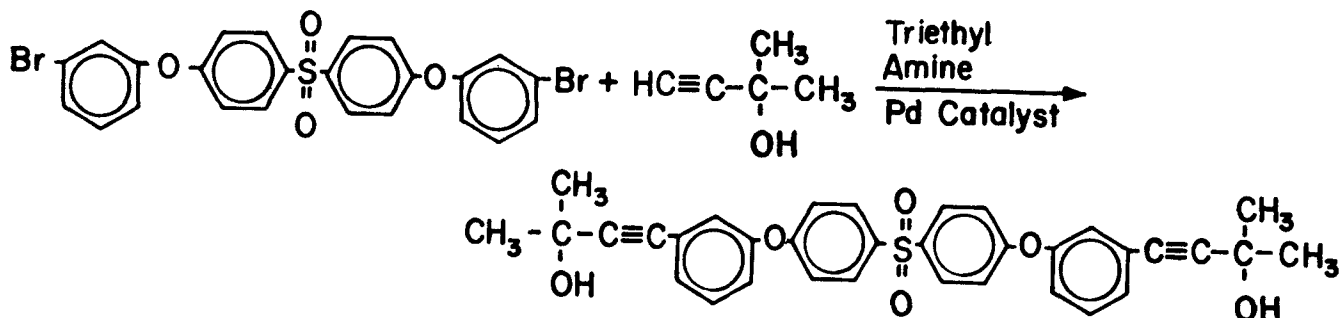
SYNTHESIS:



PERCENT YIELD: 35%

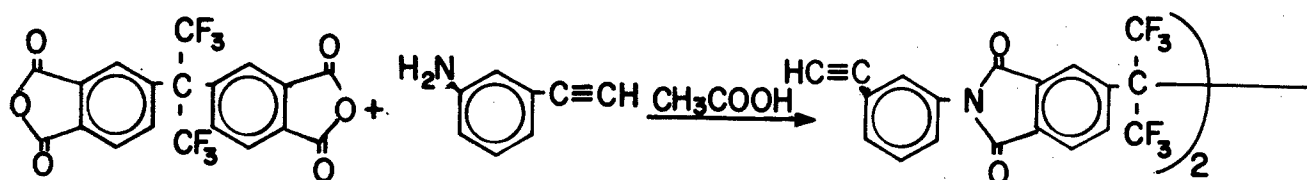
The synthesis of this compound was the most important intermediate in the synthesis of ATS. It took many months of research to find the perfect match of catalysts and reactants to meet the Air Force requirements.

SYNTHESIS:



This imide was made as one of two monomers to be utilized in a subsequent polymerization.

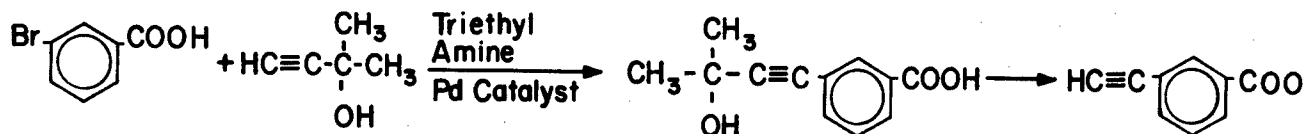
SYNTHESIS:



PERCENT YIELD: 73%

This was a novel synthetic procedure performed to test for the reactivity of this compound.

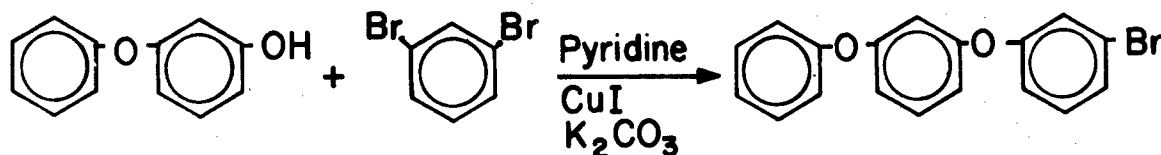
SYNTHESIS:



Reaction failed.

This compound was synthesized as a possible reactive plasticizer for Radel, a commercially available thermoplastic.

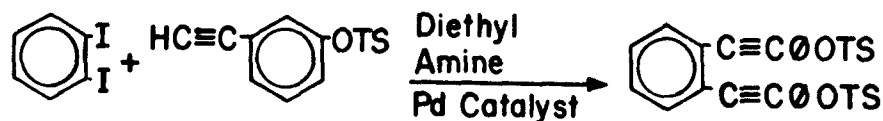
SYNTHESIS:



PERCENT YIELD: 47%

This was another try at the synthesis of a suitable compound for the IMC system similar to the ones on pages 8, 9, and 10.

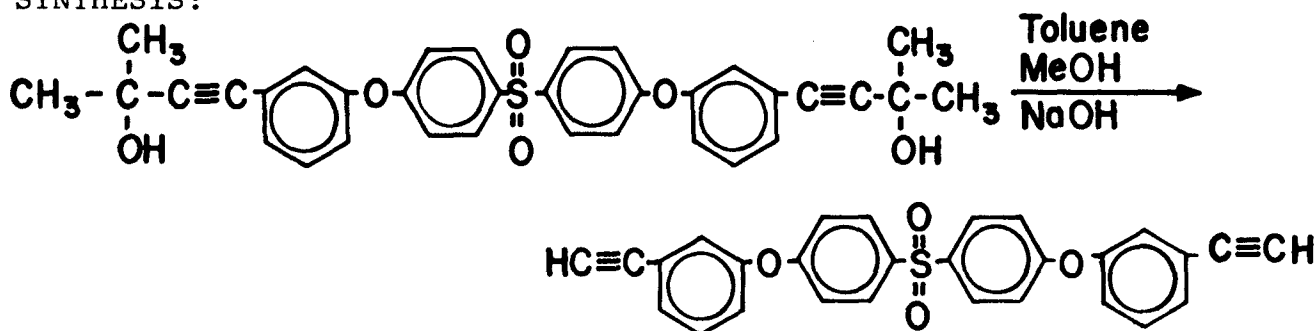
SYNTHESIS:



PERCENT YIELD: 50%

This reaction seems to be the most economical way to produce ATS for scale-up. The intermediate that was hydrolyzed in this procedure came from the reaction shown on page 10.

SYNTHESIS:



PERCENT YIELD: 55%

B. Inter and Intramolecular Cycloaddition Synthesis
(M. Unroe)

(1) SBQ Monomers

Single barreled quinoxaline monomers (SBQ) have been synthesized by reacting the benzil and diamine endcappers used to make ATQ (acetylene terminated quinoxalines) with BATQ (benzil acetylene terminated quinoxalines). An advantage of SBQ, which is in the process of evaluation at this time, is that SBQ's relatively lower molecular weight may afford a lower softening point when combined with higher molecular weight ATQ and BATQ monomers without sacrificing the physical properties of the ATQ and BATQ. Another advantage to SBQ monomers is their ease of processing. With lower molecular weight materials, one controls the outcome of the reaction more easily.

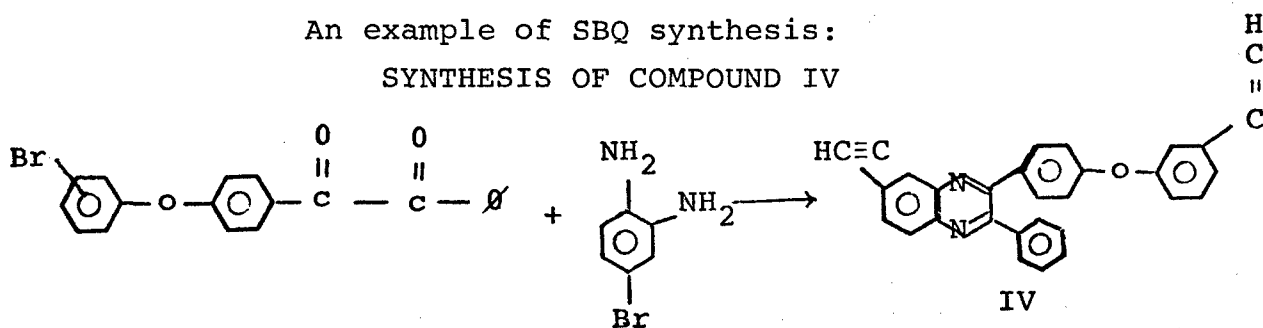
A majority of the work performed has included the synthesis of benzils and diamines to use as reactants in the SBQ syntheses. This discussion does not include benzil and diamine synthesis. Instead, the mechanism of SBQ synthesis is emphasized.

The three-step scheme of synthesis of SBQ systems is to react a benzil with a 4-halo o-phenylene diamine in a condensation reaction catalyzed by glacial acetic acid. The resulting intermediate is a halogenated quinoxaline. This intermediate is catalyzed in a basic environment with 2-methyl 3-butyne-2-ol to substitute an ethynyl group which is protected by an acetone group for the halogen. Then a base hydrolysis with sodium hydroxide causes a displacement of the acetone protector to form the acetylene termination on the quinoxaline. (See Figure 1 and Table 1.)

As a general rule the SBQ synthesis follows the scheme described in Figure 1. However, Compounds V - VIII are prepared by the reduction of the 4-halonitroanilines in situ to which are added the desired benzils. This exception to Step 1 is done only when quantitative considerations are not important.

An example of SBQ synthesis:

SYNTHESIS OF COMPOUND IV



P(3 bromophenoxy) benzil (5.48 gm, .193 oz) was heated after its preparation to the liquid state and poured into a single necked 500 ml (36.5 cu in) round-bottom flask. In 1:1 molar ratio, 3.64 gm (.128 oz) of 4-bromo o-phenylene diamine was added to the flask; in addition to 200 ml (12.2 cu in) methanol, 1 ml (.061 cu in) acetic acid was added. As the solution stirred, a yellow precipitate formed. After a 20 minute reflux, the solution was poured into 20 ml (1.22 cu in) HCl/400 ml (24.4 cu in) H₂O. The brominated quinoxaline intermediate was extracted

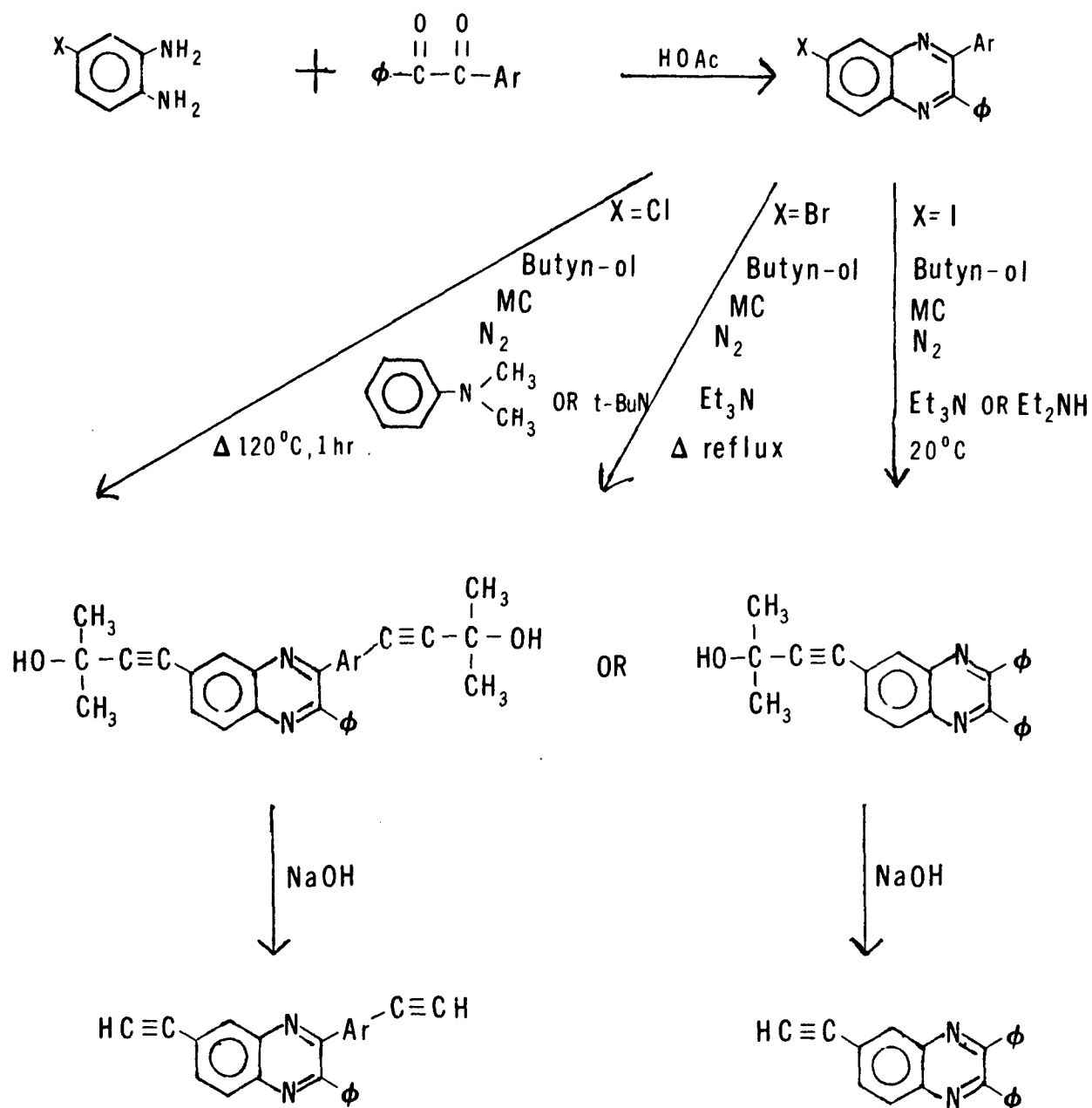

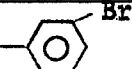

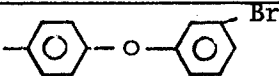
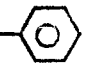
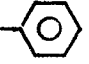
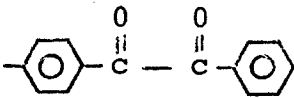
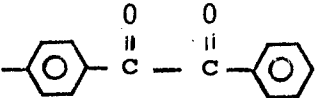
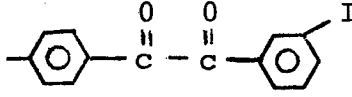
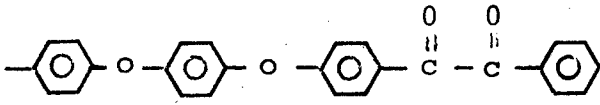


Figure 1. Mechanism of SBQ Synthesis

TABLE 1
SUMMARY OF REACTANT STRUCTURES USED IN SBQ SYNTHESIS

COMPOUND	Ar	X
I		Cl
II		I
III		Br
IV		Br
V		Br
VI		I
VII		Br
VIII		I
IX		I
X		I

with 3 X 150 ml (9.16 cu in) benzene. The yellow extract was then run through a silica gel column with dichloromethane elutant. The collected material was allowed to evaporate to dryness.

The intermediate was prepared for ethynylacetone substitution by dilution with 200 ml (12.2 cu in) triethyl amine in a 500 ml (30.5 cu in) round-bottom flask. N_2 was supplied by bubbling through the solution. To this was added 0.1 gm (.00353 oz) each of the "magic catalysts" (ϕ_3P , $(\phi_3P)_2$ $PdCl_2$, Cu I) and the solution refluxed under stirring in an oil bath for about seven hours. The solution was evaporated in a dish to an oil consistency and then added to 50 ml (3.05 cu in) fuming H_2SO_4 , 500 gm (17.6 oz) ice, and 500 ml (30.5 cu in) water. The product was extracted with 3 x 150 ml (9.16 cu in) ether and this ether layer was washed with 2 x 400 ml (24.4 cu in) water and dried.

The last step in the synthesis takes up the 9.75 gm (.344 oz) of impure acetone protected quinoxaline in minimal toluene in a 500 ml (30.5 cu in) round-bottom flask. To it was added NaOH/25 ml (1.53 cu in) methanol. The flask was filled with about 450 ml (27.5 cu in) toluene and refluxed down to ~150 ml (9.16 cu in) and refilled with toluene two more times (total reflux time = $6\frac{1}{2}$ hours). The SBQ was allowed to dry and diluted with 250 ml (15.3 cu in) CH_2Cl_2 , washed with 4 x 300 ml (18.3 cu in) water and separated. The dark brown solution was then run through a column with CH_2Cl_2 elutant. The final weight product = 1.41 gm (.0497 oz) and the yield compound IV = 30%.

The percent yields for these SBQ's synthesized range from less than 10% to a high of 44%. Work has just begun on the use of chlorinated quinoxaline intermediates because of the economics involved. Softening points are between 110-140°C (230-284°F) on the average.

ATQ (acetylene terminated quinoxaline) and IMC (intramolecular cycloaddition) synthesis have been combined to make a novel compound, BA DABA BA, that will polymerize by the pendant acetylene groups and intramolecularly within the phenylethynyl groups. The IMC occurs even after the cure temperature has been reached. As a result, this IMC polymer has a high T_g and does not emit any volatiles during the cure process.

Synthesis of ATQ monomers is accomplished by reacting benzils with tetramines in 2:1 molar ratios. (See Figure 2.)

As reported, 4.70 gm (.166 oz) of 2,2'Bis(phenylethynyl)-5,5'diaminobenzidine was dissolved in 150 ml (9.16 cu in) THF. Nitrogen was bubbled through as 6.16 gm (.0353 oz) of 4-(3 ethynylphenoxy) benzil was added. To this 2 ml (.122 cu in) acetic acid was added and the mixture was stirred for 16 hours at room temperature. The solution was poured into 750 ml (45.8 cu in) methanol and a yellow precipitate formed. Total weight of product recovered was 6.41 gm (.226 oz). The percent yield of BA DABA BA was 65%. Softening point was 107°C (224.6°F).

In contrast to ATQ synthesis, the BATQ systems (benzil acetylene terminated quinoxaline) synthesis is two stepped. First, a tetramine is reacted with a bis-benzil in a 2:1 molar ratio to form an intermediate which is then reacted with a benzil endcapper that had terminal acetylene groups. The research performed this year has been toward increasing the amounts of a BATQ called BA DABA BA.

BA DAB BA is an outgrowth of the work previously done on BATQ systems with large molecular weights. BA DAB BA ($M_w = 794$) could be added to higher weight BATQ monomers to reduce their softening temperatures. (See Figure 3.)

The compound p-diaminobenzidine (10.70 gm, .377 oz) was placed in a 3-necked 500 ml (30.5 cu in) round-bottom flask fitted with a condenser and N_2 inlet. THF (tetrahydrofuran)

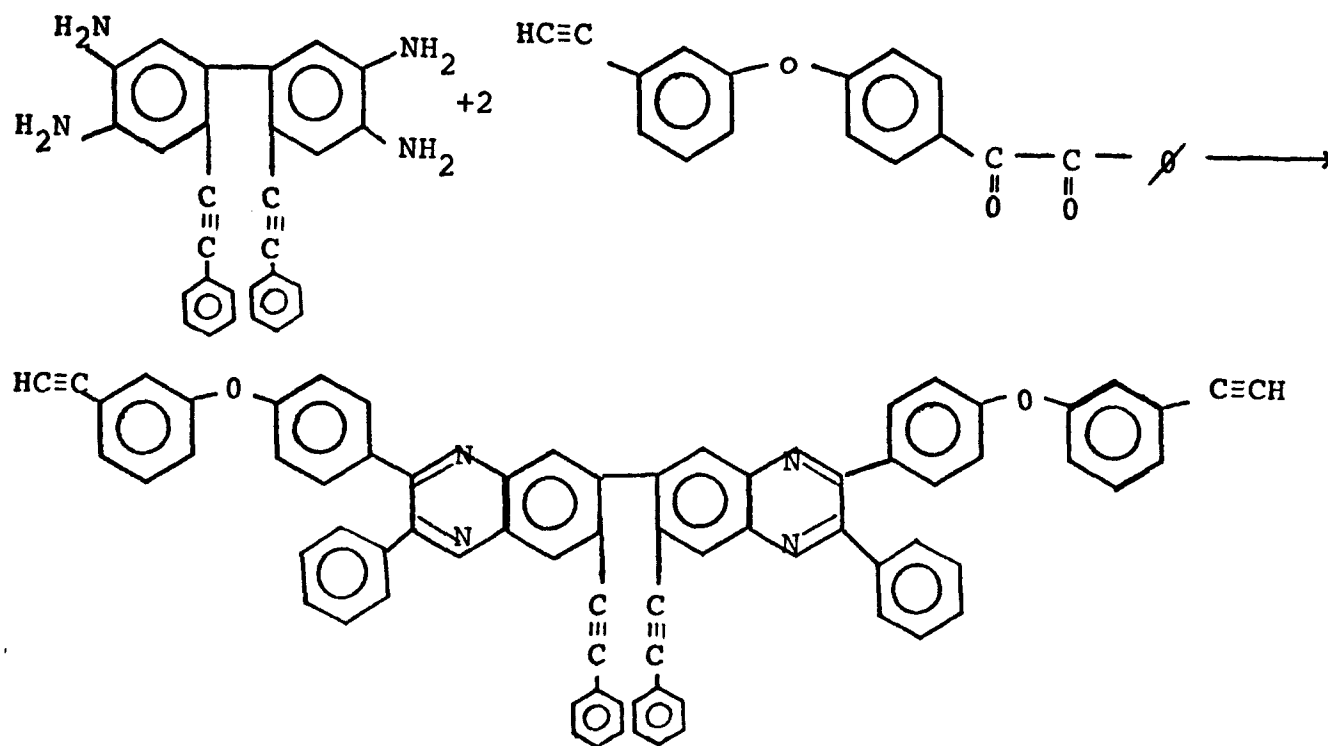


Figure 2. Synthesis Scheme of BA DABA BA

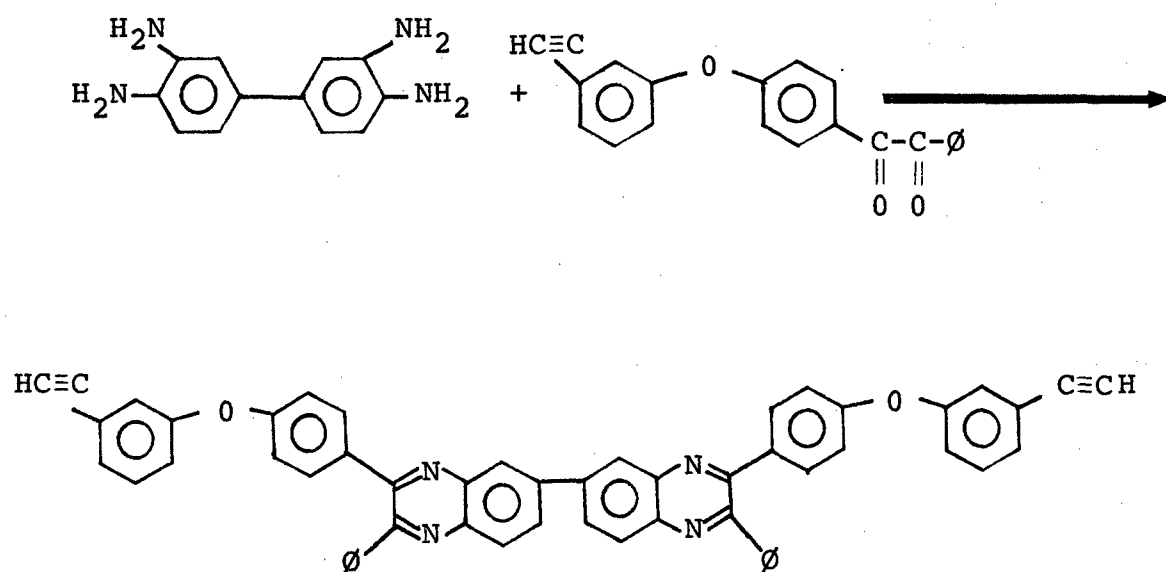


Figure 3. Synthesis Scheme of BA DAB BA

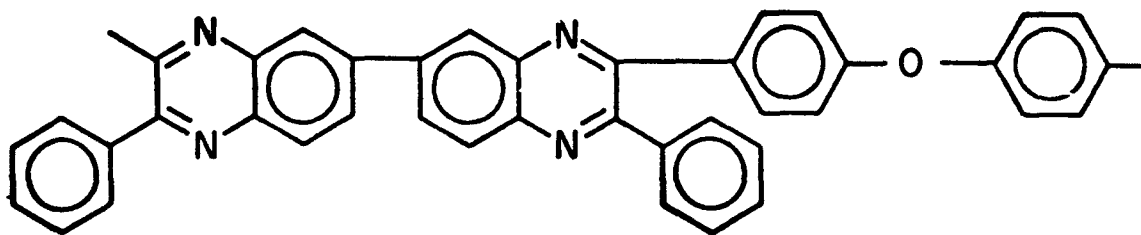
(200 ml, 12.2 cu in) and 32.60 gm (1.15 oz) 4(3'ethynylphenoxy) benzil were added. After addition of 4 ml (.244 cu in) acetic acid, the solution was heated to reflux for 30 minutes. After reflux, the THF was distilled down to about 25 ml (1.53 cu in), (total time = two hours). The dark brown solution was placed with 800 ml (48.8 cu in) methanol into a blender. After five minutes, a yellow precipitate that formed was filtered on a medium glass frit. The blender procedure was repeated for 2 x wash. The total weight of BA DAB BA was 37.51 gm (1.32 oz) (94%).

C. T_g Predictions (D. Wiff)

During the previous contractual period, preliminary efforts were directed to using the semi-empirical expression

$$\log T_g = \frac{\sum N_i K_i}{N_A \sum \Delta V_{\ell}} + 1.435$$

where $\sum \Delta V_{\ell}$ is the van der Waals volume of the repeat unit at a reference temperature T_R , N_A is Avagadro's number, and $\sum N_i K_i$ is the volume of the repeat unit at temperature T_g . For example, a typical polymer to which the technique is being applied is:



$$T_g)_{\text{calc}} = 561.5^{\circ}\text{K} \ (551^{\circ}\text{F}) \qquad T_g)_{\text{exp}} = 573^{\circ}\text{K} \ (572^{\circ}\text{F})$$

The measured value was determined by use of DSC. This technique was applied many times in an effort to test its reliability.

D. Kinetic Analysis (T. Grossman)

(1) Theory

The kinetic rate equation is:

$$\frac{dc}{dt} = A \cdot f(c) e^{\frac{-\Delta E}{RT}} \quad (1)$$

where dc/dt is the rate of change of the concentration of reactants with respect to time, A is a constant, $f(c)$ is a function of the concentration of reactants, ΔE is the activation energy of the system, R is the universal gas constant, and T is the temperature of the system in degrees Kelvin. The activation energy (ΔE), the constant (A), and the function $f(c)$ can be determined by using a differential scanning calorimeter. Assuming the area under a measured polymerization curve represents all reactants having reacted, one could measure heat evolved. If different heating rates are used, then a plot of the natural logarithm of the rate of heat evolved versus the reciprocal of the temperature in degrees Kelvin for each percent of the material's total heat evolved, then the slope of the straight line times the negative of the ideal gas constant equals the activation energy

$$\ln\left(\frac{dc}{dt}\right) = \frac{\Delta E}{-R} \left(\frac{1}{T}\right) + \ln(A \cdot f(c)) \quad (2)$$

or

$$\Delta E = -R * (\text{the slope}) \quad (3)$$

Rearranging equation (2)

$$\ln(A \cdot f(c)) = \ln\left(\frac{dc}{dt}\right) + (\text{the slope}) * \left(\frac{1}{T}\right) \quad (4)$$

From this $Af(c)$ can be computed for a given concentration of reactants present in the sample. The last two parameters needed for constructing a processing window plot are n the reaction order and A . This is accomplished by plotting the natural logarithms of $A \cdot f(c)$ versus the natural logarithm of the quantity $(1-c)$. Here we are assuming $Af(c) = (1-c)^n$, a typical reaction process. The slope of the best straight line is the reaction order (n) and $\ln(A)$ is the intercept. Finally, upon rearranging equation (1)

$$\frac{dc}{Af(c)} = e^{\frac{-\Delta E}{RT}} dt \quad (5)$$

$$\int_0^c \frac{dc}{A(f(c))} = e^{\frac{-\Delta E}{RT}} \int_0^t dt \quad (6)$$

Let us define a new function of the concentration called $g(c)$

$$g(c) = \int_0^c \frac{dc}{Af(c)} \quad (7)$$

If we substitute for $A \cdot f(c)$ the calculated values of n (reaction order) and A (the prefix of kinetic rate) then

$$g(c) = A \int_0^c \frac{dc}{(1-c)^n} \quad (8)$$

Performing the integration and rearranging

$$g(c) = t e^{\frac{-\Delta E}{RT}} \quad (9)$$

$$t = g(c) e^{\frac{\Delta E}{RT}} \quad (10)$$

and

$$\ln(t) = \frac{\Delta E}{R} \left(\frac{1}{T} \right) + \ln[g(c)] \quad (11)$$

This equation allows us to construct a processing window plot. Each line on the processing window plot represents some level of concentration (5%, 50%, and 95% conversion). There are two plots per set of kinetic analysis experiments, one using $g(c)$ from equation (7) and the other from equation (8). These reaction window plots are now ready for our use in predicting how long (under ideal kinetic assumptions, i.e., complete mobility of the reactive components) it will take to cure a sample to a specified percent of cure if we know the cure temperature.

(2) Results from Kinetic and Cure Computer Programs

Table 2 contains the results from eleven sets of kinetic experiments. Following Table 2 are the processing window plots (Figures 4 thru 25); for explanation of plot see the above section on kinetic theory.

E. Rheometrics Mechanical Spectrometer (C. Lee and J. Henes)

(1) Instrumentation

Different modes of measurement of this instrument were verified, and their limitations were evaluated.¹ The spectrometer has been used mainly in two areas: 1) characterization of the dynamic response of bulk sample, and 2) monitoring the cure rheology of thermoset systems. In addition to the parallel plate mode of operation used for measuring degree of cure, a new technique, torsion impregnated cloth analysis (TICA), was developed (see below).

(2) Radel

The thermoplastic polymer (Radel) was chosen as one of the matrix materials used in the reactive plasticizer program. Its dynamic response was characterized in the temperature range of -150°C (302°F) to 380°C (716°F).^{1,2}

(3) Torsion Impregnated Cloth Analysis (TICA)

This technique has been developed to an operational stage. This new technique allows monitoring of the cure

TABLE 2
KINETIC ANALYSIS DATA OF ACETYLENE TERMINATED SYSTEMS

SAMPLE	STRUCTURE (Figure #)	SCAN NUMBER	ΔE (KCAL/MOLE)	ENERGY OF ACTIVATION ΔE (BTU/MOLE)	LOG PRE-FIX OF LOG (A)	REACTION ORDER (N)
A-BA	1	78.8	24.965	(99.212)	8.0353	1.40
BATQ N=0	2	78.9	25.480	(101.258)	7.8567	1.34
FLH	3	78.10	27.873	(110.768)	9.4790	1.27
BA-DAB-BA	4	78.13	21.192	(84.218)	6.6291	0.23
BA-DABA-BA	5	78.14	20.817	(82.727)	7.2738	0.64
Pats X-27	6	78.15	40.395	(260.531)	13.7656	1.21
GD-37	7	78.16	24.736	(98.302)	8.6161	0.55
ATQ Batch #1	8	79.2	16.274	(64.673)	4.3280	0.86
ATZ Batch #2	8	79.3	17.474	(69.442)	4.8990	0.69
AA-BA	9	79.4	22.642	(89.980)	7.2650	0.64
BA-DAB-BA	4	79.5	19.770	(78.567)	5.9880	0.34

REACTION WINDOW PLOT
 SAMPLE: A-BA (BATQ M-II) 78.8 2 & 3 MAY
 KINETIC METHOD: FRIEDMANS MULTI-SCAN
 $\text{LOG}(A)=8.0353$ $E=24.965$ $N=1.40$

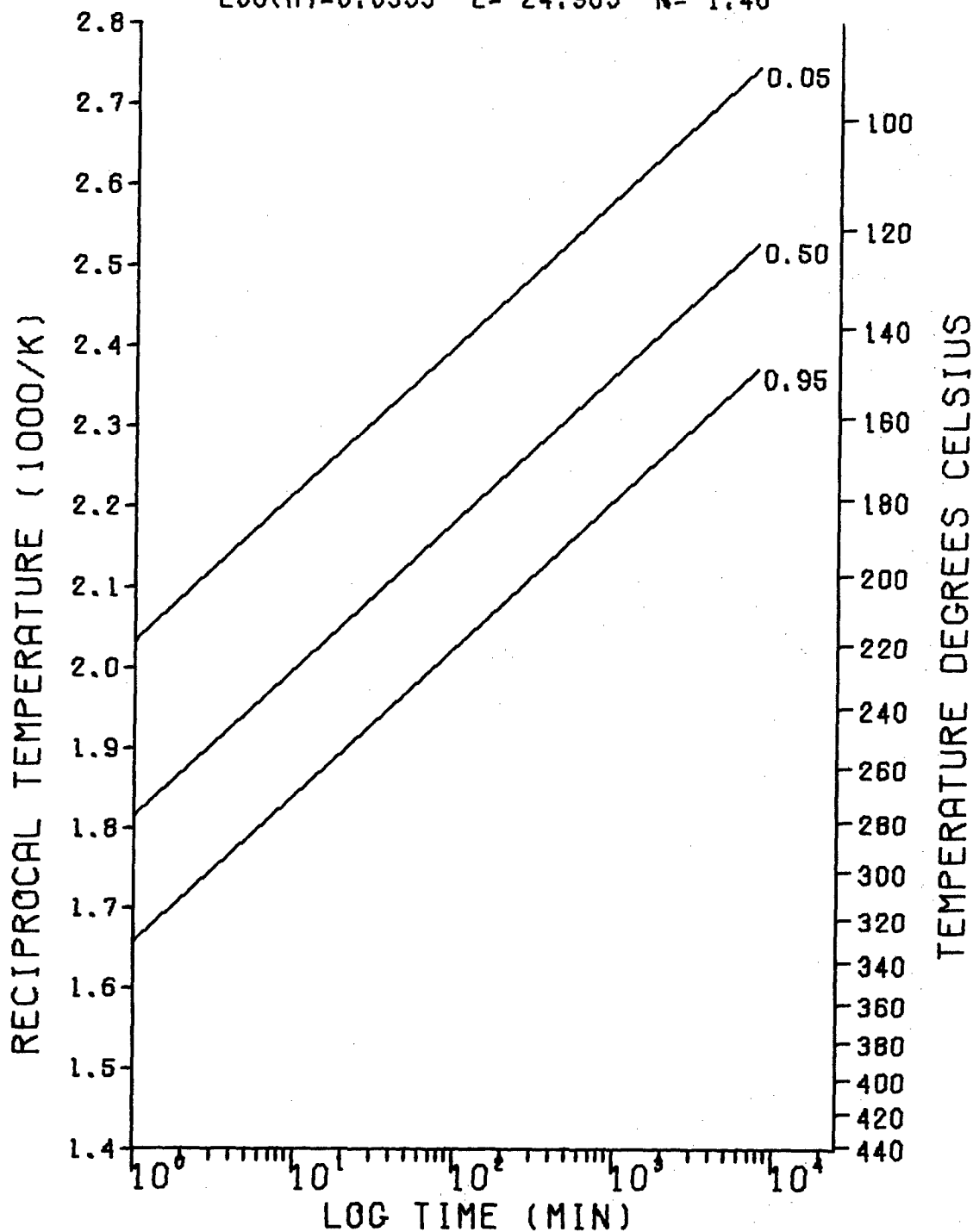


Figure 4. Ideal Processing Window for A-BA (BATQ M-II)
 ($n=1.40$).

REACTION WINDOW PLOT
 SAMPLE: A-BA (BATQ M=11) 78.8 2 & 3 MAY
 KINETIC METHOD: FRIEDMAN'S MULTI-SCAN
 LOG(A)=8.0353 E= 24.965 N= 0.00

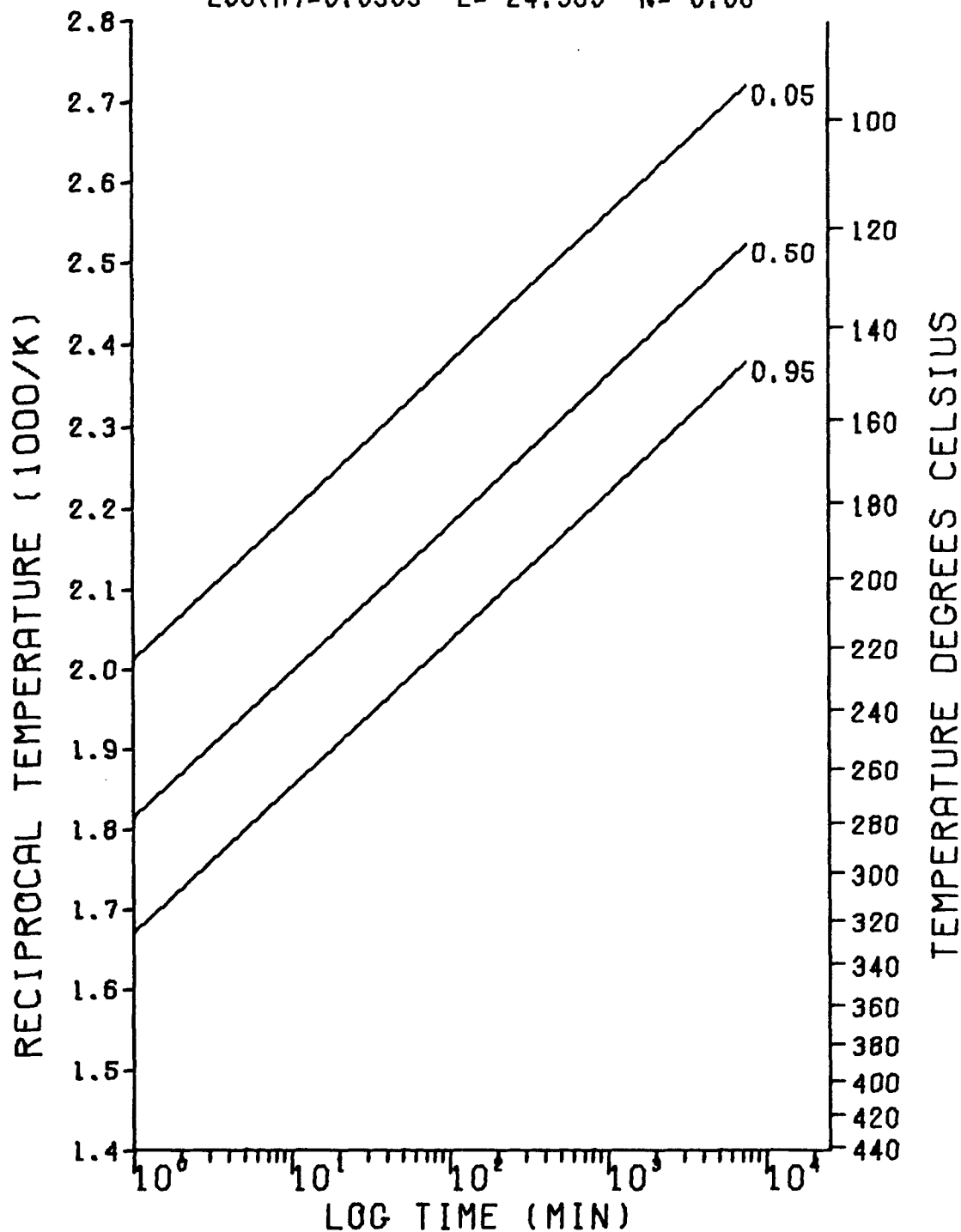


Figure 5. Ideal Processing Window for A-BA (BATQ M=11) ($n = 0.00$).

REACTION WINDOW PLOT
 SAMPLE: BATQ N=0 78.9
 KINETIC METHOD: FRIEDMAN'S MULTI-SCAN
 LOG(A)=7.8567 E= 25.480 N= 1.34

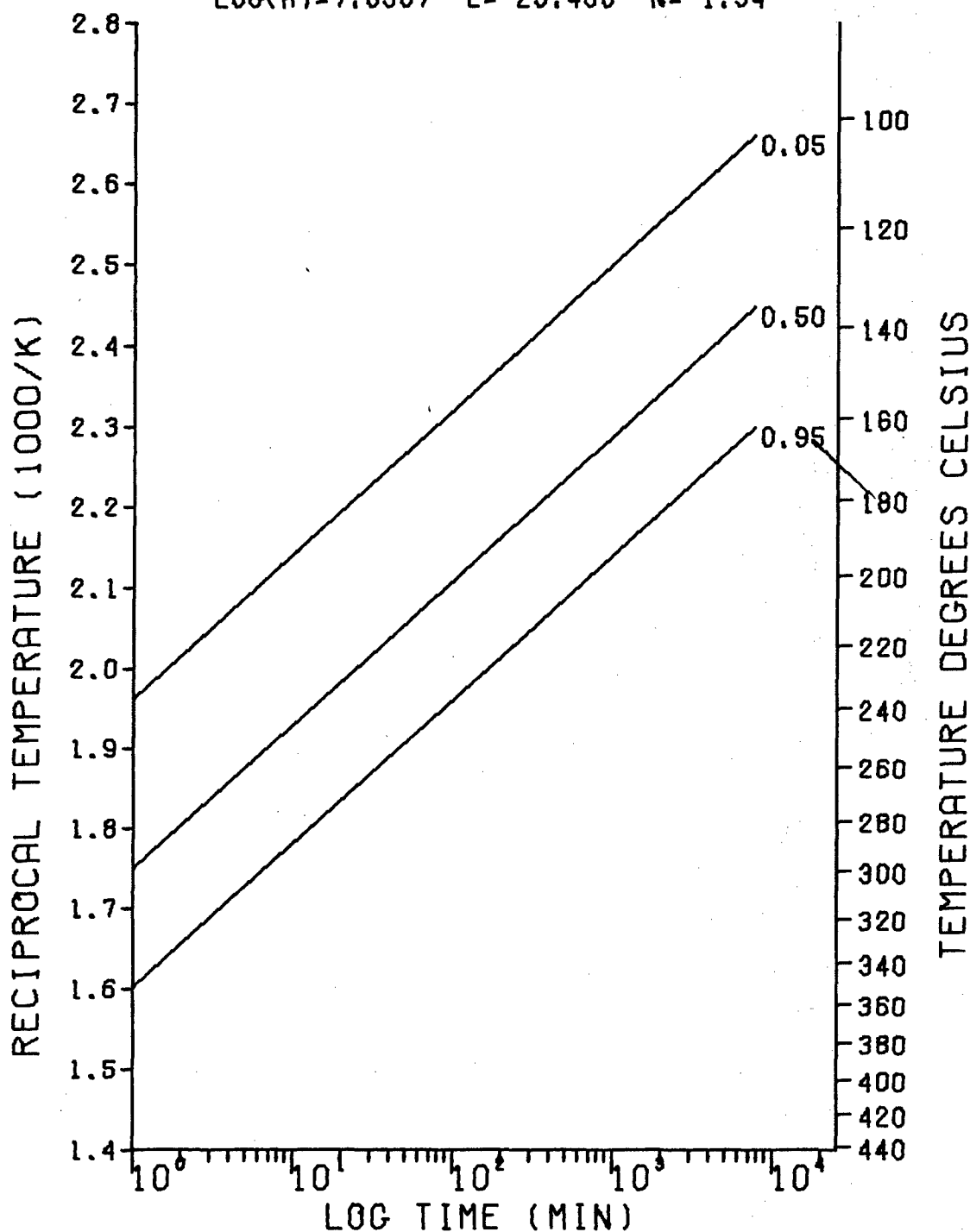


Figure 6. Ideal Processing Window for BATQ N=0
 (n= 1.34).

REACTION WINDOW PLOT
 SAMPLE: BATQ N=0 78.9 4 MAY 78
 KINETIC METHOD: FRIEDMAN'S MULTI-SCAN
 LOG(A)=7.8567 E= 25.480 N= 0.00

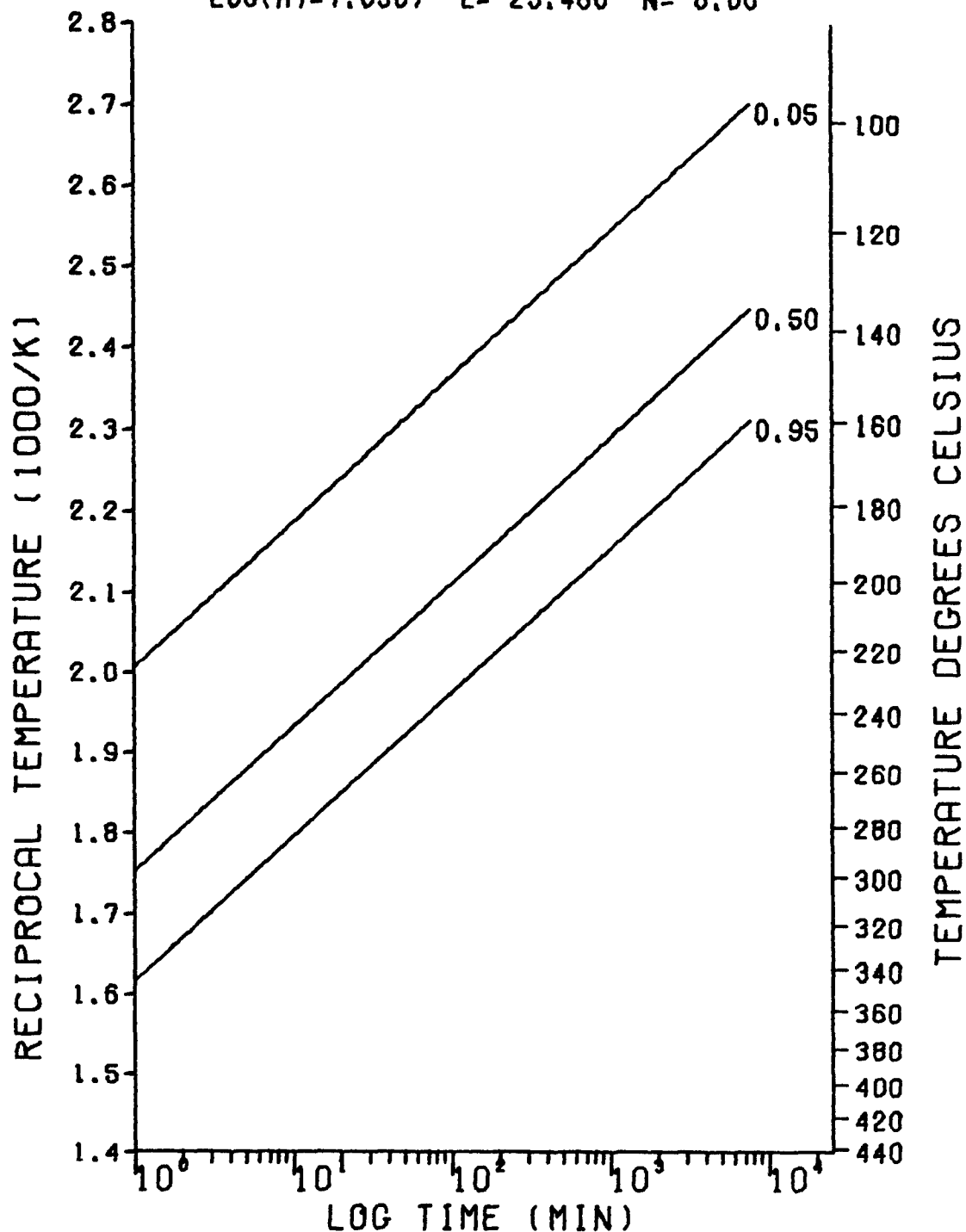


Figure 7. Ideal Processing Window for BATQ N=0 (n=0.00).

REACTION WINDOW PLOT
 SAMPLE: FLH-5-99 78.10 22 MAY 78
 KINETIC METHOD: FRIEDMAN'S MULTI-SCAN
 LOG(A)=9.4790 E= 27.873 N= 1.27

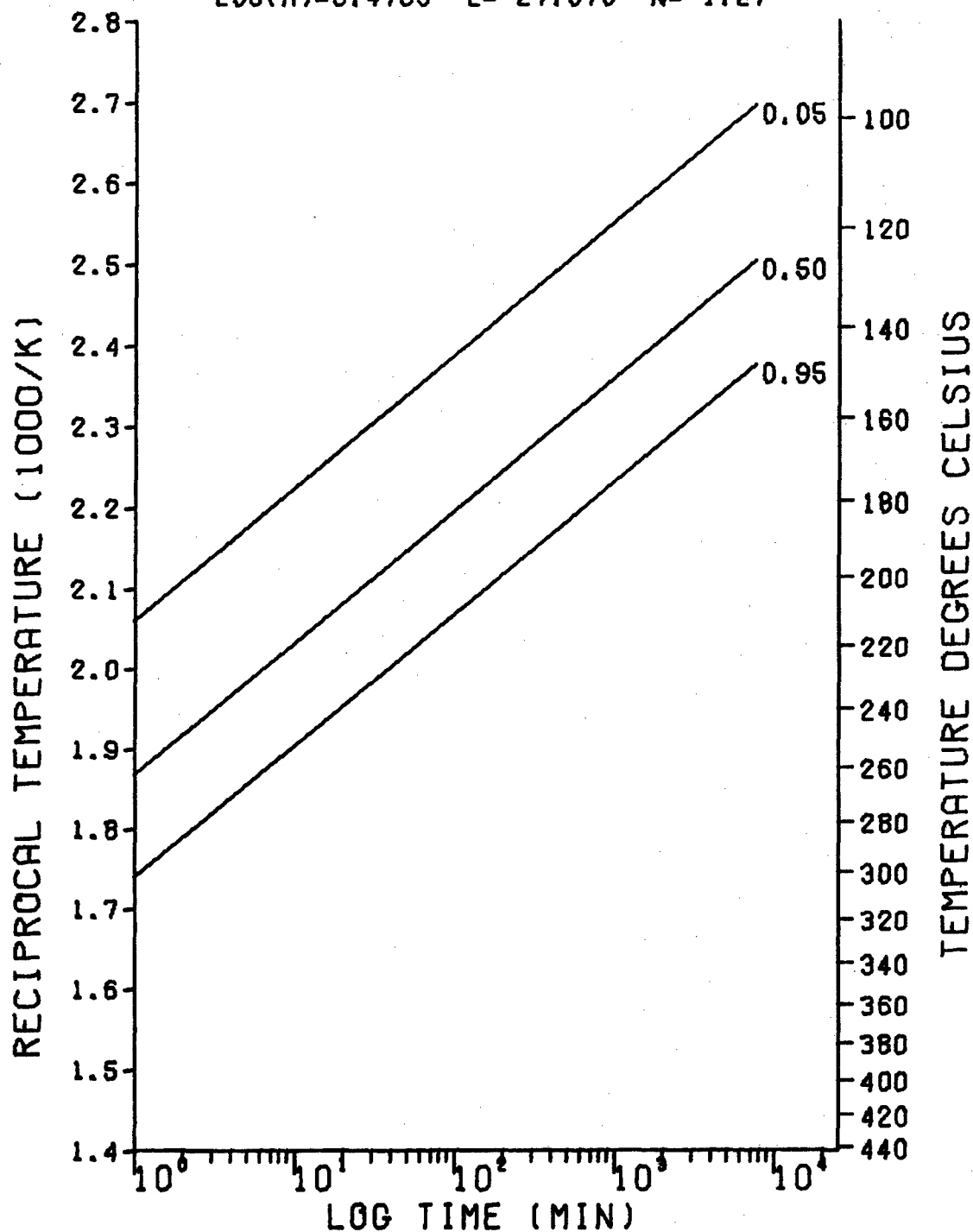


Figure 8. Ideal Processing Window for FLH-5-99
 (n= 1.27).

REACTION WINDOW PLOT
 SAMPLE: FLH-5-99 78.10 22 MAY 78
 KINETIC METHOD: FRIEDMAN'S MULTI-SCAN
 LOG(A)=9.4790 E= 27.873 N= 0.00

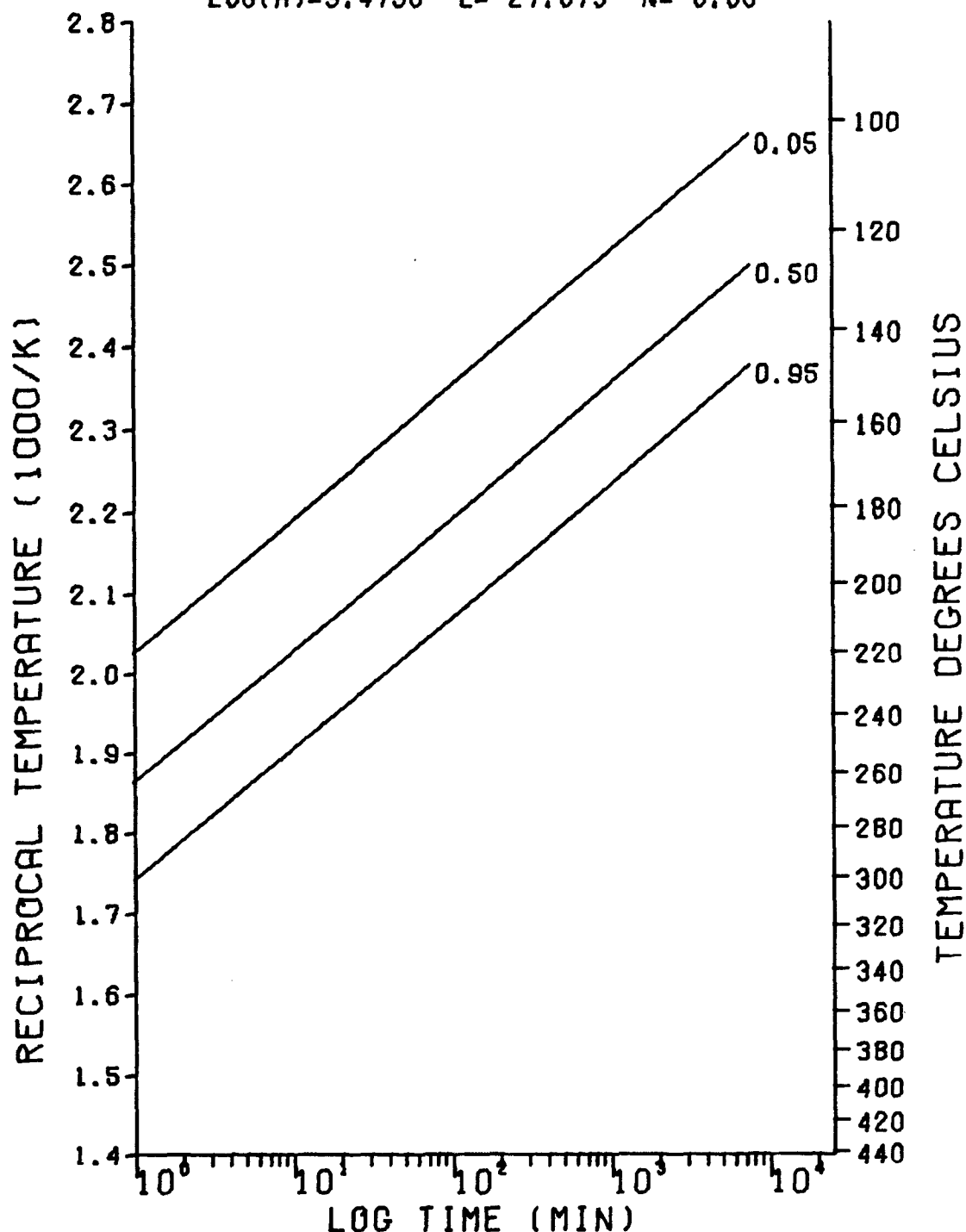


Figure 9. Ideal Processing Window for FLH-5-99
 (n= 0.00).

REACTION WINDOW PLOT
 SAMPLE: BA-DAB-BA 78.13 25 SEPT 78
 KINETIC METHOD: FRIEDMAN'S MULTI-SCAN
 LOG(A)=6.6291 E= 21.192 N= 0.23

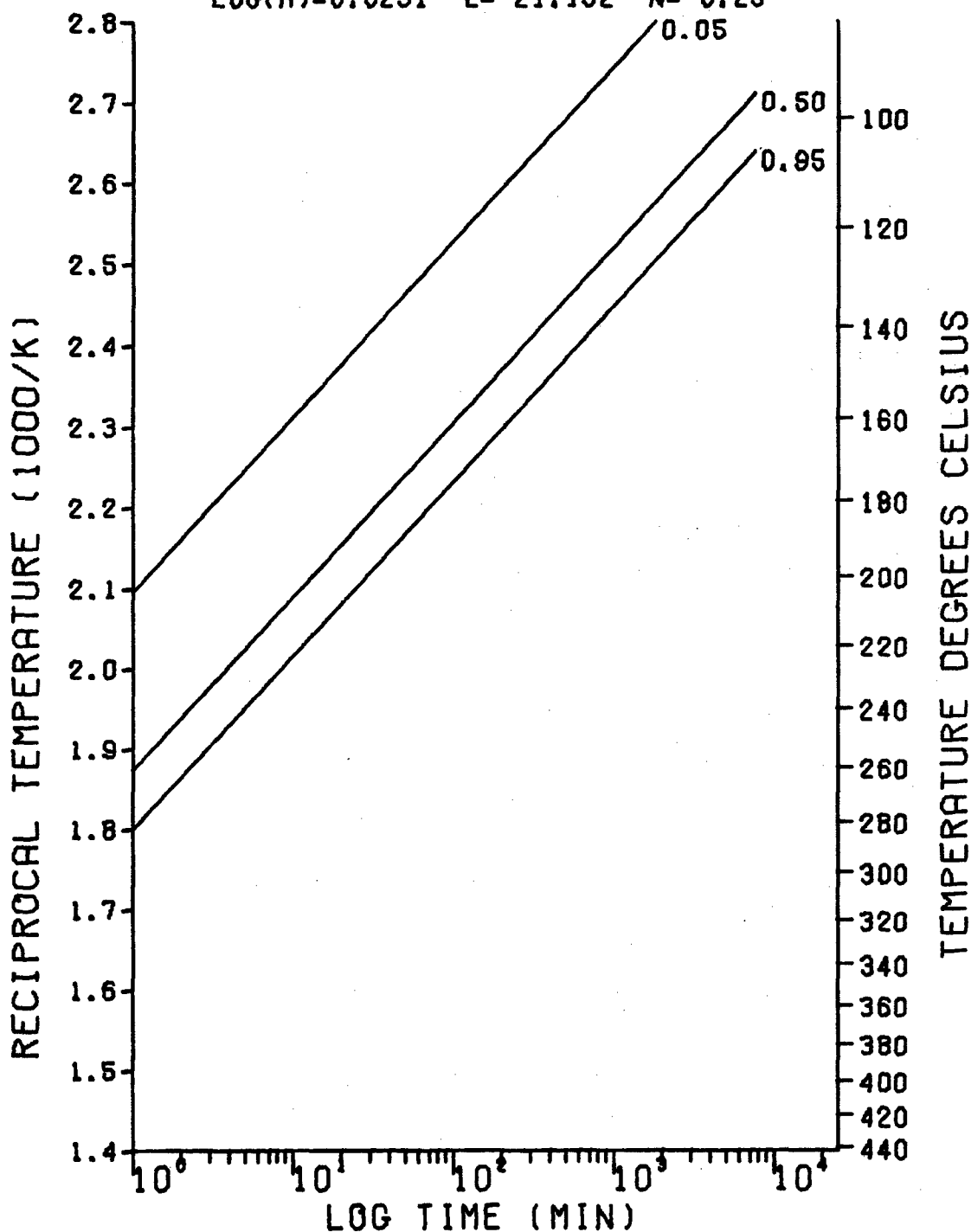


Figure 10. Ideal Processing Window for BA-DAB-BA
 ($n = 0.23$).

REACTION WINDOW PLOT
 SAMPLE: BA-DAB-BA 78.13 25 SEPT 78
 KINETIC METHOD: FRIEDMAN'S MULTI-SCAN
 $\text{LOG}(A)=6.6291$ $E=21.192$ $N=0.00$

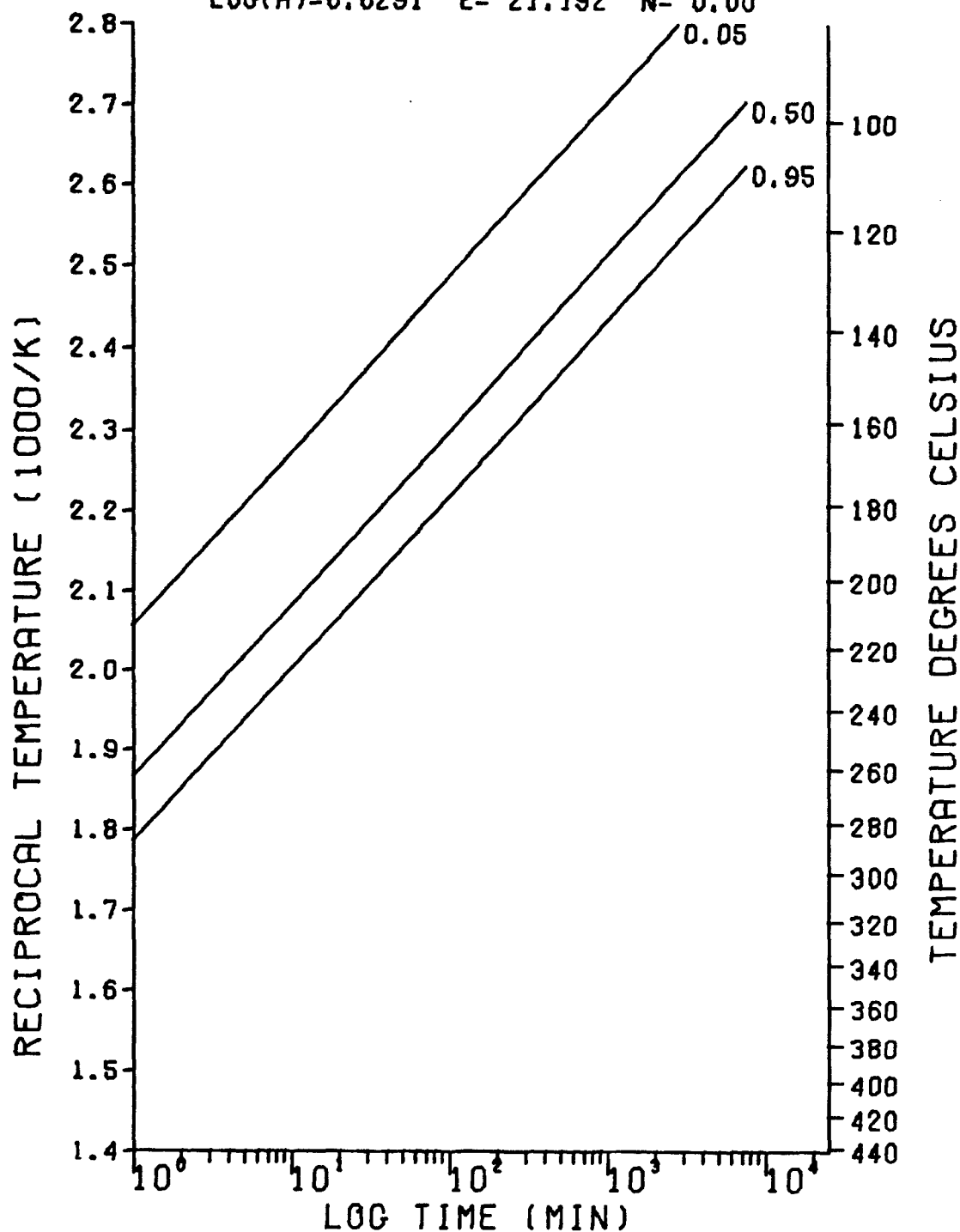


Figure 11. Ideal Processing Window for BA-DAB-BA ($n=0.00$).

REACTION WINDOW PLOT
 SAMPLE: BA-DABA-BA 78.14 26 SEPT 78
 KINETIC METHOD: FRIEDMAN'S MULTI-SCAN
 LOG(A)=7.2738 E= 20.817 N= 0.64

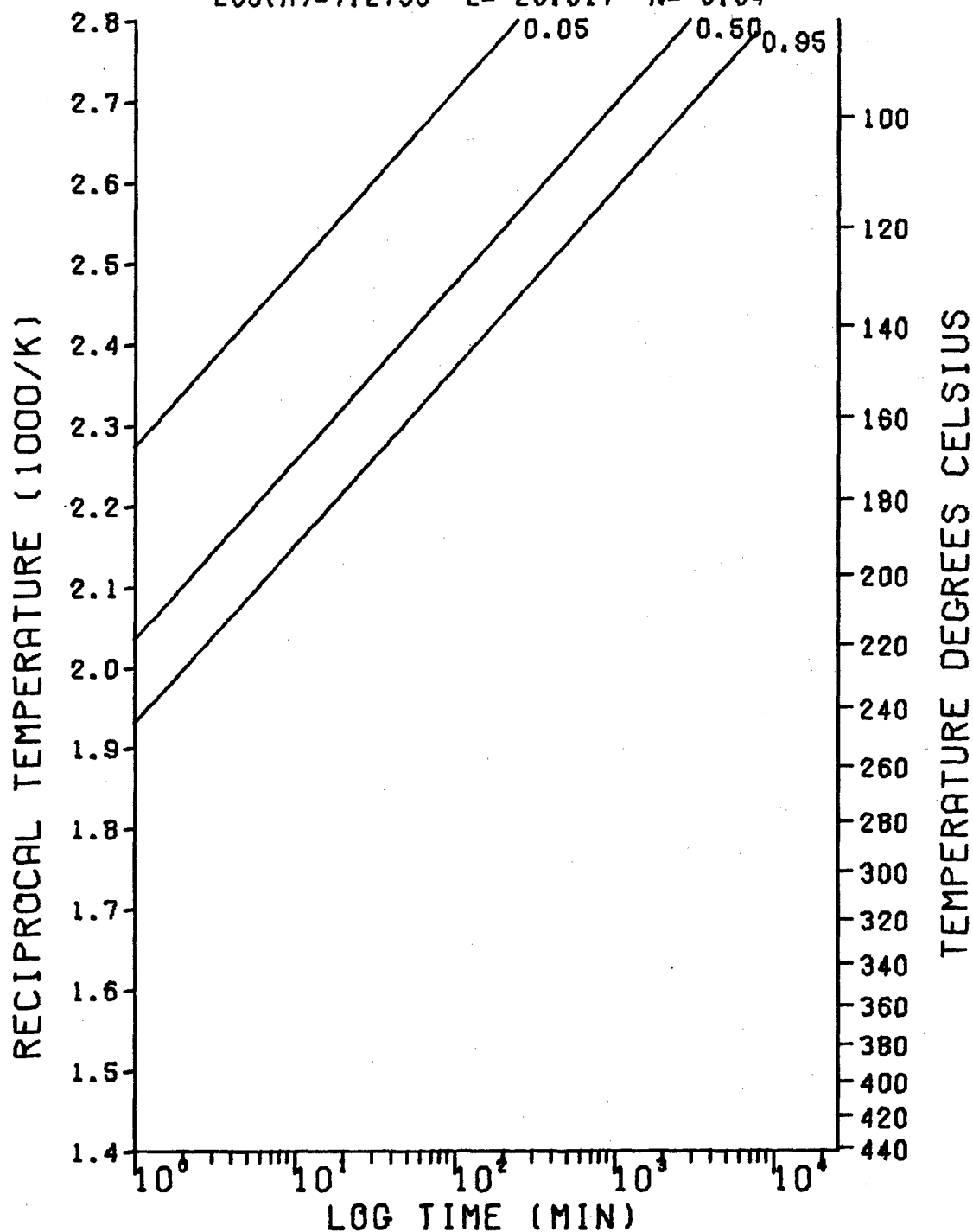


Figure 12. Ideal Processing Window for BA-DABA-BA
 (n= 0.64).

REACTION WINDOW PLOT
 SAMPLE: BA-DABA-BA 78.14 26 SEPT 78
 KINETIC METHOD: FRIEDMAN'S MULTI-SCAN
 LOG(A)=7.2738 E= 20.817 N= 0.00

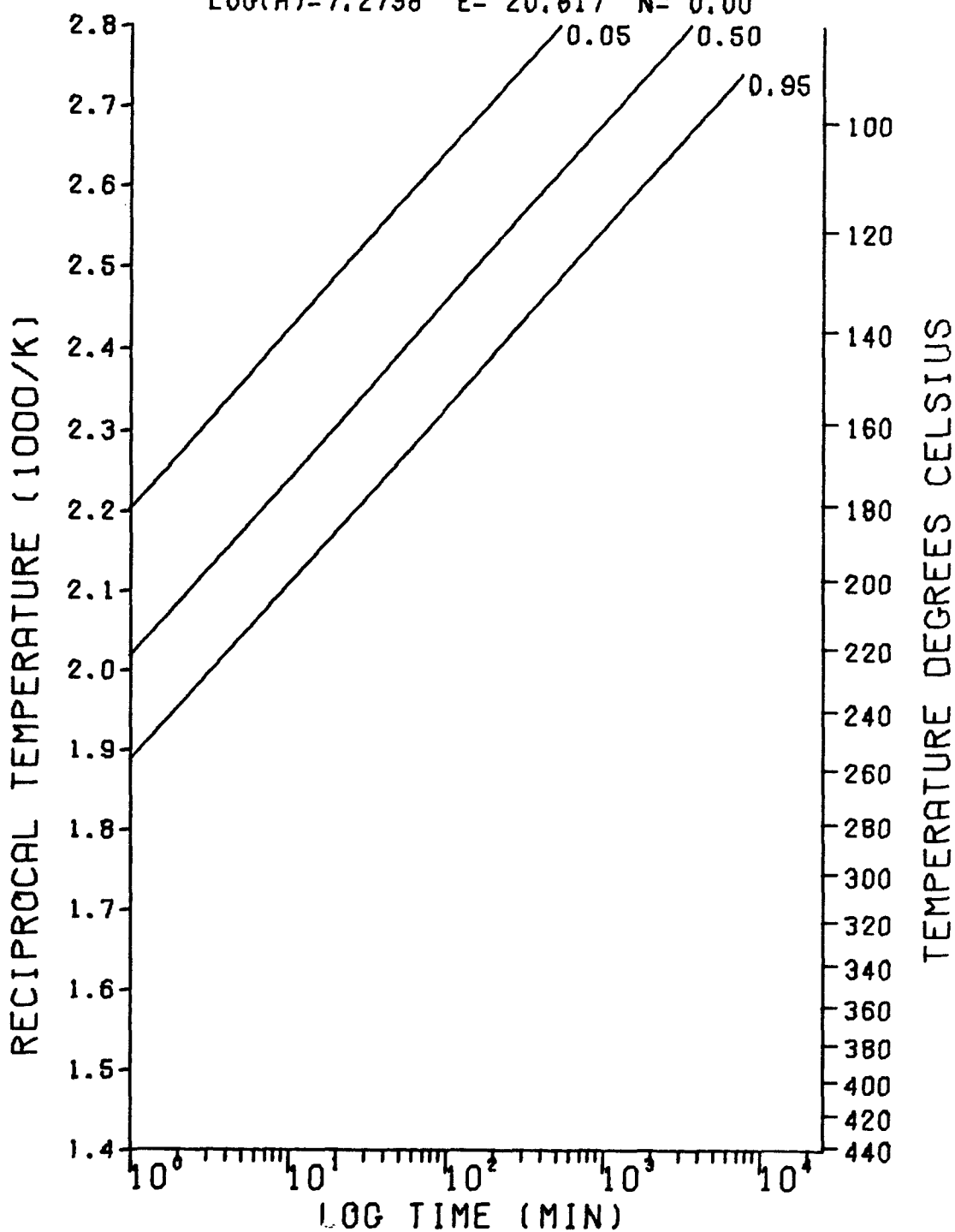


Figure 13. Ideal Processing Window for BA-DABA-BA ($n= 0.00$).

REACTION WINDOW PLOT
 SAMPLE: PATS X-27 78.15 27 SEPT 78
 KINETIC METHOD: FRIEDMAN'S MULTI-SCAN
 $\text{LOG}(A)=13.7656$ $E=40.395$ $N=1.21$

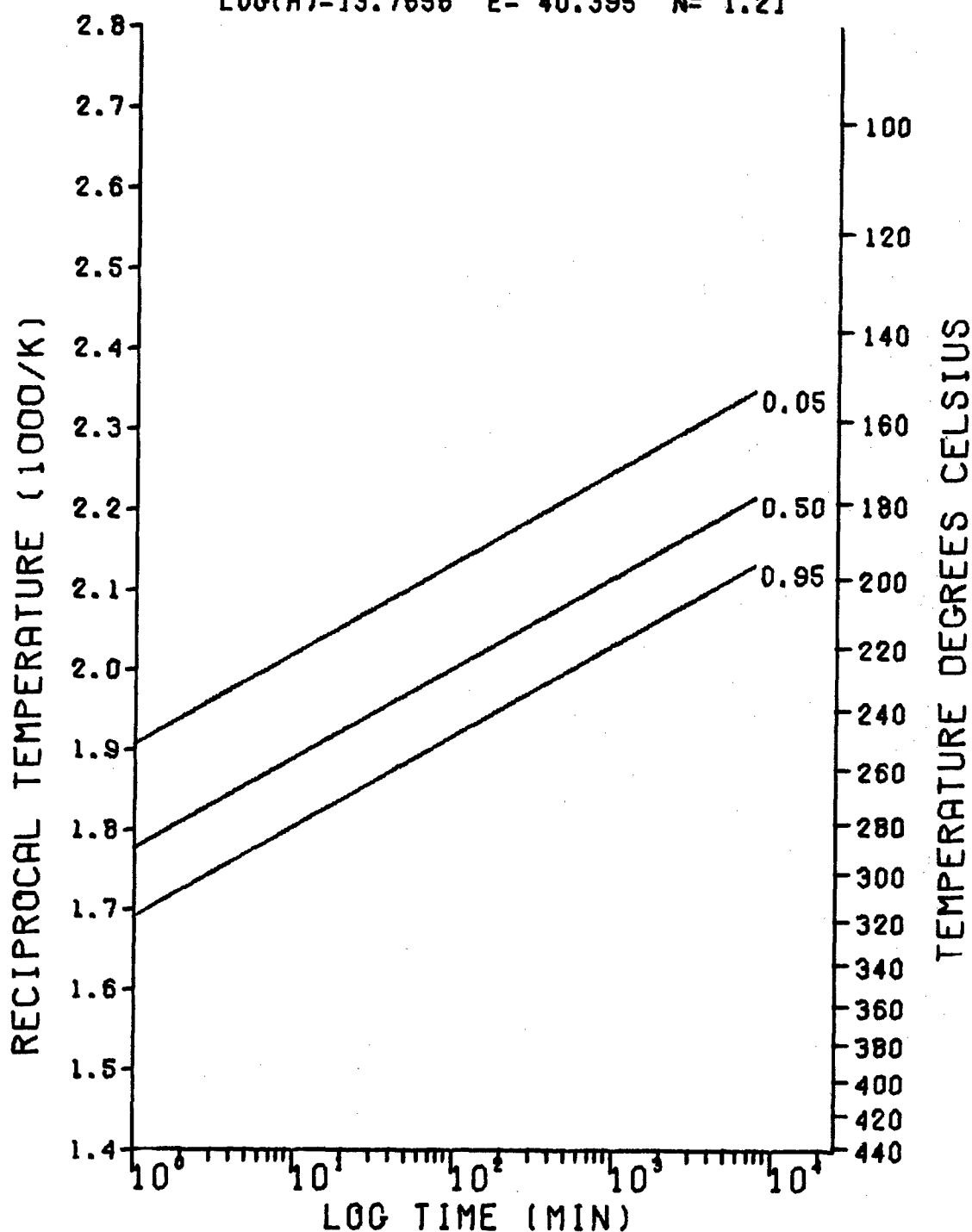


Figure 14. Ideal Processing Window for PATS X-27
 ($n=1.21$).

REACTION WINDOW PLOT
SAMPLE: PATS X-27 78.15 27 SEPT 78
KINETIC METHOD: FRIEDMAN'S MULTI-SCAN
LOG(A)=13.7656 E= 40.395 N= 0.00

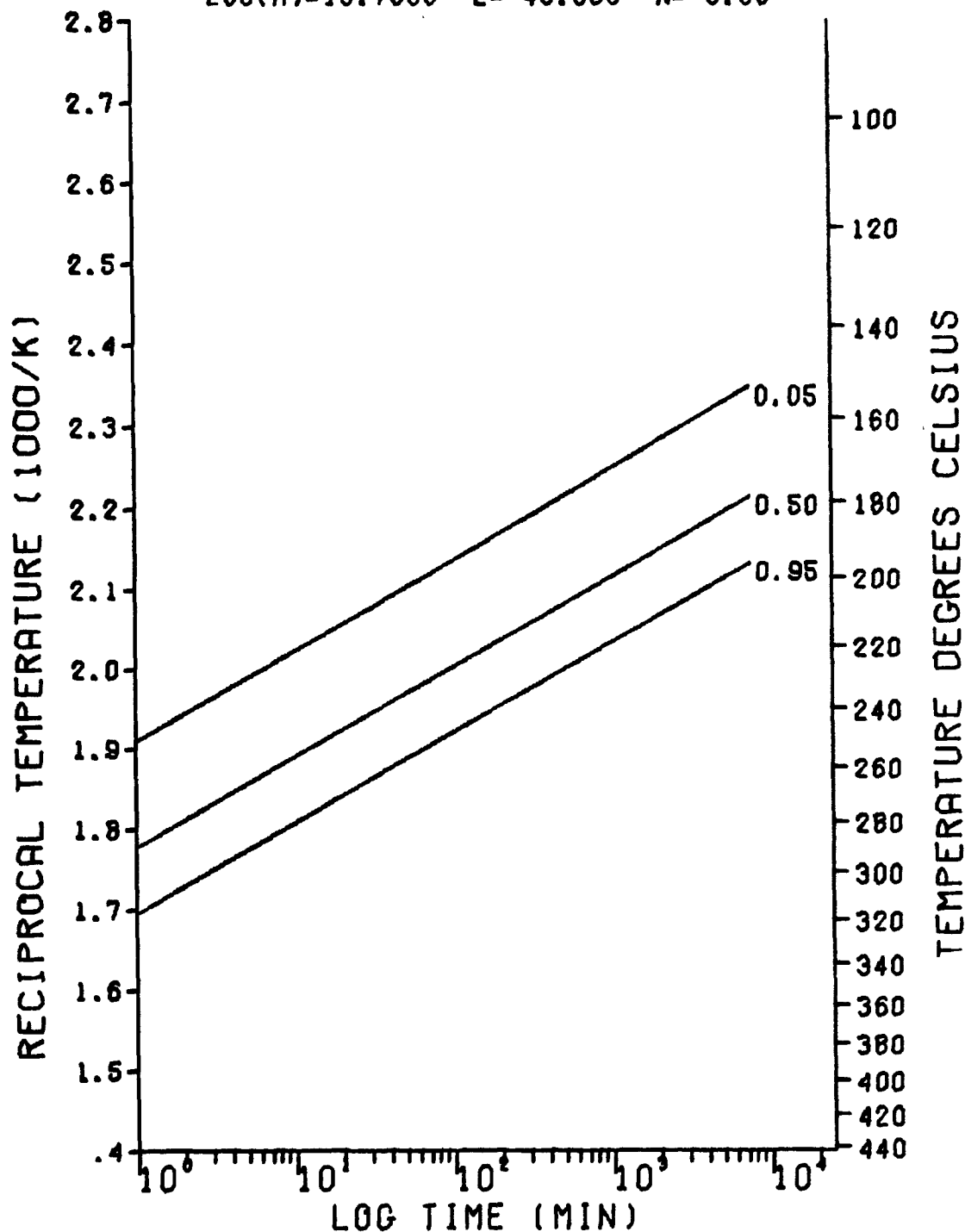


Figure 15. Ideal Processing Window for PATS X-27
(n= 0.00).

REACTION WINDOW PLOT
 SAMPLE: GD-37 RUN-2 CUT 3 78.16 28 SEP
 KINETIC METHOD: FRIEDMAN'S MULTI-SCAN
 LOG(A)=8.6161 E= 24.736 N= 0.55

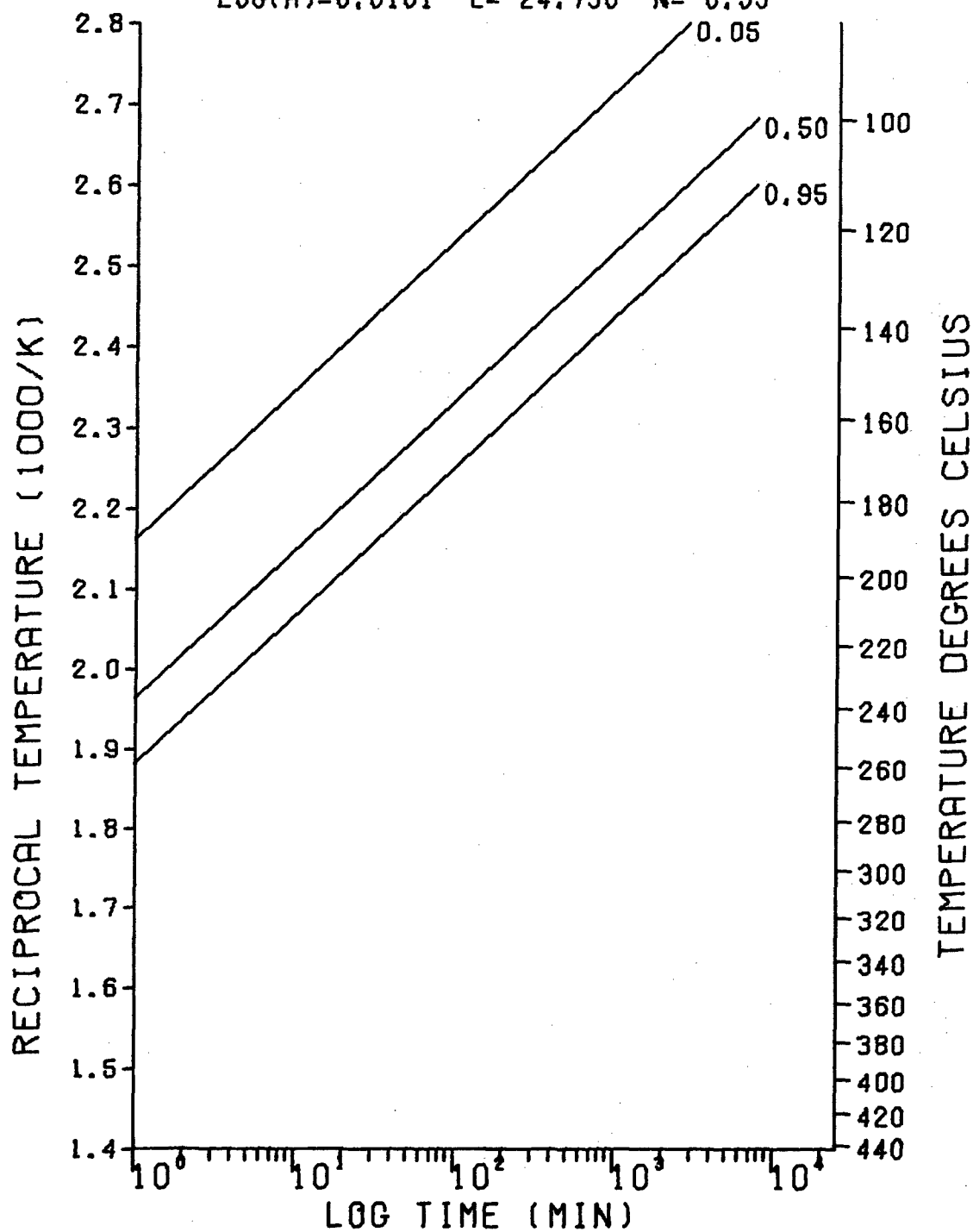


Figure 16. Ideal Processing Window for GD-37
 Run-2 Cut 3 ($n=0.55$).

REACTION WINDOW PLOT
 SAMPLE: GD-37 RUN-2 CUT 3 78.16 28 SEP
 KINETIC METHOD: FRIEDMAN'S MULTI-SCAN
 LOG(A)=8.6161 E= 24.736 N= 0.00

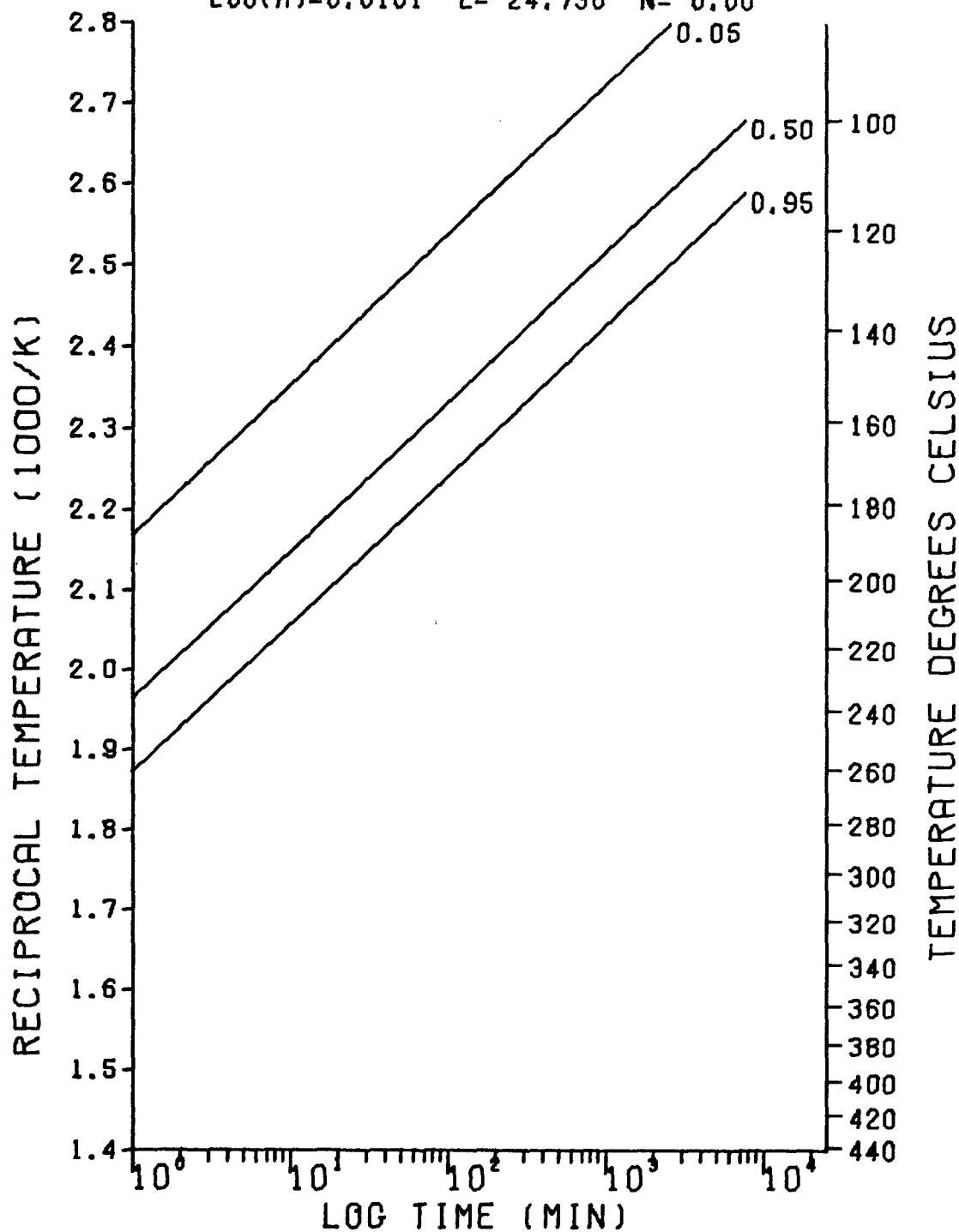


Figure 17. Ideal Processing Window for GD-37 Run-2 Cut 3 ($n=0.00$).

REACTION WINDOW PLOT
 SAMPLE: ATQ-BN-17B (79.2.3.15)
 KINETIC METHOD: FRIEDMAN'S MULTI-SCAN
 LOG(A)=4.3280 E= 16.274 N= 0.86

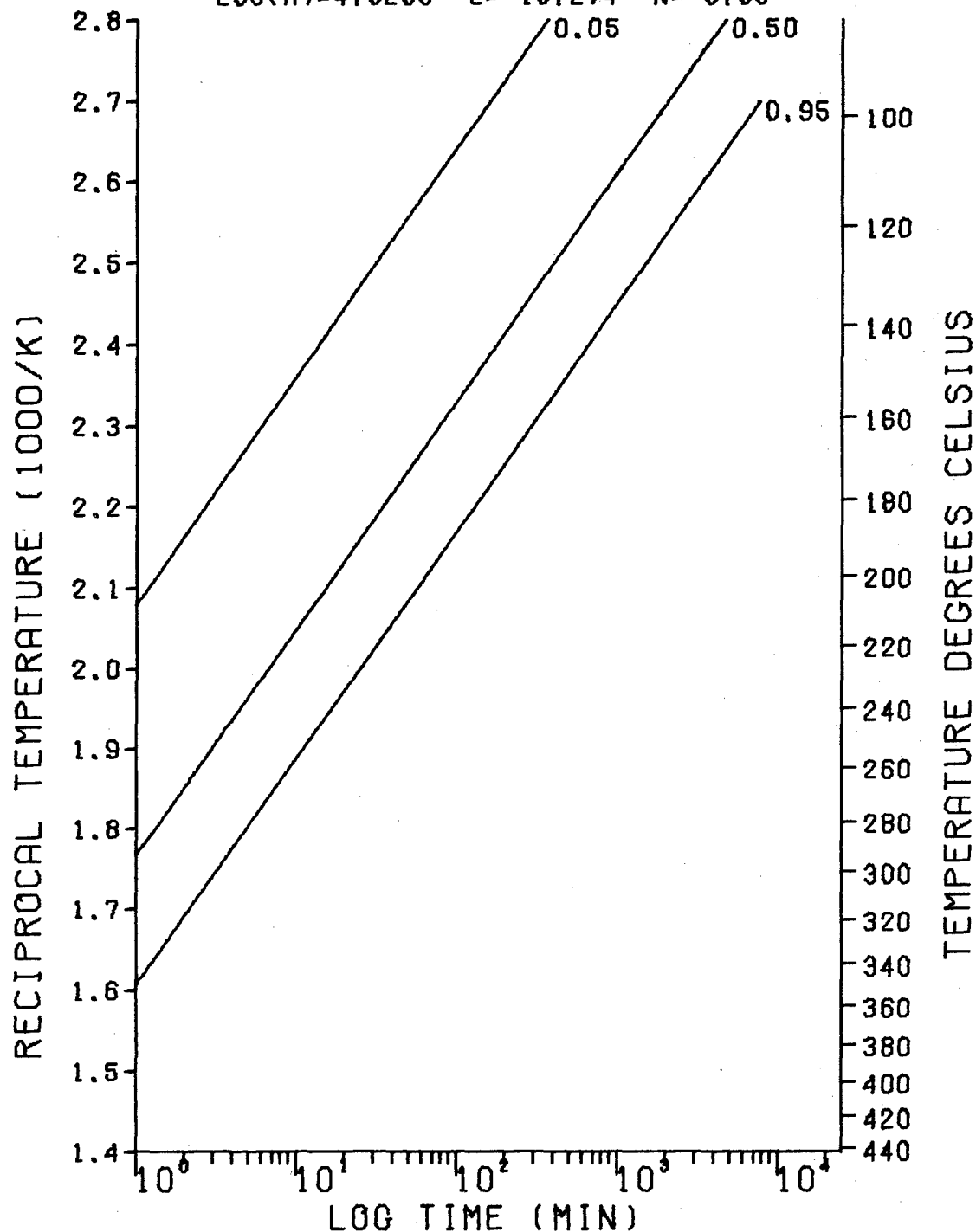


Figure 18. Ideal Processing Window for ATQ-BN-17B (n= 0.86).

REACTION WINDOW PLOT
 SAMPLE: ATQ-BN-17B (79.2.3.15)
 KINETIC METHOD: FRIEDMAN'S MULTI-SCAN
 LOG(A)=4.3280 E= 16.274 N= 0.00

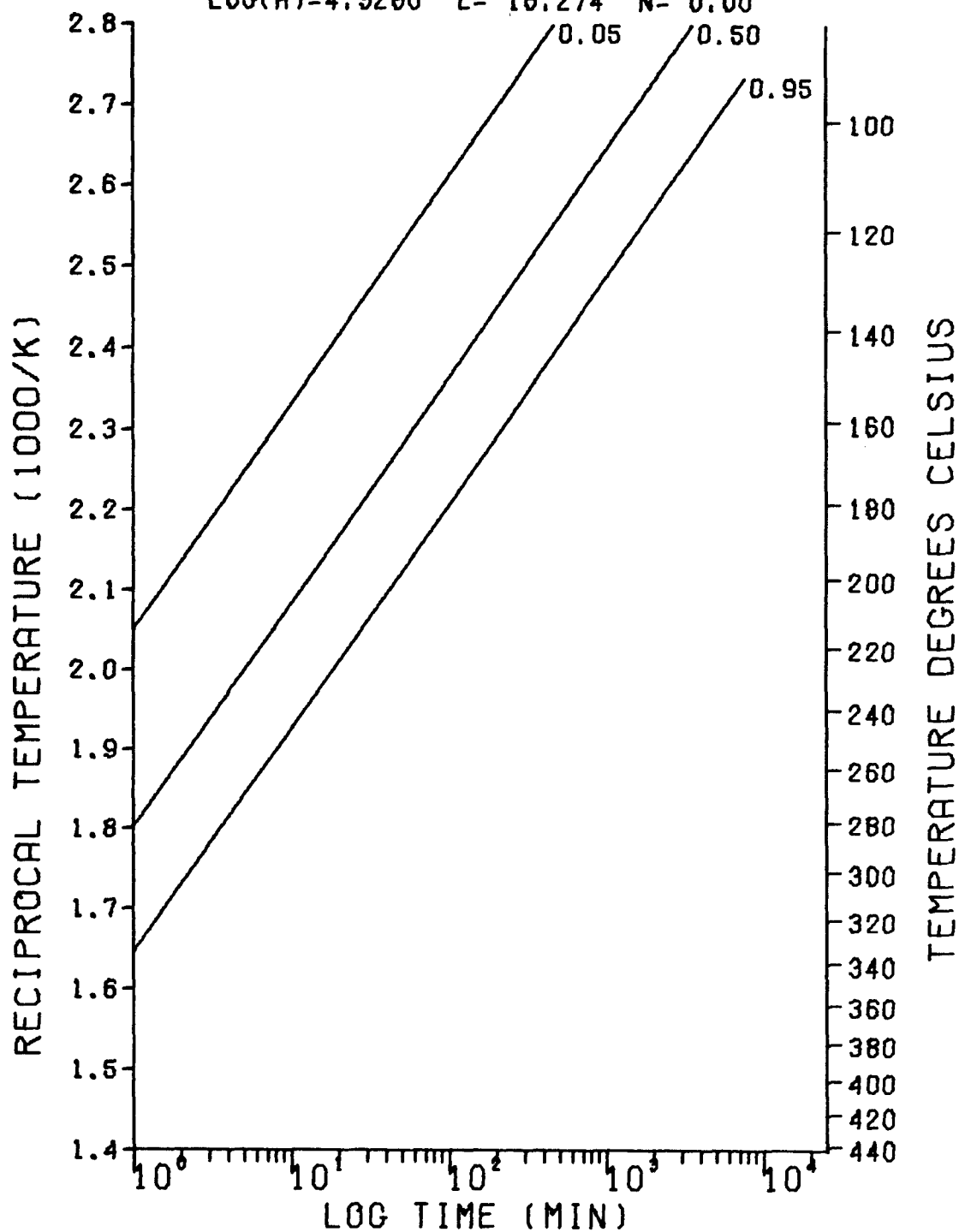


Figure 19. Ideal Processing Window for ATQ-BN-17B
 ($n= 0.00$).

REACTION WINDOW PLOT
 SAMPLE: ATQ-BN-17A (79.3.3.16)
 KINETIC METHOD: FRIEDMAN'S MULTI-SCAN
 $\text{LOG}(A)=4.8990$ $E=17.474$ $N=0.69$

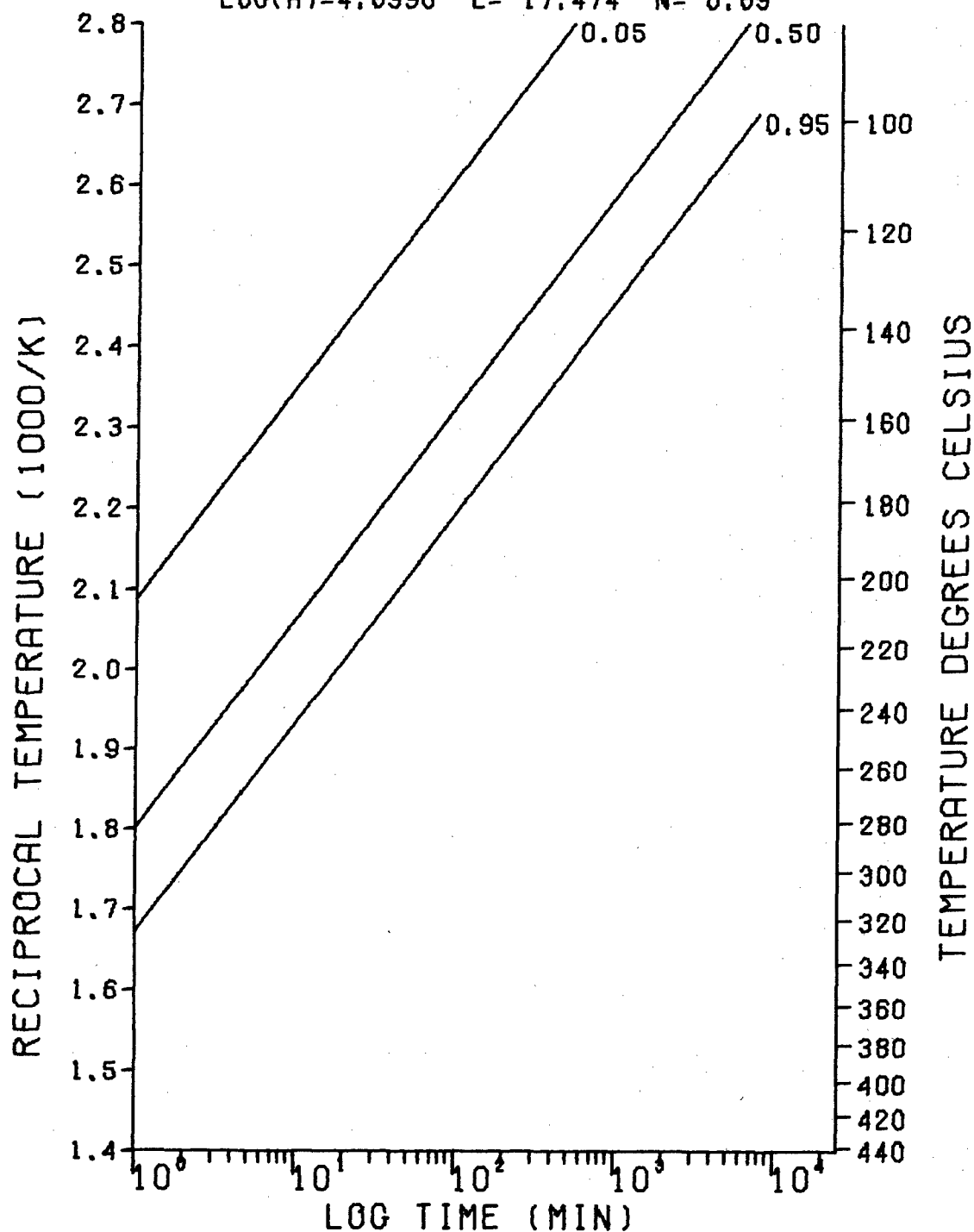


Figure 20. Ideal Processing Window for ATQ-BN-17A
 ($n=0.69$).

REACTION WINDOW PLOT
 SAMPLE: ATQ-BN-17A (79.3.3.16)
 KINETIC METHOD: FRIEDMAN'S MULTI-SCAN
 LOG(A)=4.8990 E= 17.474 N= 0.00

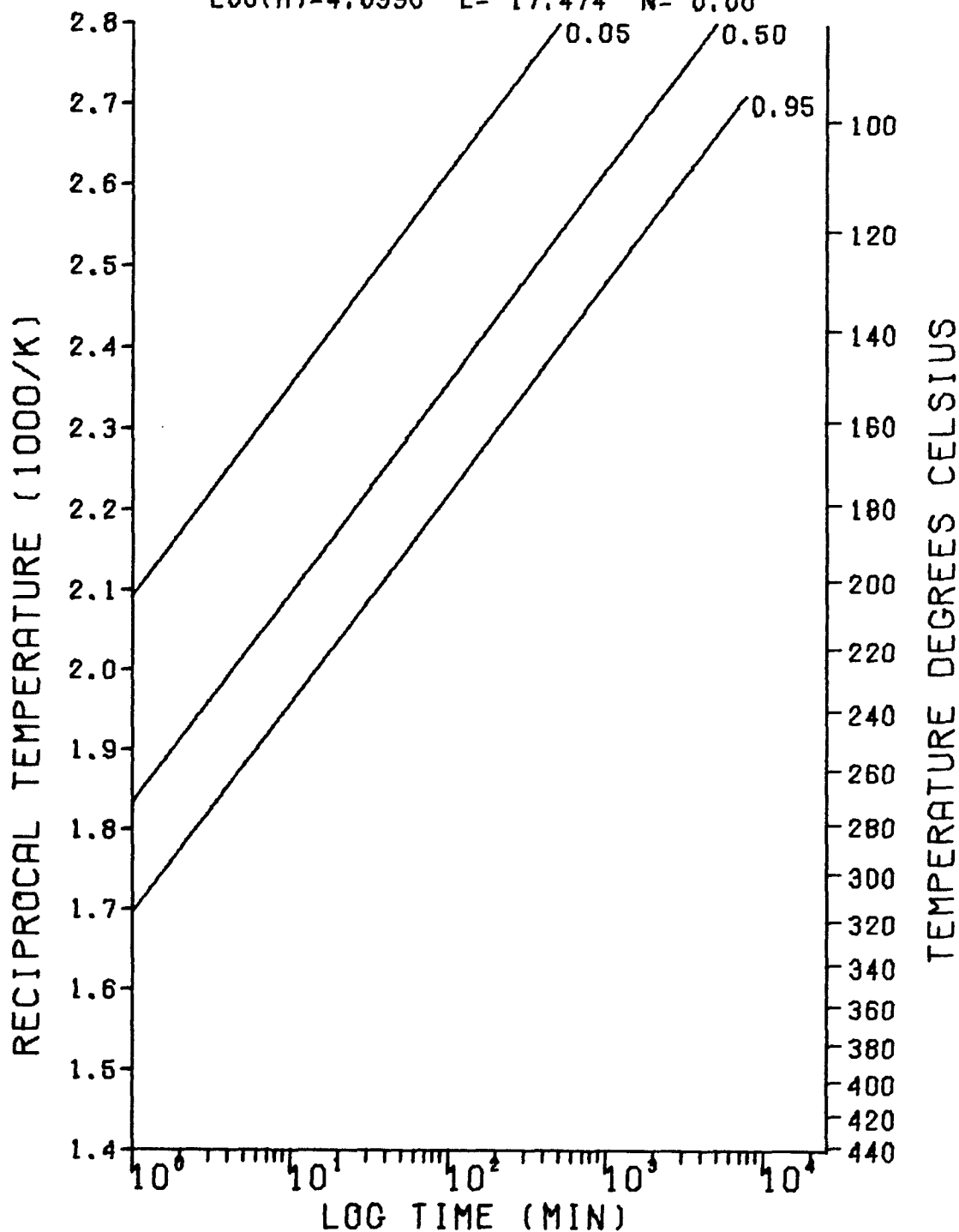


Figure 21. Ideal Processing Window for ATQ-BN-17A
 ($n= 0.00$).

REACTION WINDOW PLOT
 SAMPLE: AA-BA-BN-13A (79.4.3.20)
 KINETIC METHOD: FRIEDMAN'S MULTI-SCAN
 LOG(A)=7.2650 E= 22.642 N= 0.64

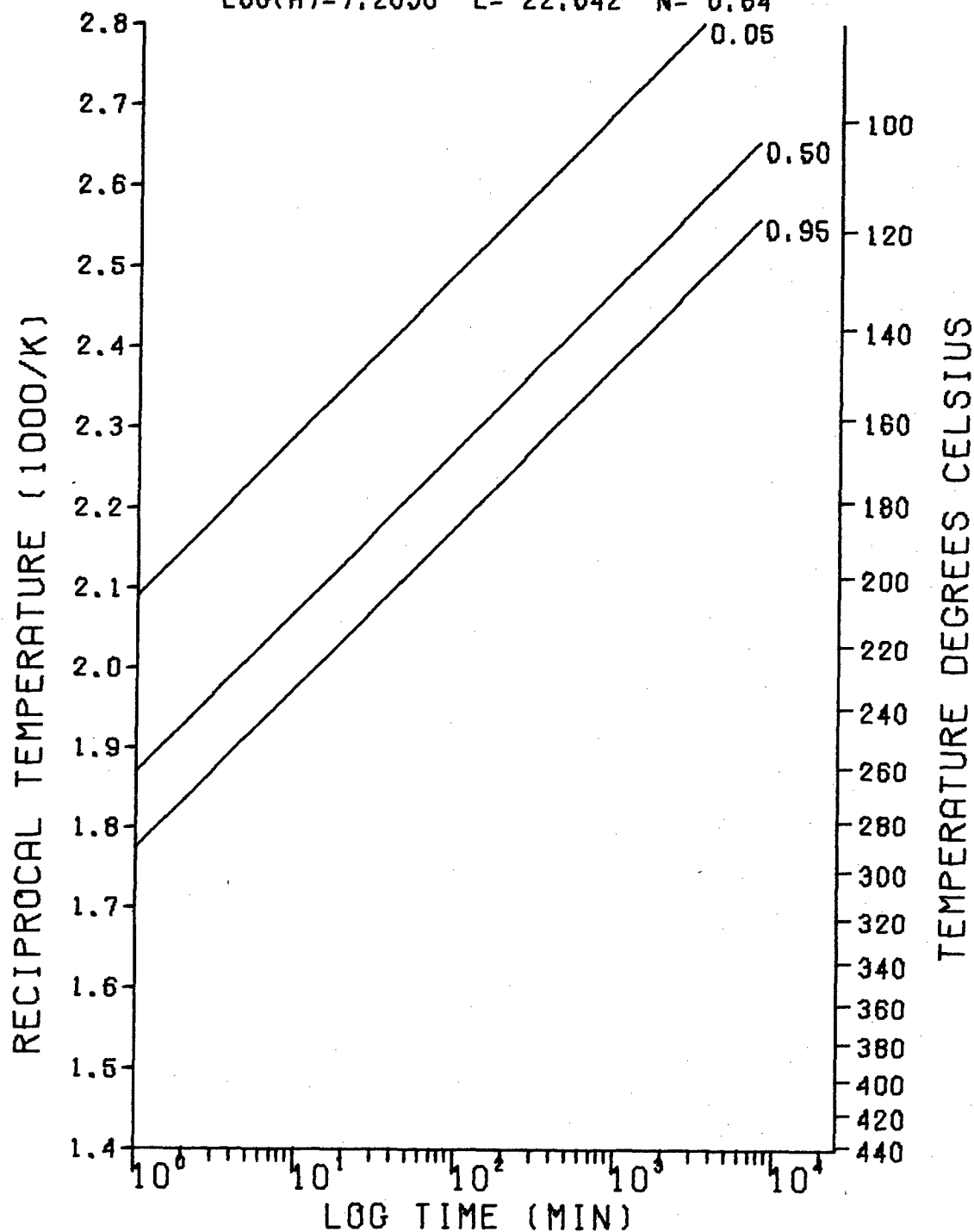


Figure 22. Ideal Processing Window for AA-BA-BN-13A (n= 0.64).

REACTION WINDOW PLOT
 SAMPLE: AA-BA-BN-13A (79.4.3.20)
 KINETIC METHOD: FRIEDMAN'S MULTI-SCAN
 LOG(A)=7.2650 E= 22.642 N= 0.00

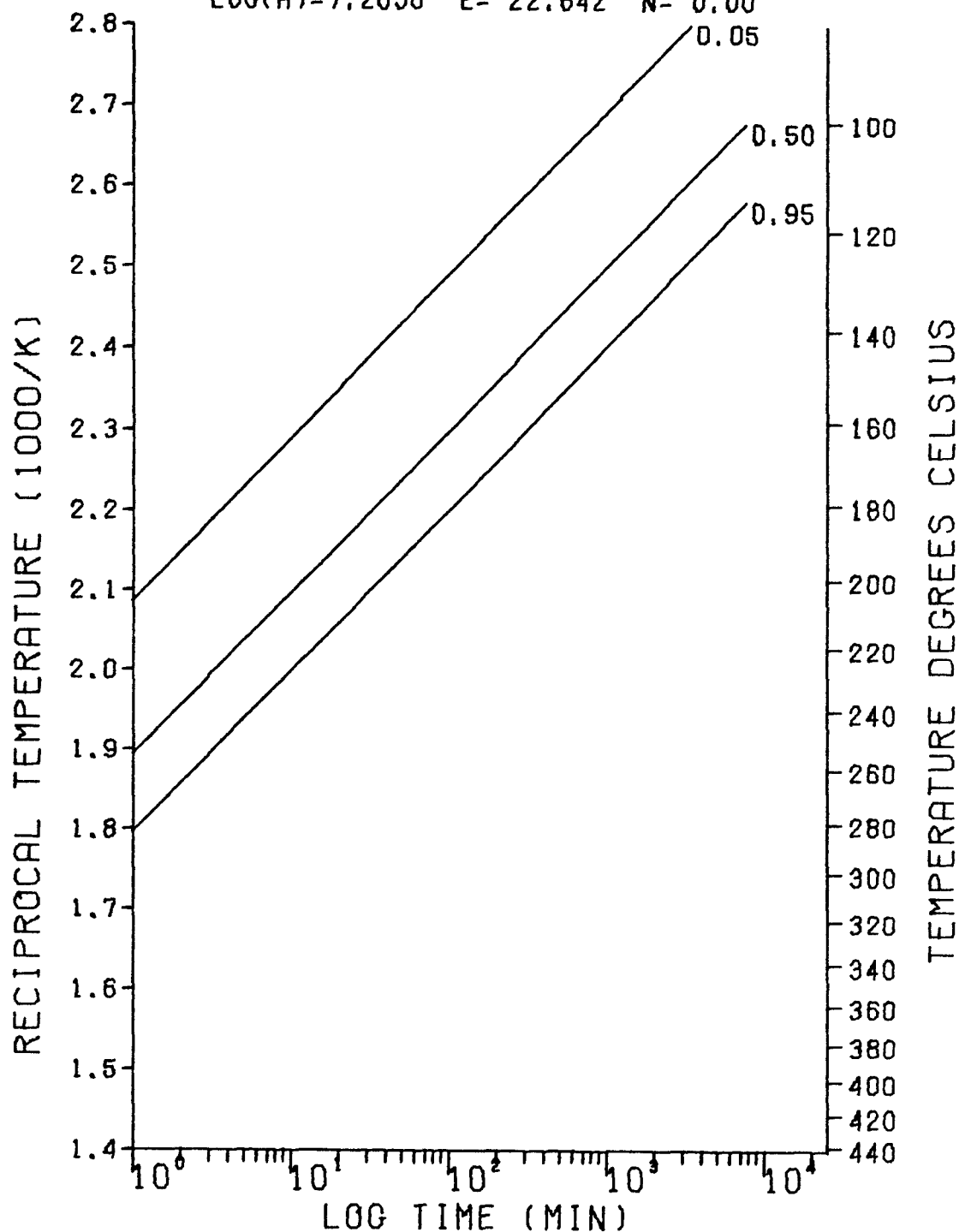


Figure 23. Ideal Processing Window for AA-BA-BN-13A (n= 0.00).

REACTION WINDOW PLOT
 SAMPLE: BA-DAB-BA (FLH-335-160-1) 79.5
 KINETIC METHOD: FRIEDMAN'S MULTI-SCAN
 LOG(A)=5.9880 E= 19.770 N= 0.00

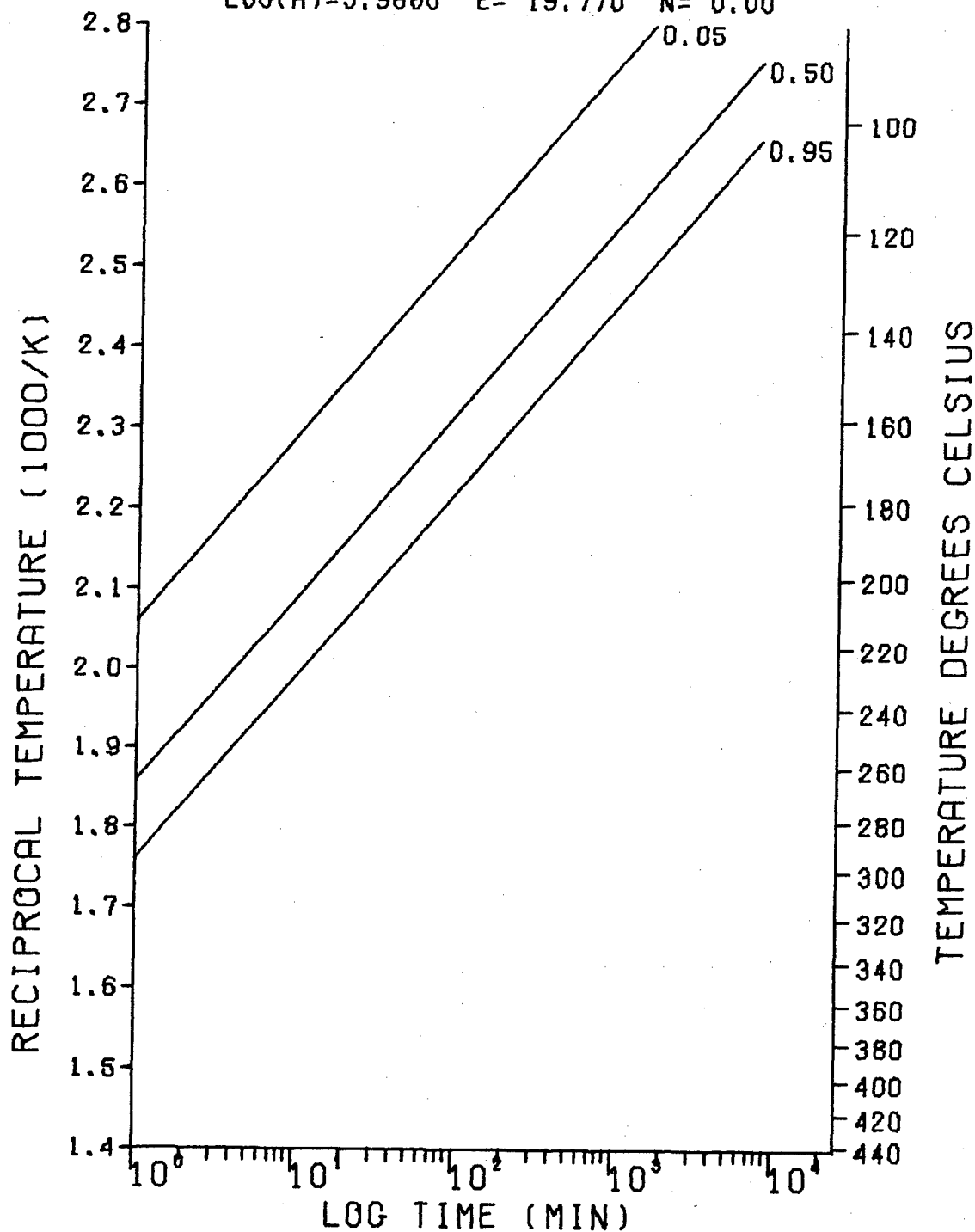


Figure 24. Ideal Processing Window for BA-DAB-BA (FHL-335-160-1) (n= 0.00).

REACTION WINDOW PLOT
 SAMPLE: BA-DAB-BA (FLH-335-160-1) 79.5
 KINETIC METHOD: FRIEDMAN'S MULTI-SCAN
 LOG(A)=5.9880 E= 19.770 N= 0.34

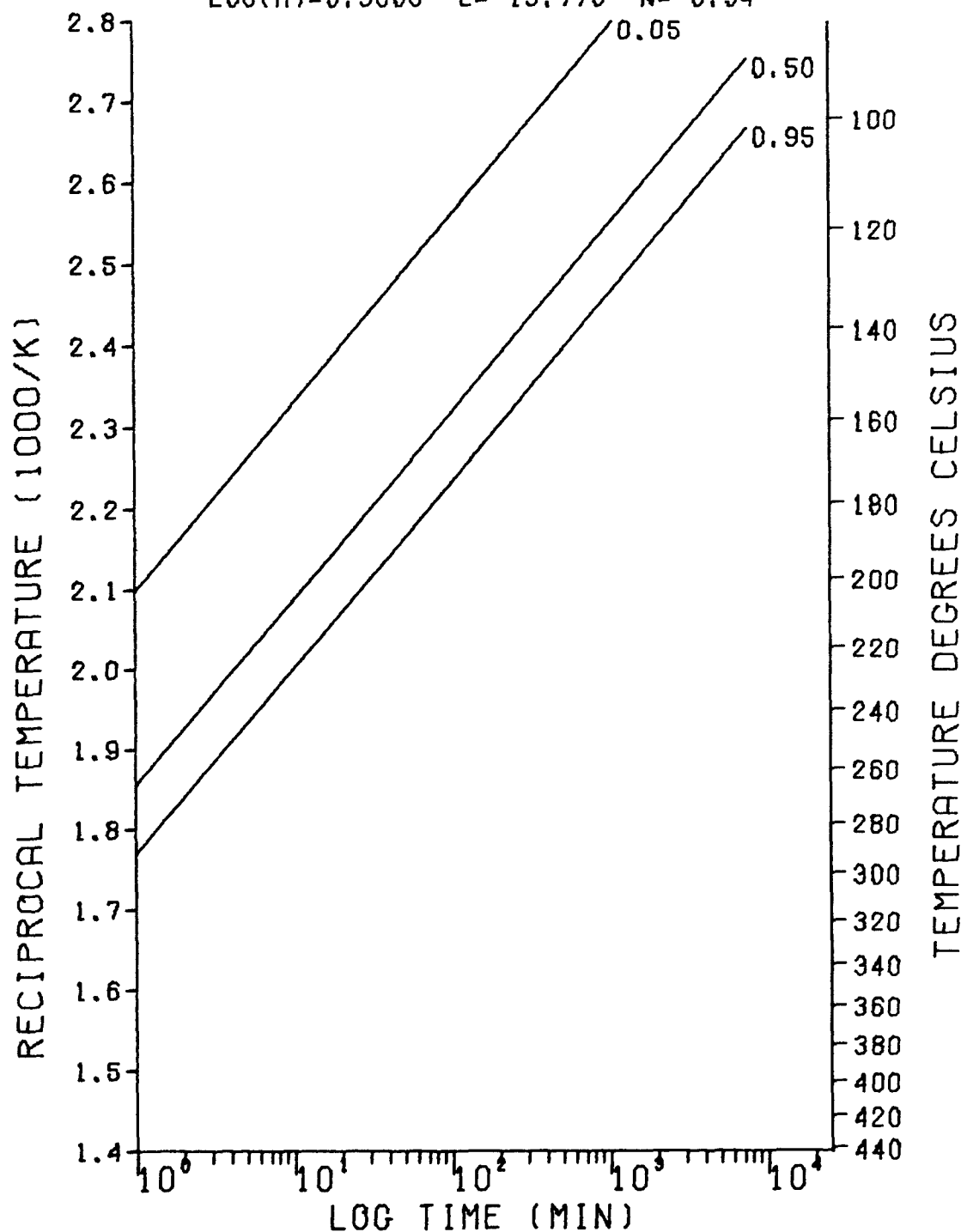


Figure 25. Ideal Processing Window for BA-DAB-BA (FLH-335-160-1) (n= 0.34).

rheology of the same specimen through the various states of matter.³ The full understanding of the cure behavior awaits further experimental work on the technique.

(4) Epoxy

A cure phase diagram of an epoxy system has been constructed with TICA measurements. Experiments have shown that further curing during thermal scan of a partially cured specimen is not negligible.⁴ The thermal scan behavior of the partially cured specimen was analyzed with the time derivative function of the expression $(T-T_g)$.

(5) Intramolecular Cyclization (IMC) System

The two thermoset resins, BA-DAB-BA and BA-DABA-BA, were used to test the feasibility of curing in the glassy state with proper engineering of the chemical structures. The intrinsic cured T_g of the BA-DAB-BA system at 200°C (392°F) cure was estimated from experimental results to be about 260°C (500°F). Similar experiments are currently in progress using BA-DABA-BA.

F. Inferring Relaxation Spectra (D. Wiff and C. Lee)

The approach toward inferring a mechanical relaxation spectrum from relaxation modulus, loss modulus, or storage modulus master curve data used by this laboratory has been to apply the regularization quadratic programming (RQP) technique.⁵ This technique performs the inverse transformation of the Fredholm integral equation of the first kind

$$u(\omega) = \int_{\tau_1}^{\tau_2} K(\omega, \tau) f(\tau) d\tau \quad (12)$$

where $u(\omega)$ are the experimentally determined data, $K(\omega, \tau)$ is the appropriate kernel, $f(\tau)$ is the sought after relaxation spectrum, and $f(\tau)$ is bounded i.e., for $\tau \geq \tau_2$ and $\tau \leq \tau_1$, $f(\tau)=0$. The usual

technique used in determining the spectral distribution $f(\tau)$ would be to minimize

$$N \left[f(\tau), \bar{u}(\omega) \right] = \int \left[u(\omega) - \bar{u}(\omega) \right]^2 d\omega \quad (13)$$

where $\bar{u}(\omega)$ is the "true" experimental data containing error

$$\bar{u}(\omega) = u(\omega) + \epsilon$$

This least squares approach usually yields a reliable spectral distribution $f(\tau)$. However, given an appropriate kernel, the inverse transformation operating on the experimental set $\bar{u}(\omega)$ can produce a wildly fluctuating distribution $f(\tau)$. This happens because $\bar{u}(\omega)$ contains error and computational techniques cause the functional space containing $f(\tau)$ to shift to a functional space which yields a fluctuating spectrum. One way to handle and/or control this numerical problem is to introduce a regularization term. One now minimizes

$$M^\alpha \left[f(\tau), \bar{u}(\omega) \right] = N \left[f(\tau), \bar{u}(\omega) \right] + \Omega \left[f(\tau) \right] \quad (14)$$

where $\Omega^\alpha \left[f(\tau) \right]$ is the regularizing term.

$$\Omega^\alpha \left[f(\tau) \right] = \sum_n \alpha_n \int \left[\frac{d^n f(\tau)}{d\tau^n} \right]^2 d\tau \quad (15)$$

Usually $n=1$ or 2 , and one term is quite sufficient. Applying this technique to master curve data obtained from the rheometrics mechanical spectrometer has resulted in relaxation spectra whose envelopes give expected results, but sporadically throughout the spectra there are points which are zero. (Figure 26)

Computationally this can be controlled by putting constraints on the differences $\Delta[f(\tau)]$ between adjacent points. However, before doing this, the RQP algorithm and various

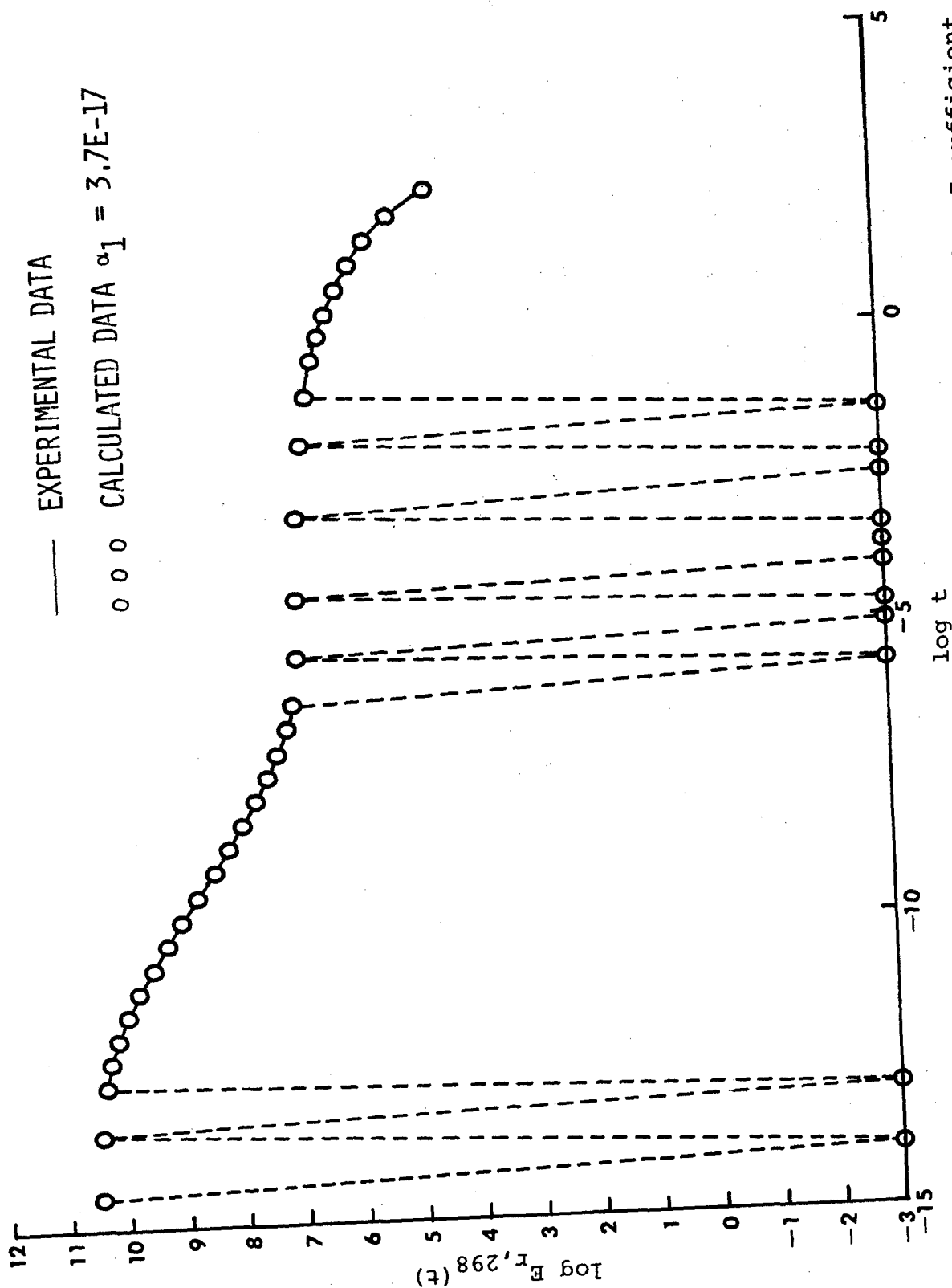
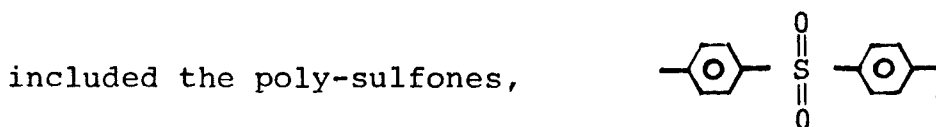


Figure 26. A Typical Relaxation Spectrum which may be Inferred when Insufficient Numerical Analysis Techniques are Used. Present techniques eliminate these discontinuities.

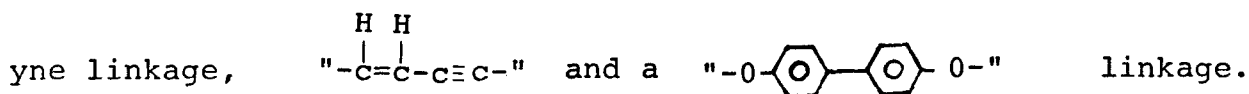
integration approximations used are being investigated. Also the criterion used for choosing the appropriate $f(\tau)$ might be under question. We have treated the problem such that mapping $f(\tau)$ onto the space containing $u(\omega)$ is a mathematically well posed problem and that the inverse operation, i.e., mapping $u(\omega)$ onto $f(\tau)$ is a mathematically ill-posed problem. This is an important point since if $\bar{f}(\tau)$ maps to $\bar{u}(\omega)$, then the inferred distribution $\tilde{f}^\alpha(\tau)$ will map to $\tilde{u}(\omega)$. If we knew $\bar{f}(\tau)$ we could compare it with $\tilde{f}^\alpha(\tau)$, however all we have is the experimental set of values $\{\bar{u}(\omega)\}$. In order to obtain the best $\tilde{f}^\alpha(\tau)$ we have used that spectrum in correspondence with the minimum of the variance, $\{|\bar{u}_i(\omega) - \tilde{u}_i(\omega)|/\bar{u}_i(\omega)\}$. Other such criterion are presently being investigated.

G. Characterization by Thermal Methods (E. Soloski)

One of the areas of research currently under investigation is of thermoplastic materials. Within this group are



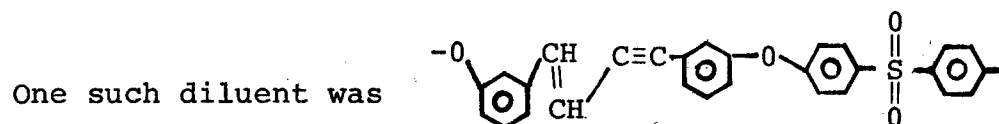
To this basic diphenyl sulfone, desirable thermal characteristic compounds can be achieved by adding various chemical moieties which have been incorporated into this backbone and ene-



By increasing the ratio of $\text{-O-}\langle\text{benzene ring}\rangle\text{-O-}$ to $\text{-C=C-C}\equiv\text{C-}$ from 1:1 to 9:1, not only is there an increase in the polymerization temperature, but more importantly, there is a glass transition T_g after cure, $T_{g\infty}$.

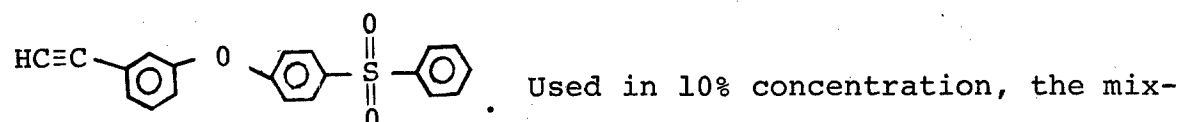
Several samples with Radel-like structures were received. Since Radel has a glass transition above 225°C (437°F), diluents have been added in an attempt to make the material

processable at lower temperatures, i.e., lower the effective T_g .



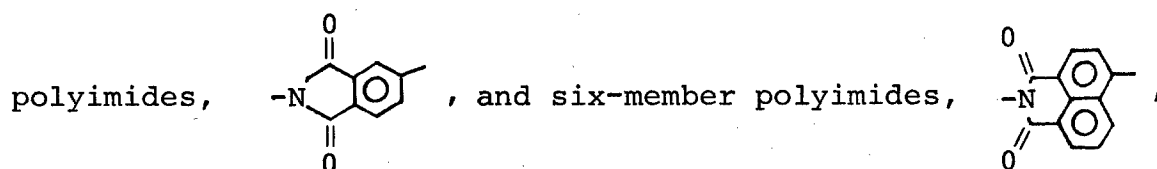
In one sample the concentration of diluent was 15%, in the other 35%. The polymerization peak temperatures were similar, 342°C (647°F) (35%) and 369°C (696°F) (15%), and as we expected, the glass transition temperatures of the cured materials showed a higher T_g for the 35% compound (257°C , 495°F) compared to the 15% compound (227°C , 441°F). This is probably due to the increased stiffness resulting from cycloaddition and/or crosslinking of the ene-yne moiety.

Another diluent which was added to the Radel was



exhibited a T_g (180°C , 356°F) only after previously being heated to 325°C (617°F). The components do not appear compatible and the lowering of T_g may be due simply to dilution.

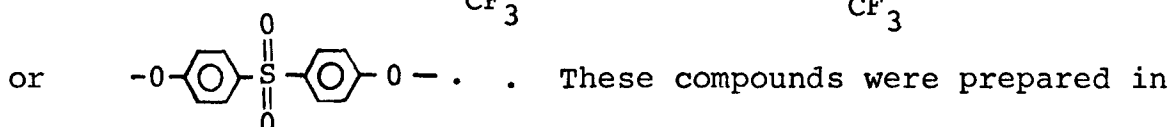
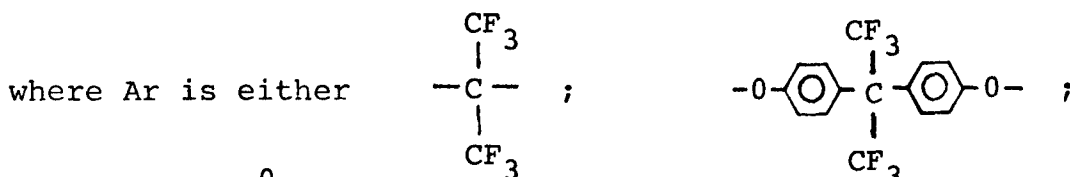
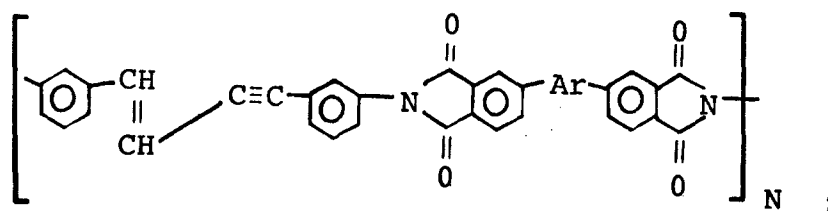
The polyimides comprise another classification of compounds receiving a great deal of attention. Both five-member



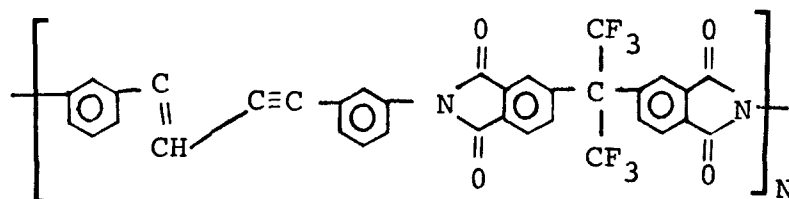
were investigated. The six-member polyimides exhibit limited solubility, therefore, most of our studies were on the five-member systems.

As with the polysulfones, several polyimides containing ene-yne linkages in the backbone were compared. Structurally

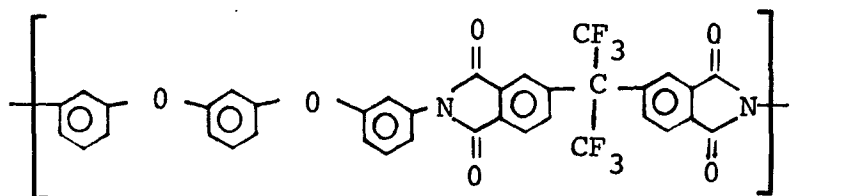
these compounds are:



hopes of widening the processing window of the polyimides. Since the glass transition and the onset of polymerization are so close [e.g., $T_g = 212^\circ\text{C}$ (414°F) and onset of T_g is at 255°C (491°F)] , an expanded window is necessary for material processing. Also received were two samples in which the ene-yne linkage in the repeat unit



was incorporated into the backbone of the polyimide

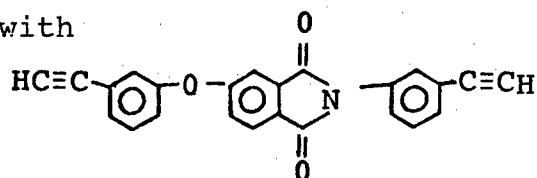


The samples contained 25% and 50% of the ene-yne segment or unit. DSC studies show a lower initial T_g in the 25% sample [208°C (406°F) versus 222°C (432°F)]. Due to the cycloaddition

and/or crosslinking during polymerization, the 50% sample has a higher T_g in the cure material [270°C (518°F) versus 229°C (444°F)].

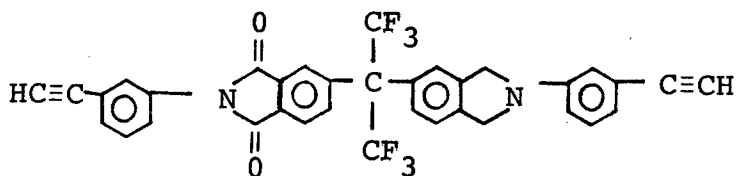
Another effort in attempting to understand the problem of processing difficulties in curing polyimides led us to look at a therimide containing 20% ATS. It was hoped the ATS would provide the operating window therimide alone did not possess. DSC measurements showed that the two materials are not compatible unless sufficient heat is applied. With the addition of heat more and more ATS tends to mix with the therimide ultimately resulting in a single phase system.

Therimide was also mixed with



This sample containing 30% plasticizer also appears counter-productive. Even though the components are compatible, the combination increases the T_g of the uncured material with little change in the polymerization temperature (T_{poly}). The result was a narrower processing window than for pure therimide.

The exact mechanism by which acetylene terminated monomers react is not fully understood. In an attempt to better understand this,

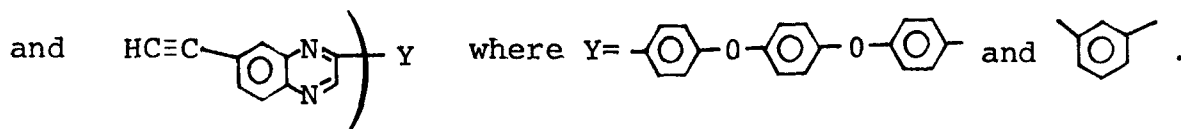
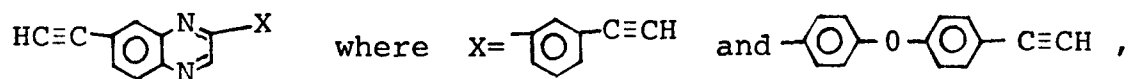


was prepared. This crystalline material has a $T_m \approx 211^{\circ}\text{C}$ (411°F) and upon completion of its melt immediately starts its polymerization with $T_{\text{poly}} \approx 231^{\circ}\text{C}$ (448°F). This material is being heated (polymerized) and later hydrolyzed to cleave the N-C bonds. The products of "end-group" reaction will be isolated and characterized thus providing a better understanding of the acetylene cure mechanism.

The polyquinoxalines comprise a portion of the thermosetting resins. Their development has proceeded along two similar courses: one consisting of quinoxaline molecules containing terminal acetylene groups, (BA-DAB-BA; see sections B, D, and E) and the other consisting of quinoxaline molecules containing terminal acetylene groups plus pendant phenyl-acetylene groups. These phenyl-acetylene groups can undergo intramolecular cycloaddition (IMC) (BA-DABA-BA; see sections B, D, and E).

While looking for the processing window of these compounds, the question was raised as to whether or not these materials were completely cured. Transitions on the DSC curves noted in earlier studies, and at that time considered glass transitions of fully cured materials, may be transitions in materials possessing only partial cure. Additional studies are underway to clarify these doubts.

Several quinoxaline monomers of low molecular weight were received and characterized. These were prepared so that we could observe changes in thermal characteristics brought on by small changes in chemical structure. These monomers are:



As might be expected, the first two monomers showed T_g of 20°C (68°F) and 33°C (91°F). The third monomer, however, showed no glass transition while the polymerization peaks of all three ranged around 250°C (482°F) - near that of the polyquinoxalines.

The fourth compound had a glass transition at 96°C (205°F) while its polymerization peak was at 215°C (419°F). Curing for six hours at 215°C (419°F), however, did not

produce complete cure. Although this material was looked at as a 371°C (700°F) use temperature material, isothermal aging at that temperature showed 100% weight loss after 100 hours. Isothermal aging repeated at 316°C (600°F) showed 52% material remaining after 200 hours. More studies of the first three monomers are needed before final evaluation of these materials can be made.

H. Solution Thermodynamics (C. Benner)

(1) Intrinsic Viscosity

Intrinsic viscosity measurements were made on various samples of polysulfone and polyimide in N,N'-Dimethylacetamide (DMAC) at 30°C (86°F). The solutions were prepared by weighing the polymers into tared flasks and adding 15 milliliters (.916 cu in) of DMAC. The flasks containing the solution were reweighed and the concentration calculated in gms solute/100 gms (3.53 oz) of solution. The concentration was converted to the needed gms/dl by multiplying by the density of solvent. The solutions were pipetted into a size 75 Cannon - Ubbelohde dilution viscometer and diluted successively with solvent after obtaining several flow times for each concentration. The flow times for the solvent and four concentrations of each solution were obtained with a stopwatch. The data were reduced to η_{sp}/C and $\ln(\eta_{sp}/C)$ and plotted versus concentration. After plotting the data, the plot was extrapolated to zero concentration to get the intrinsic viscosity. The results are shown in Table 3.

TABLE 3
INTRINSIC VISCOSITY

SAMPLE	$[\eta]$ (dl/gm) (cu ft/lb)
Polysulfone P1700 CB-5 F2	0.50 (0.80)
" BR-1-81	0.44 (0.71)
" BR-1-82	0.61 (0.98)

TABLE 3 (Concluded)
INTRINSIC VISCOSITY

SAMPLE		η (dl/gm) (cu ft/lb)
Polysulfone	BR-2-17	0.28 (0.44)
"	BR-2-22	0.62 (1.00)
Polyimide	BR-2-14	0.51 (0.82)
"	BR-2-15	0.35 (0.56)
"	BR-2-21	0.46 (0.73)
"	BR-2-30	0.42 (0.67)
"	BR-3-1	0.70 (1.12)

(2) Radel Fractionation

A sample of Radel polyphenylsulfone was fractionated to provide samples of varying molecular weight for use in the reactive plasticizer research. Five grams (.176 oz) of Radel were dissolved in 500 milliliters (30.5 cu in) of DMAC. Enough methanol was added to bring the solution to the point of turbidity (87 ml, 5.31 cu in). Some of the sample precipitated and could not be redissolved by either raising or lowering the temperature. An additional 470 ml (28.7 cu in) of DMAC were added, but the precipitated sample would not redissolve. Next 100 ml (6.10 cu in) of the nonsolvent (methanol) were removed by vacuum distillation. When the precipitated sample still did not redissolve, it was removed by filtration through a 5 micron teflon filter. Additional methanol was added and the resulting precipitate was removed again by filtration. The process was repeated to obtain a third fraction. The remaining polymer was recovered by vacuum distillation of the DMAC-methanol mixture. The fractions were dried at 120°C (248°F) under vacuum. The weight of each fraction is given in Table 4.

TABLE 4
RADEL FRACTIONS

Fraction	Weight (grams) (oz)
1	1.42 (0.050)
2	2.11 (0.074)
3	0.99 (0.035)
4	0.10 (0.0035)

(3) Number Average Molecular Weight

The number average molecular weight was determined for the polysulfone Pl700 fractions by osmometry. The measurements were made in DMAC at 37°C (98.6 °F). Solutions were prepared by dissolving the appropriate concentration of sample in 10 ml (.611 cu in) of solvent. After a reference solvent value had been determined, the osmometer sample stock was filled with solution by drawing three 0.2 ml (.012 cu in) portions of solution through it and drawing a fourth one down to the etch mark for the measurement. The data were reduced to π/C and plotted versus concentration. The plot was extrapolated to zero concentration. The number average molecular weight is calculated from:

$$(\pi/C)_{c=0} = \frac{RT}{M_n}$$

where R is the Universal gas constant and T the temperature in degrees Kelvin. Results are given in Table 5.

TABLE 5
NUMBER AVERAGE MOLECULAR WEIGHT

Fraction	Mn
CB5-F1	50,000
CB5-F2	46,000
CB5-F3	33,000

SECTION II

ORDERED POLYMERS

1. INTRODUCTION

The ordered polymers task was initially involved with the use of x-ray diffraction (XRD) in texture analysis studies of fibers or films and model compound studies. The fiber studies were performed on PBO and PBT rigid-rod polymer fibers processed at Carnegie-Mellon University and then at Celanese Research Corporation. Our contractual effort is one part of the larger U. S. Air Force - Ordered Polymer Research (OPR) program. Therefore, when early in the present contract period we were directed to work totally on rigid-rod/flexible coil (RRFC) aromatic heterocyclic polymer blends, the fiber texture analysis thrust was terminated. Presently, one area of research involves the study of various model compounds leading to inter and intramolecular bonding distances and angles. This, it is anticipated, will aid other contractors working in the OPR program to better understand their results in light of these measured molecular structure parameters and molecular packing in the crystalline state. These molecular parameters will be used to theoretically predict XRD patterns and relate selected diffraction planes to those detected in RRFC blends.

Another area of research applied using XRD techniques involves plotting of polefigures. Once specific diffraction planes are found to have their orientation vary significantly with the mechanical properties and with the percentage composition of blends, these planes will be mapped onto a two dimensional stereo projection of the reflection sphere. Each specimen having specific mechanical properties will have an associated unique polefigure plot of the distribution of these diffraction planes.

The preparation of polymer blends for this study has involved casting and precipitation techniques using methane sulfonic acid (MSA) as the solvent. To date, mechanical properties comparable with glass-filled composites have been obtained. These measured values closely follow the predictions one would expect by extrapolating chopped fiber composite theories to these molecular level composites.

In order to allow for more efficient packing of the rigid-rod polymers, swivels have been added to the PBO polymer backbone. The synthesis, XRD studies, and mechanical properties of these copolymers are briefly discussed within this report.

2. EXPERIMENTAL AND RESULTS

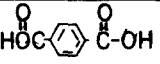
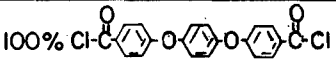
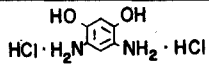

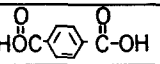
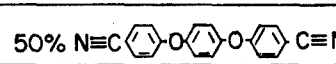
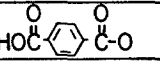
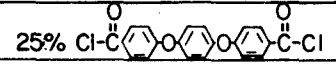
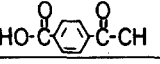
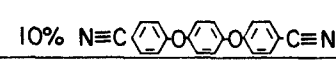
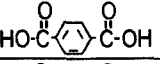
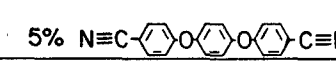
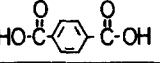
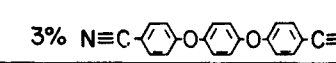
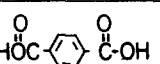
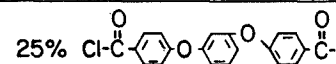
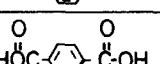
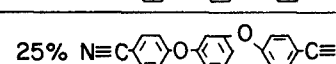
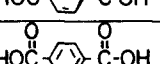
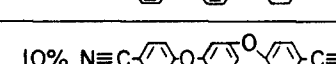
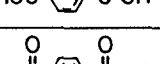
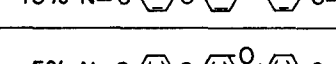
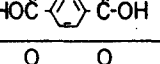
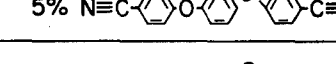
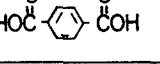
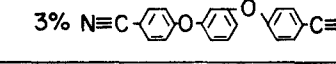
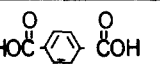
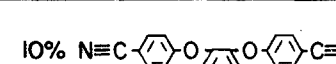
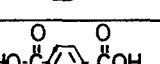
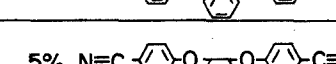
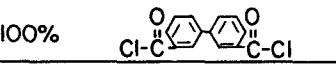
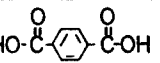
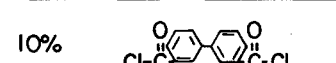
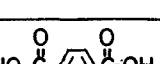
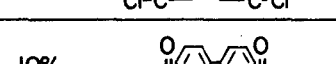
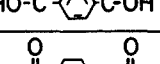
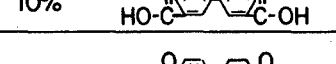
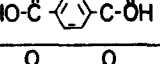
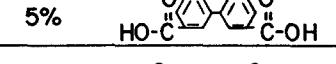
A. Articulated PBO and Model Compound Synthesis (J. Burkett)

The objective of this program was to improve the physical properties of para-ordered polybenzoxazole (PBO) polymers by synthesizing new chemical variations on the basic PBO polymer backbone structure. The modulus of 100% para-ordered PBO polymer is excellent but to process a desirable product, the polymer has to have high molecular weight. In addition, cast films of the polymer must have high modulus and high tensile strength. Para-ordered polybenzoxazoles have high modulus but cannot be cast to films and have low tensile strength because of low molecular weight and inability to easily assume conformational changes. A flexible unit within the polymer chain was used with the hope it would improve molecular weight, improve solubility and increase molecular flexibility, thus enabling films to be cast which are not brittle such that they crumble and fall apart. Table 6 presents the monomer synthesis performed during this year and the model compounds synthesized. Table 7 shows the copolymers data. Model compounds were prepared for x-ray studies and were given to Dr. D. R. Wiff and Dr. A. V. Fratini to evaluate. Copolymers were given to C. Benner who cast films and measured their modulus and tensile strengths.

TABLE 6
SYNTHESIZED ARTICULATED PBO MONOMERS AND MODEL COMPOUNDS

	+ HCl	→		H ₂ N-Br-	· HCl	
HCl · H ₂ N-Br-	NH ₂ · HCl + NaNO ₂ + H ₃ PO ₂	→		Br-		
Br-	+ Cu Cn	→	N≡C-	C≡N		
N≡C-	+ KOH (Ethylene glycol)	→	HOOC-	COOH	(MONOMER)	
HCl · H-	HCl + NaNO ₂ + H ₃ PO ₂	→	HOOC-	COOH		
HOOC-	+ PCl ₅ & POCl ₃	→	Cl-	C-Cl	(MONOMER)	
N≡C-	+ HO-	(K ₂ CO ₃ & DMSO)	→	N≡C-	O-	C≡N
N≡C-	O-	C≡N + KOH (Ethylene glycol)	→	HOOC-	O-	COOH
HOOC-	O-	COOH + PCl ₅ & POCl ₃	→	Cl-	O-	C-Cl
N≡C-	NO + HO-	(K ₂ CO ₃ & DMSO)	→	N≡C-	O-	C≡N
N≡C-	O-	C≡N + KOH (Ethylene glycol)	→	HOOC-	O-	COOH
HOOC-	O-	COOH + PCl ₅ & POCl ₃	→	Cl-	O-	C-Cl
N≡C-	NU ₂ +	(K ₂ CO ₃ & DMSO)	→	N≡C-	O-	C≡N
N≡C-	O-	C≡N + KOH (Ethylene glycol)	→	HOOC-	O-	COOH
N≡C-	NO ₂ + HO-	(K ₂ CO ₃ & DMSO)	→		O-	C≡N
N≡C-	O-	C≡N + KOH (Ethylene glycol)	→		O-	COOH
	O-	COOH + PCl ₅ & POCl ₃	→		O-	C-Cl
N≡C-	O-	C≡N + HS-	(POLYPHOSPHORIC ACID)	→		C-
HO-C-	O-	C-	(POLYPHOSPHORIC ACID)	→		C-

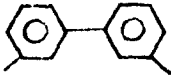
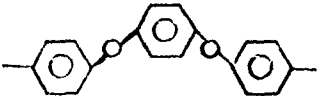
TABLE 7
SYNTHESIZED COPOLYMER DATA

MONOMERS			INHERENT VISCOSITY
0% 	100% 	 HCl · H ₂ N-  -NH ₂ · HCl	1.96
50% 	50% 	"	1.40
75% 	25% 	"	2.34
90% 	10% 	"	3.18
95% 	5% 	"	5.18
97% 	3% 	"	6.75
75% 	25% 	"	1.94
75% 	25% 	"	1.72
90% 	10% 	"	4.37
95% 	5% 	"	3.75
97% 	3% 	"	9.88
90% 	10% 	"	5.44
95% 	5% 	"	6.74
97% 	3% 	"	6.86
0% —	100% 	"	1.40
90% 	10% 	"	6.81
90% 	10% 	"	5.24
95% 	5% 	"	6.92
97% 	3% 	"	7.29

B. Articulated PBO - Film Casting and Mechanical Properties
(C. Benner)

A series of films were prepared from PBO copolymers containing various percentages of articulated units. Films were cast using 2% solutions prepared in methane sulfonic acid. The solution was poured into a flat bottom casting dish and placed in a sublimator. The sublimator was assembled and continuously evacuated with a vacuum pump. The bottom of the sublimator was immersed in a water bath held at 60°C (140°F). The cold finger of the sublimator was thermostated at -25°C (-13°F) with a Kryomat. After the films formed, they were cut into 6.35 mm (0.25 inch) wide test specimens and elongated at a rate of .508 mm (0.02 inch) per minute in an Instron tensile tester. Typical results are shown in Table 8.

TABLE 8
MECHANICAL DATA OF ARTICULATED PBO POLYMERS

Structure of flexible molecule	mole. %	Tensile Strength MPa (PSI)	Modulus (PSI)
	10	24.8 (3600)	979 (142,000)
"	5	53.1 (7700)	2158 (313,000)
"	3	52.4 (7600)	1475 (214,000)
	10	77.2 (11,200)	3765 (546,000)
"	5	48.9 (7100)	2317 (336,000)
"	3	62.0 (9000)	2365 (343,000)

C. Molecular Composites (Blends) (C. Benner)

(1) Cast Films Preparation

Recent developments in the synthesis of rod-like aromatic heterocyclic polymers has generated a great interest in

the development of these polymers as structural materials. One potential concept for the utilization of the rod-like polymers is molecular composites. This concept consists of blending a rod-like aromatic heterocyclic polymer with a coil-like aromatic heterocyclic polymer. The intent is to reinforce the coil-like polymer with the rod-like polymer, thus forming a composite on the molecular level analogous to chopped fiber reinforced composites. Films of the molecular blends were prepared for tensile testing by the film casting technique. Solutions were prepared by dissolving 0.2 gm (.0071 oz) of blended polymer into 10 ml (.610 oz) of methane sulfonic acid. The solution was poured into a specially constructed flat-bottom film casting dish 63.5 mm (2.5 inches) in diameter placed in the bottom of a sublimator. The sublimator was assembled and leveled by means of a swivel clamp while observing the overall thickness of the solution in the casting dish. The sublimator was continuously evacuated during the film casting process. The cold finger of the sublimator was cooled to -30°C (-22°F) by a circulating bath. The outer shell of the sublimator was heated to 60°C (140°F) to enhance the removal of the methane sulfonic acid.

After the film had formed, it was removed from the casting dish by soaking the film in methanol. The film was air dried and cut into 0.64 cm (.25 in) wide test specimens using a razor blade, a 0.64 cm (.25 in) wide template bar, and a cutting surface plate. Tests were performed with an Instron tensile tester at a crosshead speed of .508 mm (0.02 in) per minute. After initial specimen breaks occurred, remaining pieces were retested until the length became too short to reasonably grip the specimen [approximately 1.5 cm (.59 in)]. This provided not only "as-cast" data, but also "mechanically-stretched" data. Some specimens were plasticized with methanol to permit further stretching. After these specimens were dried of the methanol, they were mechanically tested to determine the effect of the stretching. Blends studied are listed in Table 9. The best mechanical data were obtained with the AB-PBI/PBT blends and are shown in Table 10.

TABLE 9
POLYMER BLENDS

MATRIX		RODLIKE POLYMER	WEIGHT % of RODLIKE POLYMER
1.	PBI-M	PD/AB	0, 2.5, 5 10, 20, 75
2.	P-PBI	PD/AB	0, 10, 20
3.	AB-PBI	P-PBI	0, 10, 20, 30
4.	PPBT	PBT	0, 25, 50, 75, 100
5.	PePBO	PBO	0, 25, 50, 60, 75
6.	AB-PBI	PD/AB	0, 10, 20, 30, 57, 75
7.	AB-PBI	PBO	0, 10, 20, 30
8.	AB-PBI	PBT	0, 10, 20, 30
9.	PPQ 401	PBT	0, 10, 20, 30, 50, 90

TABLE 10
MECHANICAL PROPERTIES OF AB-PBI/PBT BLENDS

% Rod Polymer	Stretch/ % Area Reduction	Tensile Strength (MPa) (PSI)		Modulus (MPa) (PSI)		Strain (%)
0	none	80.0	11,600	1031	149,500	98
0	mech./20	134.5	19,500	2002	290,300	43
0	solvent/60	108.8	15,200	3372	489,100	12
10	none	100.7	14,600	2272	329,500	50
10	mech./40	215.1	31,200	5534	802,600	18
10	solvent/?	365.4	53,000	8639	1,253,000	9
20	none	22.8	3,300	420.3	60,960	93
20	mech./55	244.1	35,400	4473	648,800	22
20	mech./70	404.0	58,600	8729	1,266,000	18
20	solvent/70	501.2	72,700	13,707	1,988,000	3

During the testing of the AB-PBI blends, the 80%/20% ABPBI/PBT sample elongated much more than expected. This was thought to be due to plasticization of the test specimens by methane sulfonic acid. Therefore, a test specimen was elongated 100% and cut into two pieces. One piece was tested without further treatment, while the second piece was neutralized with dilute ammonium hydroxide and air dried. The unneutralized half was elongated an additional 39.2% and the neutralized portion was elongated an additional 22.2%. Utilizing this information, a test specimen 90/10 ABPBI/PBT was soaked in a mixture of 70% methane sulfonic acid and 30% methanol in order to plasticize it to the point where the specimen could be oriented by stretching. After the specimen was removed from the mixture, it was allowed to absorb water from the atmosphere (four hours) before it was wiped free of surface acid with a paper towel. It was elongated 300% and neutralized with dilute ammonium hydroxide. This was followed by washing with methanol while keeping the specimen under tension in the Instron tensile tester and dried at 100°C before being tested. The tensile strength was 365 MPa (53,000 PSI) and the modulus was 8618 MPa (1,250,000 PSI) compared to 213.7 MPa (31,000 PSI) tensile strength and 5515 MPa (800,000 PSI) modulus for the mechanically stretched as-cast sample.

(2) Precipitated Films - Preparation and Mechanical Properties

Another approach used to achieve molecular level composites was to precipitate a solution containing a mixture of the matrix (coil-like) polymer and the rod-like reinforcing polymer. Solutions were prepared by dissolving 0.2 gm (.0071 oz) samples containing various mixtures of the two polymers in 10 ml (.610 cu in) of methane sulfonic acid. The solution was poured into the casting dish and the dish was placed in a desiccator containing some water in the bottom. The desiccator was covered and the sample was allowed to precipitate by absorbing the water vapor. The resulting film was removed, rinsed with water to remove excess acid, and flattened somewhat between two parallel

plates in a press. The films containing a high percentage of matrix generally gave good films while the ones containing more rod-like polymer were prone to breaking apart during the pressing operation. A new matrix polymer (PPQ401) was used in place of the ABPBI. None of the PPQ401 samples were usable films. The results are shown in Table 11.

(3) Polymer Reclamation

The sample of PDIAB-LS-1, one of the rigid rod polymers used for making films, was entirely consumed during the film making processes. It was reclaimed for future use by filtering the slurry in the reclaim flask through a five micron teflon filter. The resulting solution was precipitated by adding methanol slowly to it. Methane sulfonic acid was added to the filtrate until a suspension of very fine particles was formed. Both portions were poured into a beaker containing 1500 ml (91.6 cu in) of stirring double distilled water. The precipitated sample was collected on a teflon filter where it was washed with a liter (61.0 cu in) of methanol, 100 ml (6.10 cu in) portions of a benzene-methanol mixture (80% MeOH/20% BZ, 60% MeOH/40% BS, etc.) and finally washed with one liter of benzene also in 100 ml portions. The sample was transferred to a tared sample jar and freeze-dried from the benzene. After the benzene had been removed, the sample was heated for 1 1/2 hours at 120°C (248°F) under a vacuum of one micron.

D. Morphology

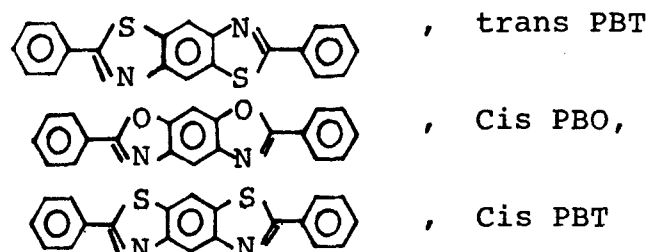
(1) Model Compound Studies Via XRD (D. Wiff and A. Fratini)

Model compounds of aromatic heterocyclic rigid-rod polymers being investigated in the ordered polymers research area, Polybenzoxazole (PBO) and Polybenzathiazole (PBT), were synthesized by Dr. F. E. Arnold and colleagues at AFML Polymer Branch and by Dr. J. Wolfe, SRI International under contract with AFML. These model compounds have been studied in order to better understand macromolecular packing

TABLE 11
MECHANICAL PROPERTIES OF
SELECTED PRECIPITATED BLEND FILMS

Sample	Tensile Strength		Modulus	
	(MPa)	(PSI)	(MPa)	(PSI)
90% AB-PBI/ 10% PDIAB	122.0	17,700	3999	580,000
80% AB-PBI/ 20% PBT	137.9	20,000	6334	918,700

and polymer conformation, and determine intra and inter-atomic distances. Some of the model compounds studied to date have been



and presently collecting data on

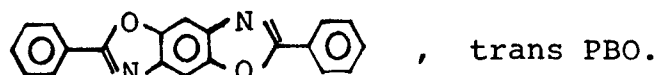


Figure 27 shows the packing scheme for the Cis PBT model compound. All of the geometric centers of the molecules shown are almost planar within a few Angstrom units. Plots such as these help one visualize how polymer chains most easily pack. If the crystal packing does not lend itself to alignment of long chain molecules, there must be other driving forces available if processing engineers are to achieve liquid crystalline type packing. The most productive path from a processing viewpoint would be to have a polymer which readily consolidates into that configuration exemplified by the crystal packing. The 5.83 and 3.95A spacings are the same as the dominant equatorial reflections determined by wide angle x-ray scattering (WAXS) from highly oriented PBT fibers (Figure 27). The 12.2A spacing is the same as the meridional reflection.

(2) Texture Analysis (G. Price and D. Wiff)

X-ray diffraction (XRD) characterizations were made on several polymer fibers and several new polymer blends (molecular composites). The molecular ordering (degree of orientation) in these materials is of particular interest, and this degree of ordering can be determined with XRD data.

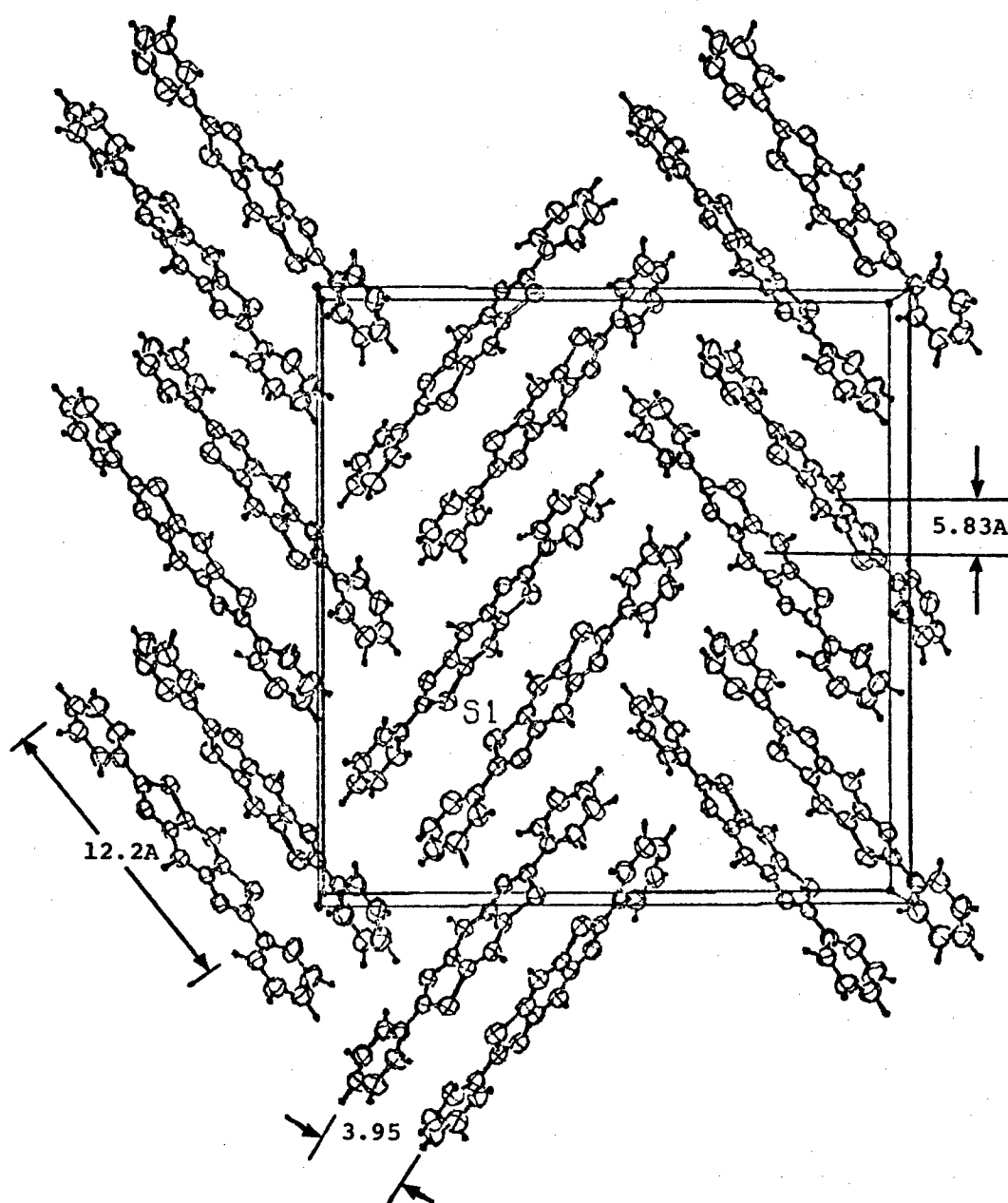


Figure 27. Molecular Packing Scheme for the Trans-PBO Model Compound. The 12.2 spacing is the meridional reflection and 5.83 and 3.95 spacings are equatorial in fiber XRD photographs (see Figure 33).

X-ray diffraction patterns were obtained on 21 different PBT fibers and 15 different polymer blends.^{6,7}

Flat film wide angle XRD patterns were made for the following percentage blends of ABPBI/PBT and ABPBI/PDIAB:

<u>ABPBI/PBT</u>	<u>ABPBI/PDIAB</u>
90/10 as cast, flat & edge	90/10 stretched, flat & edge
90/10 stretched, flat	70/30 as cast, flat & edge
80/20 stretched, flat & edge	43/57 as cast, flat & edge
80/20 solvent stretched, flat & edge	43/57 stretched, flat & edge
70/30 as cast, flat	90/10 precipitated, stretched, flat & edge
80/20 precipitated, stretched, flat & edge	
80/20 as precipitated, flat & edge	
20/80 as precipitated, flat.	

Figures 28 through 30 show the collective results of these studies where we have included the intensity by the height of the bar and the width of the diffraction ring or arc by the width of the bar. Flat film wide angle XRD patterns were also made for films of 100% ABPBI as-cast (flat) and stretched (flat) and 100% PBO as-cast (flat and edge) and stretched (flat). A Debye-Scherrer XRD pattern was made for PDIAB powder for comparison with predicted powder pattern using model compound study results.

Small angle XRD patterns with a sample-to-film distance (SFD) of 17 centimeters (6.69 in) were made of the 80/20 ABPBI/PBT solvent stretched, (flat) sample, and the 43/57 ABPBI/PDIAB stretched, (flat) sample. Only meridional arcs corresponding to a d-spacing of 12.2 Angstroms could be seen for the 80/20 ABPBI/PBT sample with a 234 hour exposure time. No small angle x-ray scattering (SAXS) pattern could be seen for the 43/57 ABPBI/PDIAB sample with 48 hours exposure time. A small angle (SFD = 29.0 cm, 14.4 in) x-ray exposure for 258 hours

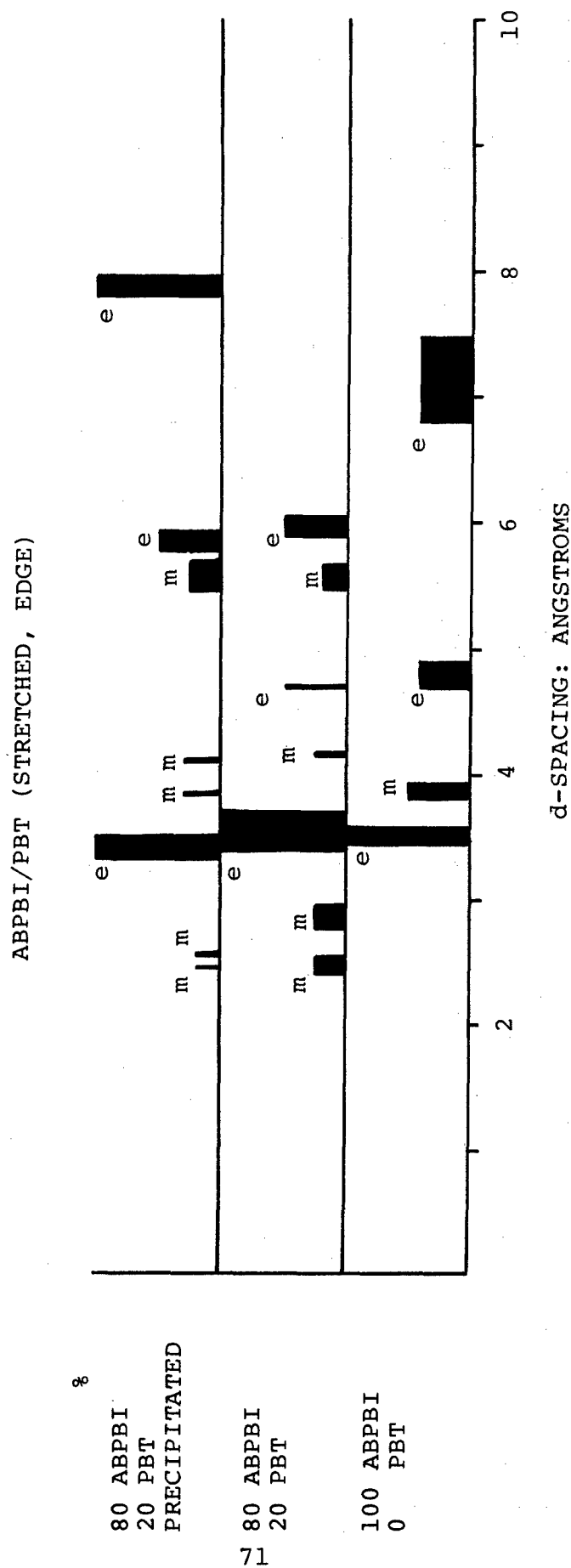


Figure 28. Comparison of D-spacings Present in WAXS Photographs of ABPBI/PBT Blends for Edge Specimen View. The percent combination of blends is indicated on the ordinate. The height of the bar is a relative comparison of the intensity; the width of the bar relates to the breadth of the debye ring; if orientation is present (e = equatorial, m = meridional).

STRETCHED (FLAT)

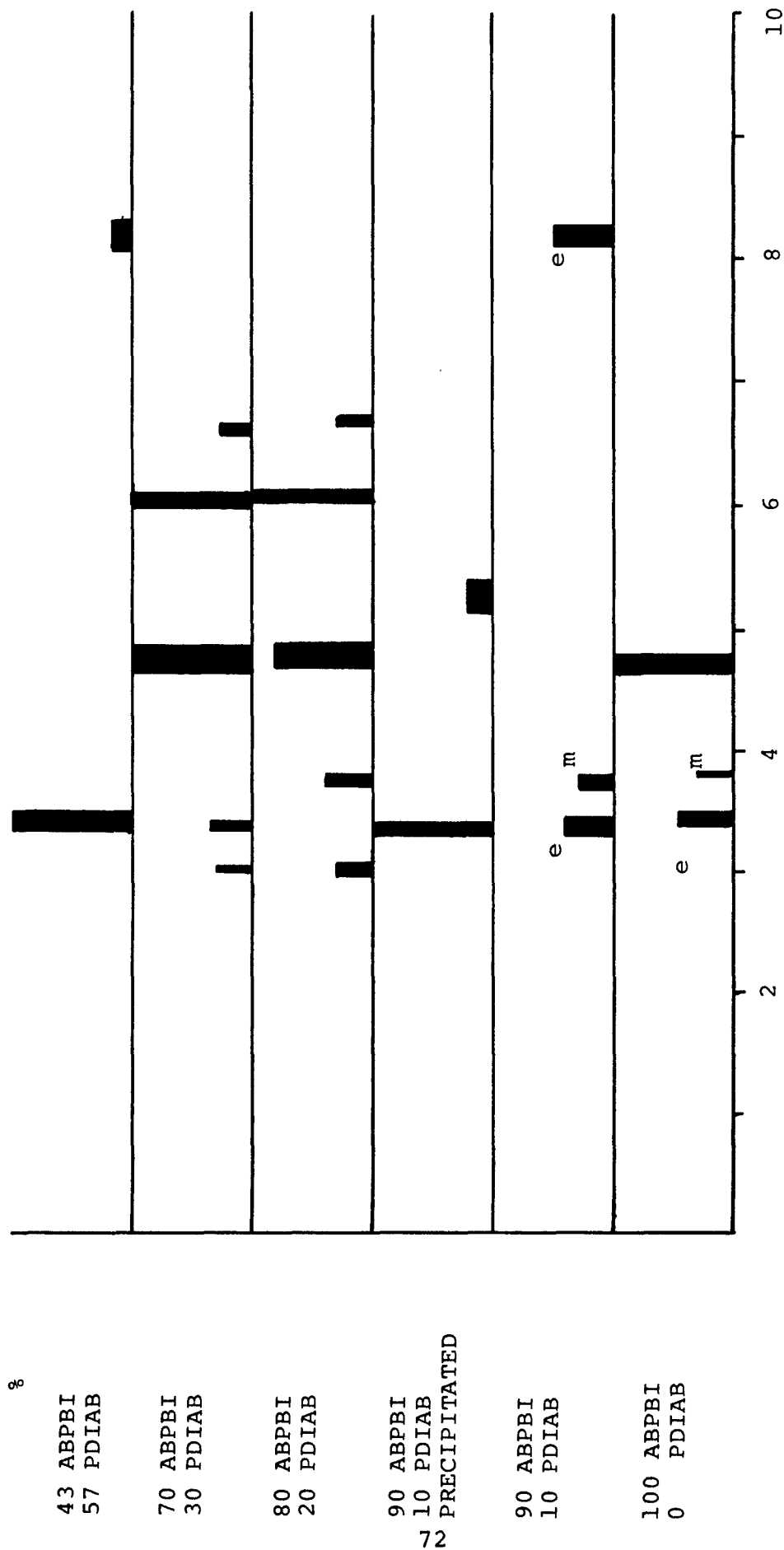


Figure 29. Comparison of D-spacings Present in WAXS Photographs of ABPBI/PDIAB Blends for Flat View of the Specimen. The percent combination of blends is indicated on the ordinate. The height of the bar relates to the intensity; the width of the bar relates to the breadth of the debye ring; if orientation is present (e = equatorial, m = meridional).

ABPBI/PDIAB (STRETCHED, EDGE)

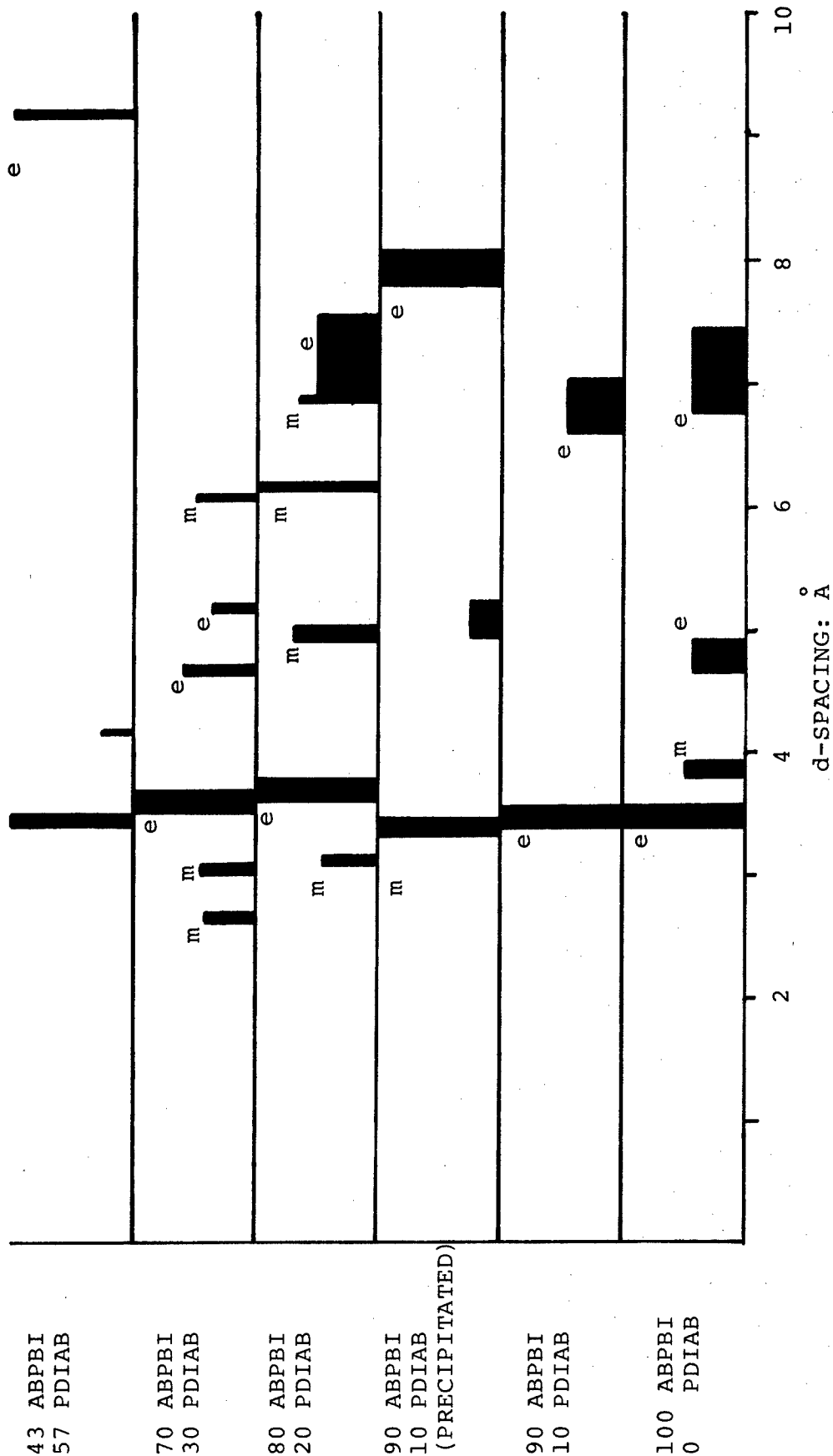


Figure 30. Comparison of D-spacings Present in WAXS Photographs of ABPBI/PDIAB Blends for Edge View of the Specimen. The percent combination of blends is indicated on the ordinate. The height of the bar relates to the intensity; the width of the bar relates to the breadth of the debye ring; if orientation is present (e = equatorial, m = meridional).

was made on the 100% ABPBI unstretched flat sample but nothing appeared on the negative. The SAXS pattern (SFD = 29.0 cm, 14.4 in) for the 80/20 ABPBI/PBT precipitated, stretched, edge sample showed only an equatorial streaking at the center of the negative indicative of microvoid scattering. A sample of the 80/20 ABPBI/PBT blend was mounted on the ten meter SAXS system at Oak Ridge National Laboratories. The contour map of this specimen (Figure 31) shows contours at powers of two (i.e., 2,4,8,16...). The machine direction is oriented -20° from north. The pattern shows a large broadening in the transverse (AA') direction. A scan along the AA' path is shown in Figure 32. We would guess the basic microstructural unit is rod-like, but the 80/20 and 90/10 (ABPBI/PBT) solvent stretched samples give a diffraction pattern that is much sharper than any of the other patterns. The XRD patterns for the 80/20 and 90/10 ABPBI/PBT solvent stretched samples are the only pattern that show any arcs with the sample in the flat position.

Flat film XRD patterns were developed on several PBT fibers. The following fibers were examined with a Jarrel-Ash Laue camera with a 24 hour exposure time and a sample-to-film distance (SFD) equal to 6.3 cm (2.48 in).

PBT-071927	PBT-071937
28	38
30	38 H1
31	38 H2
32	43
33	45
34	PBT#53-54.

Flat film wide angle XRD patterns were made of PBT#53-54, PBT#46, and PBT#2122-57 in a polymer camera with a sample-to-film distance of 5.0 cm (1.97 in). The d-spacings and orientation angles were calculated for all the fibers tested (see Table 12 and 13). The XRD pattern for PBT#46 was unique in that it showed a split meridional arc (quadrant arcs) for the d-spacing of 5.61 Angstroms. (See Figure 33.) The fiber which showed the smallest orientation

80 ABPBI/20 PBT

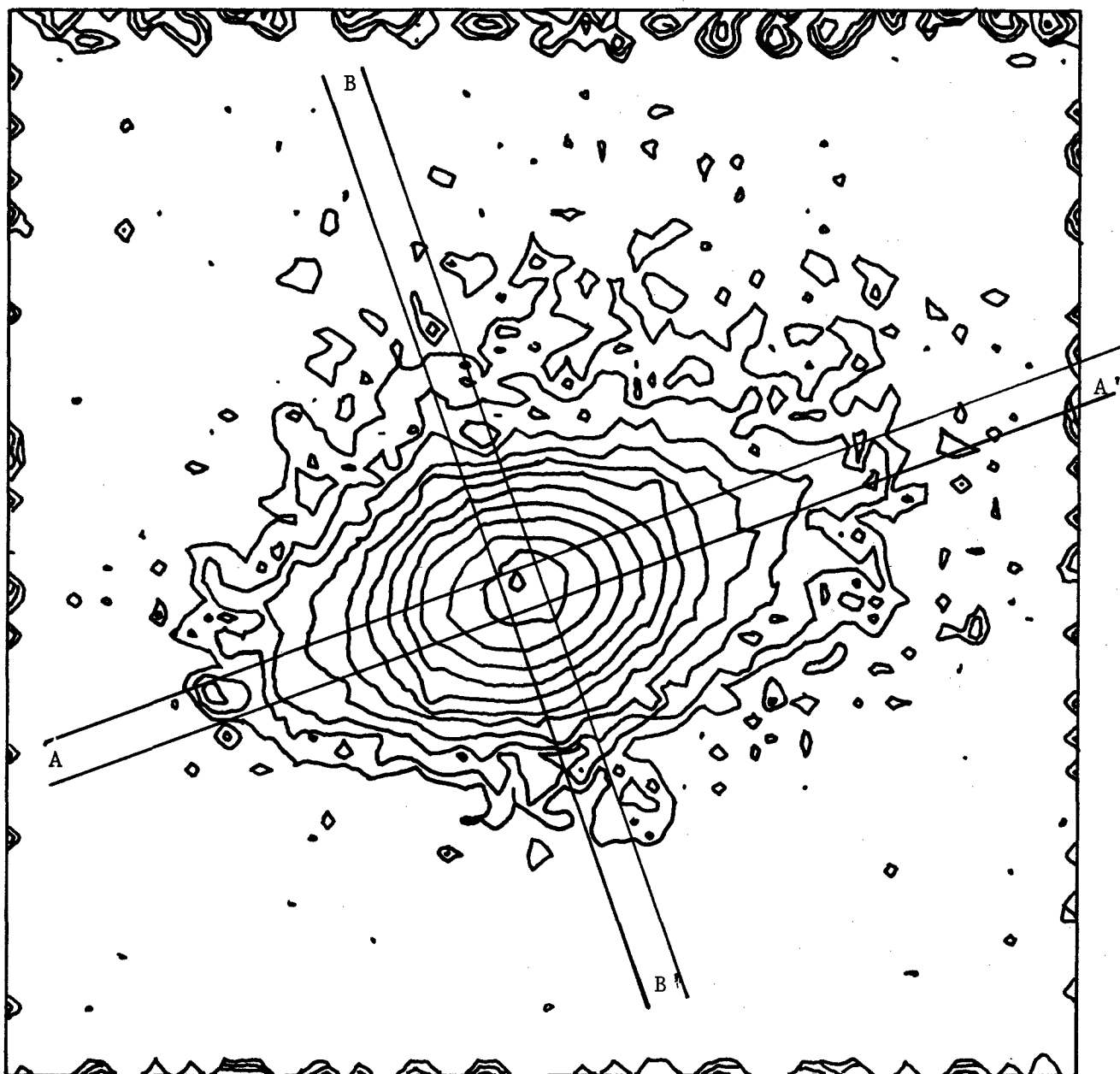


Figure 31. SAXS Results of 80/20 (ABPBI/PBT) Taken on the ORNL 10 Meter System. The intensity contours are indicated. The machine direction is oriented -20° from the north.

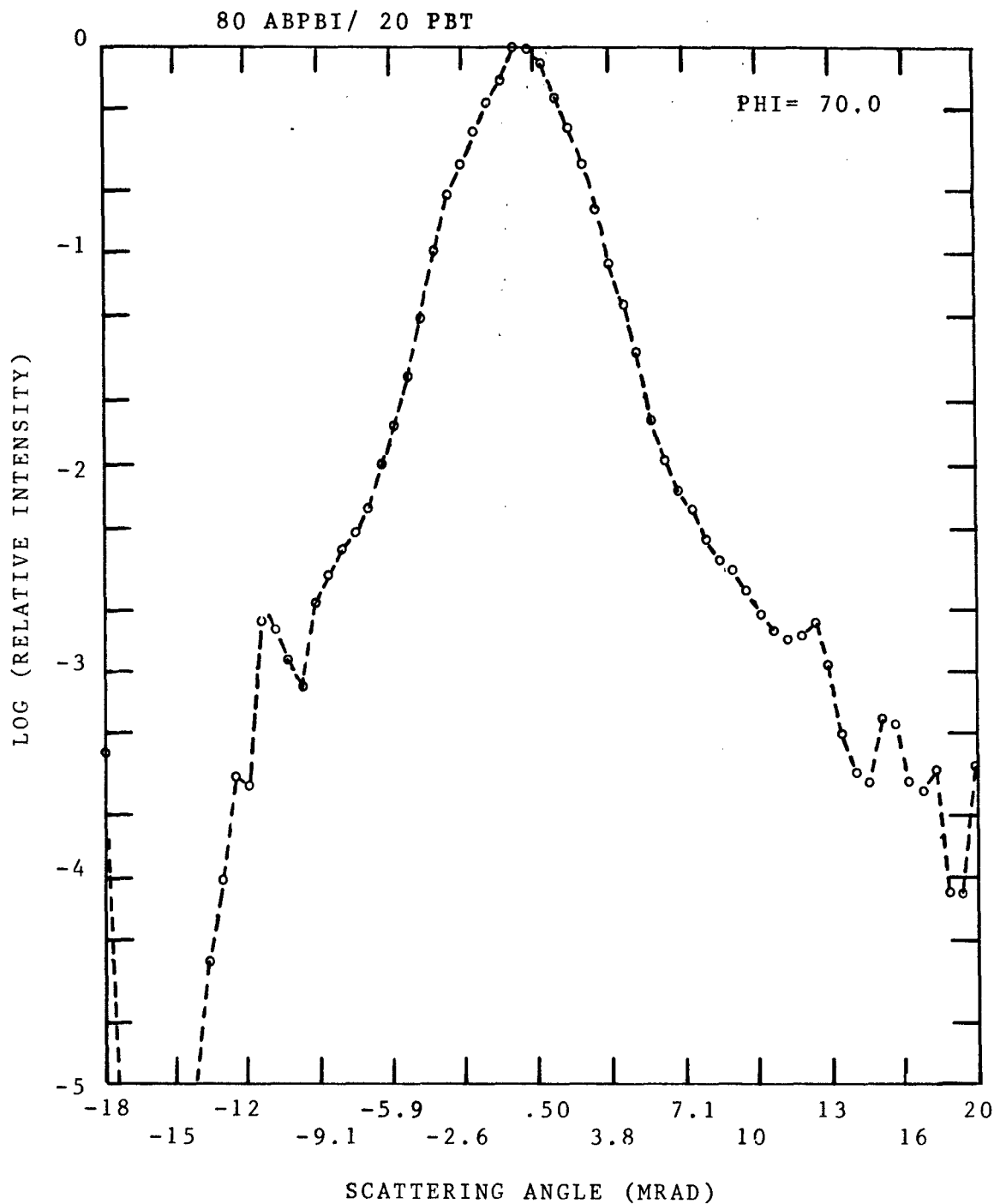


Figure 32. An Intensity Scan Along the AA' Path Shown on the Contour Plot in Figure 31.

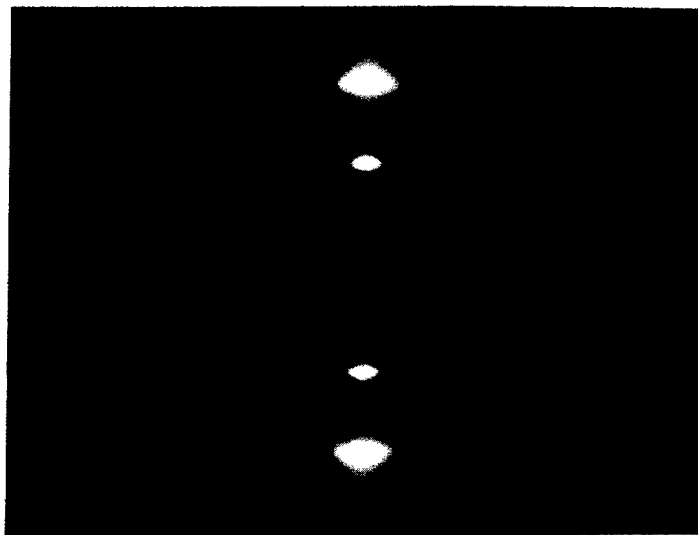


Fig. 33. WAXS Photograph of PBT46 Fiber. Note the meridional 12.2A spacing, the 3.95 and 5.83A equatorial arcs and the split (quadrant) meridional arc for the 5.61A d-spacing.

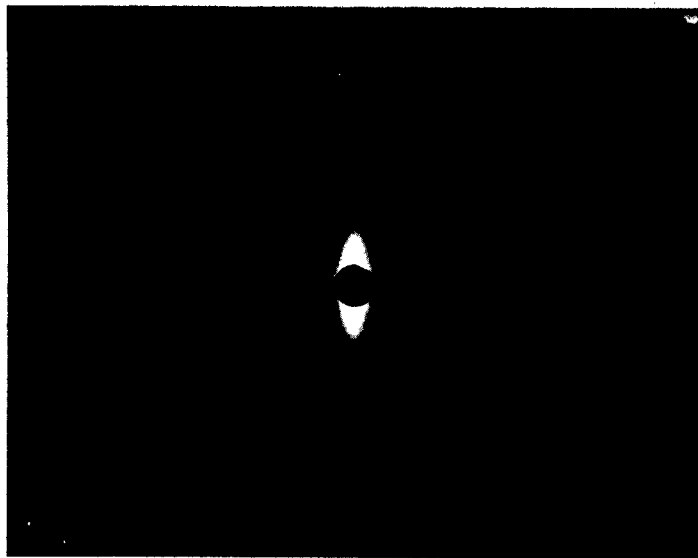


Fig. 34. SAXS Photograph of PBT#46 Fiber Using the 29 cm Setting in a Statton Camera. Note the 12.2A d-spacing is present as a meridional arc. No other spacings are present. The equatorial streaks are attributed to micro-void scattering.

TABLE 12
RESULTS OF PBT #33, 38, 38 H1 FIBER MORPHOLOGY STUDY

	Modulus (gpd)	Tenacity (gpd)	d-spacing (A)	degree	f	Crystallite Size (A)	Comments
PBT #33			3.47	11	-0.44	17	Equatorial
	432	3.76	5.58	--	--	23	Equatorial
PBT #38			3.47	--	--	29(14)	Equatorial
	820	4.1	5.58	13	-0.42	19	Equatorial
PBT #38 H1			3.47	5.5	-0.49	--	Equatorial
	1000	5.2	5.58	11.2	-0.44	--	Equatorial

TABLE 13
CHARACTERISTICS OF THE X-RAY DIFFRACTION PATTERNS
OF PBT 26554-9-5 (AS SPUN) AND PBT #46 FIBER

PBT 27554-9-5 (AS SPUN), IV = 18

θ degrees	d-spacing A	Comments	Orientation Angle degrees
18.80	2.39	w,d	
14.80	3.02	vw,d	
12.99	3.43	s,vd	17 e
10.88	4.09	m,b	
10.40	4.27	m,vd	
7.58	5.84	s,vd	17 e
7.31	6.06	w,f	
3.70	11.93	m,vd	17 e
3.62	12.21	s,f	

PBT #46, IV = 14 (T/E/M; 11.58 gpd/1%/1220 gpd)

18.60	2.42	w,d	
15.10	2.95	w,d	19 e
14.80	3.02	w,vd	
14.20	3.15	w,d	19 e
12.70	3.50	s,d	21 e
10.80	4.11	m,f	
7.90	5.61	w,f	split meridional arcs
7.50	5.93	s,f	21 e
3.80	11.76	w,vd	19 e
3.60	12.40	m,f	

angle was PBT-071938 H1 with an orientation angle of 10 degrees. The next lowest orientation angles were for fibers PBT-071938, 53-54, 46 and 2122-57 all with orientation angles of about 17 degrees.

Small angle XRD patterns were developed on PBT-071943, PBT#46 (Figure 34), and PBT#2122-57. These three fibers all gave the same SAXS patterns that consist of meridional arcs corresponding to a d-spacing of approximately 12.2 Angstroms and equatorial streaking attributed to microvoid scattering.

(3) Polefigure Analysis (D. Wiff)

A polefigure is the stereographic projection of the normals (poles) of diffracting planes. Even though there are many diffraction planes (e.g., a single crystal) it is customary, when illustrating orientation or texture, to show the poles of only one type of diffraction planes on each figure and to indicate the pole diversities by contour lines. In Figure 35 we illustrate the relationship between the x-ray beam, the Debye ring on a flat-plate photograph, and the polefigure. All crystal planes which can diffract the x-ray beam make an angle θ with the beam and the normals to these planes make an angle of $90^\circ - \theta$ with the beam. Thus the poles of those diffracting planes which give rise to Debye rings in a flat plate photograph are projected into circles on the polefigure. As the Debye ring increases, the corresponding circle representing the locus of the poles decreases. That is, the Debye ring is determined by a cone having a half angle of 2θ whereas the corresponding locus of poles is determined by a cone with the half angle $90^\circ - \theta$.

In considering the polefigures of a film sample, it is customary to orient the sample with the machine (roll or stretch direction in a vertical position (see Figure 36) and the transverse direction in a horizontal position. It is necessary to rotate the sample in many different ways in order to actually examine or record the various diffraction intensities arising from the distribution of a given set (specified 2θ) of diffraction planes within the sample.

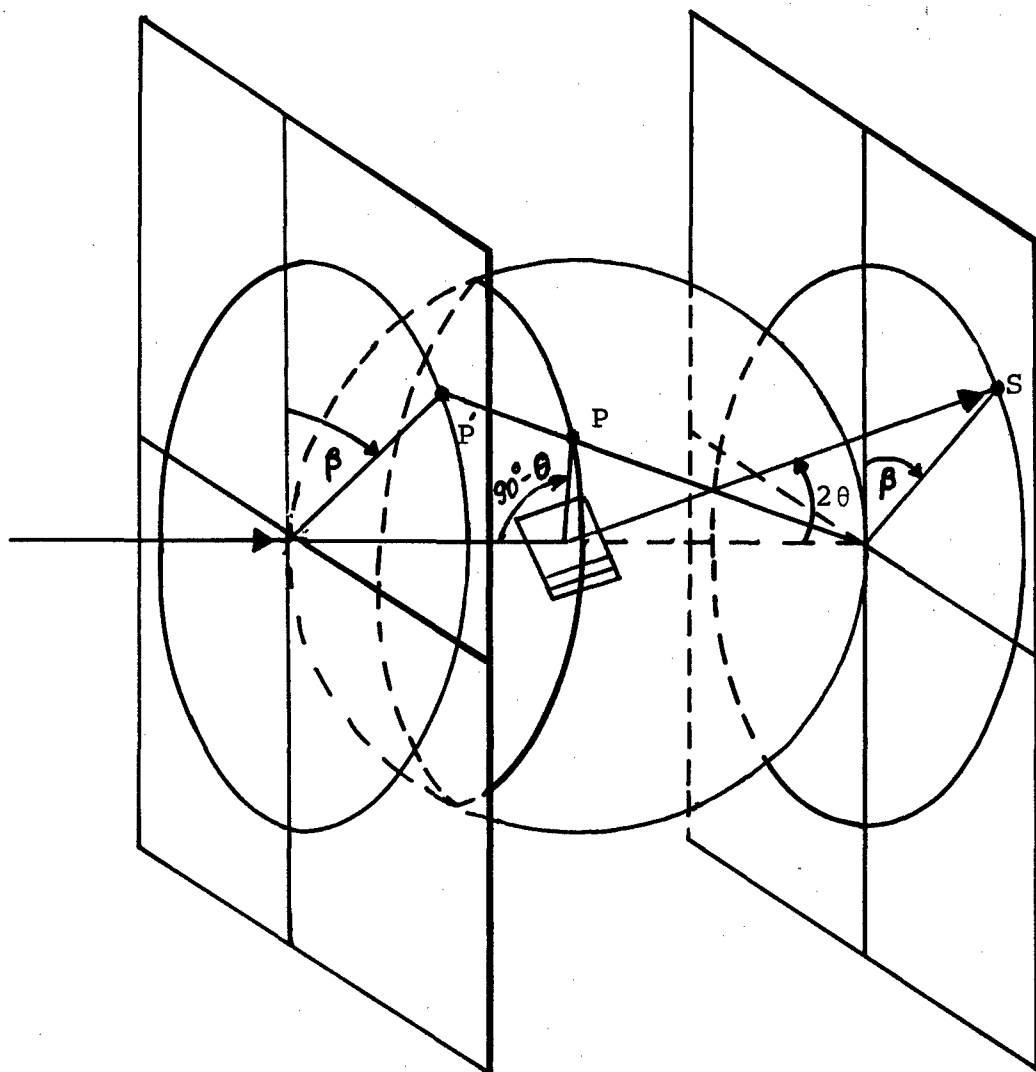


Figure 35. Schematic Showing the Geometrical Polefigure Plotting of a Point P' , the Projection of the Pole P and the flat film XRD spot S . The point S is located on a debye ring. Note that the angle β is preserved in the projection scheme.

In spite of experimental difficulties required to obtain a complete polefigure, the advantages become apparent when one compares the amount of information available on such a polefigure with the information which is obtained from the usual flat-plate photograph.

Usually the only information obtained is a single flat-plate photograph with the x-ray beam normal to the film. For a specified set of diffraction planes, this yields information only about those planes whose normals or poles make an angle θ (typically $10-13^\circ$) with the plane of the film.

Application of this technique to various fibers (PBO and PBT) of interest in this contractual effort and various blends has been achieved. Typical of these is a polefigure scan (Figure 37) of a PBO heat treated fiber for diffraction planes separated by a distance $d=3.81\text{\AA}$. The angle χ is zero along the vertical direction (MD). It was varied by equal intervals (40°) for the entire 360° . This is a 360° rotation of the fiber about an axis perpendicular to the fiber direction. The latitude angle was ω . It was varied by equal intervals (20°) of $\sin \omega$ from $0 \leq \sin \omega \leq 1$. In this case the fiber starts out in the plane of the χ -circle of the instrument (here $\omega=0$). The angle χ is stepped through 360° giving rise to the intensity distribution on the circumference of the circle (Figure 37). Then the fiber is tilted relative to this instrument χ -circle (or relative to the incident χ -ray beam) and again stepped through 360° for χ . This process is continued until the specified angular limits are reached. In Figure 37, the labelling of intensity is symbol $D \rightarrow$ unit intensity, normalized to the averaged background, $E \rightarrow \sqrt{2} \times D$, $F \rightarrow \sqrt{2} \times E = 2D$, etc.

All data is collected with a Picker FACS-1 fully automated x-ray diffractometer. The instrument control programs and data reduction programs used for this analysis were originally written by Desper.⁸

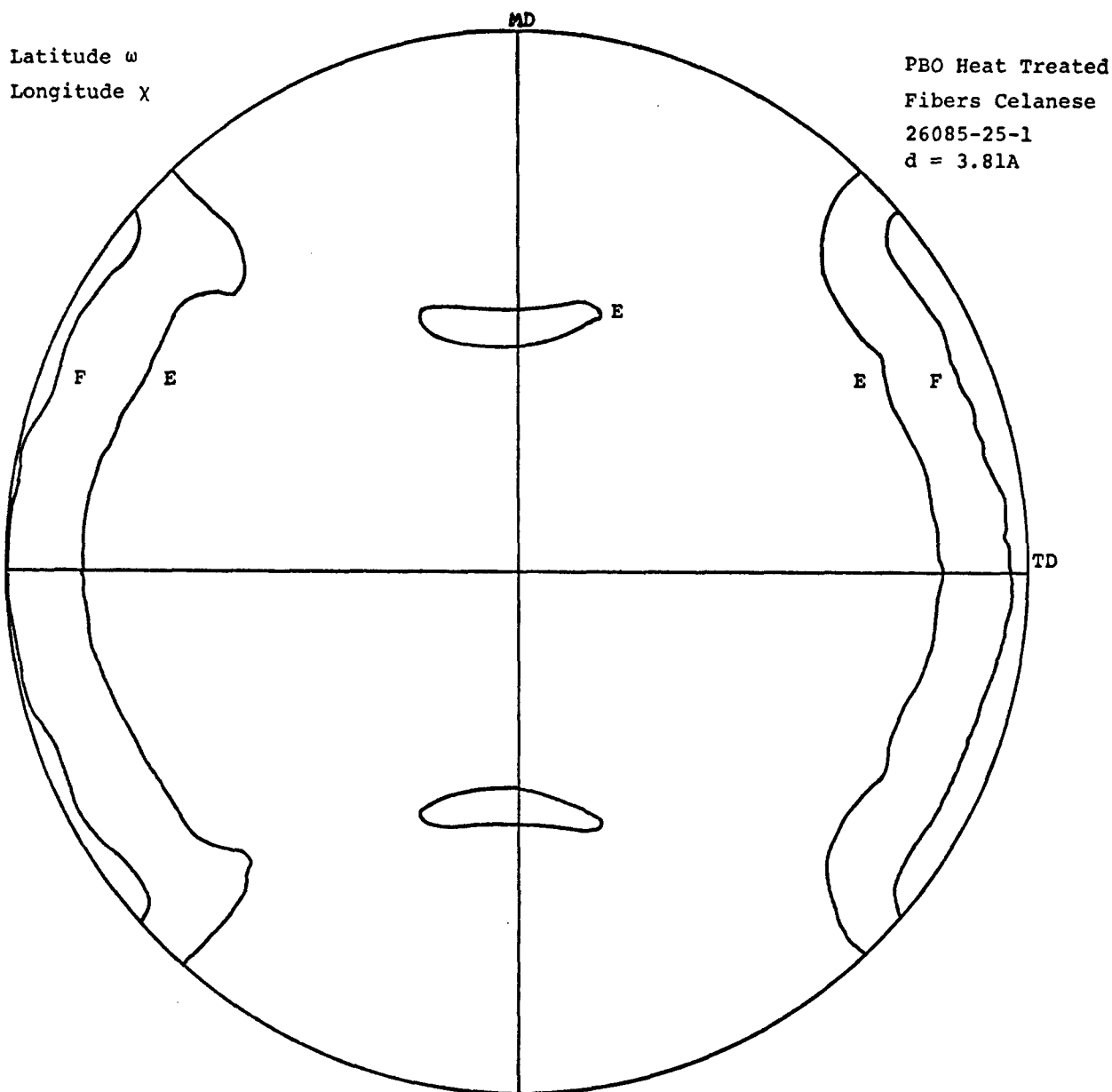


Figure 37. A Measured Polefigure of a PBO Heat-treated Fiber (Celanese 26085-25-1). The contoured intensities displayed represent the distribution of the d-spacings 3.81\AA . Starting with the vertical axis (MD direction), the longitudinal angle is χ . The latitude angle is ω , with $\omega = 0$ at the circumference and 90° at the center.

(4) Dynamic Imaging (D. Wiff and G. Price)

The dynamic imaging of x-ray diffraction pattern system (Figure 38)⁹ has been transferred from the original Siemens x-ray generator to a Rigaku microfocus x-ray generator. It was felt that the increased intensity (even though a very small increase) could only help in the operation of the equipment. While located in the Rigaku x-ray generator, we have been able to record prominent x-ray diffraction Debye rings and definitely detect orientation of these rings with this system. These results are now recorded on video tape for future reference. Achievement of these photographs has only been possible by storing the picture on the vidicon phosphor for 40 seconds. Every 1/60th of a second a picture is added to the phosphor. Thus to get a good picture we are storing 2400 frames or pictures. The next problem which arises is that the read pulse originally only scanned the phosphor once, thus leaving a residual signal. We are presently scanning the phosphor twice at each read command, thus reducing the residual signal.

The experimental capability has now been increased. There is presently a heated specimen holder allowing us to achieve a maximum temperature of 250°C (482°F). Also the Air Force Materials Laboratory has purchased a video digitizer to allow for better data manipulation and a rotating anode x-ray generator is scheduled to arrive before the end of this calendar year. This increased x-ray beam intensity ≈ 10 times will allow us to detect weaker diffraction rings, shorten the storage time, and minimize the residual signal. We will then be in a position to begin to apply this system on a regular basis to better understand the time dependent structural changes occurring during the processing and mechanical deformation of the polymer specimens of interest to the Air Force.

Several samples were examined with the dynamic imaging system and the Rigaku x-ray generator. The clearest diffraction patterns were seen for the PBO-26085-25-1 fiber and

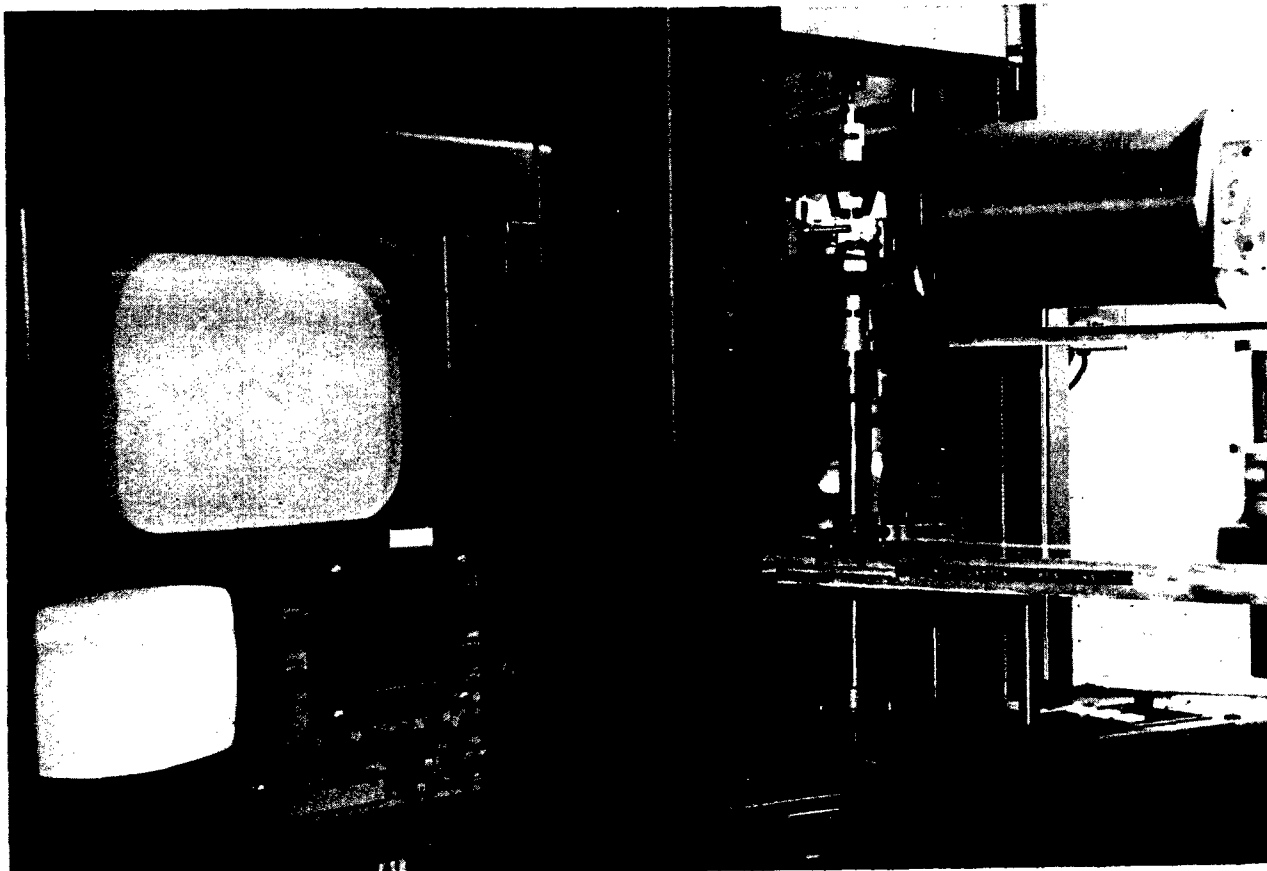


Figure 38. Photograph of the Dynamic Imaging of X-ray Diffraction Pattern System.

for the 25 m-PBI/75 PDIAB blend sample, but only the very strong rings or arcs could be seen. These two samples were heated to 250°C (482°F) while the XRD patterns were being observed, and no change was seen in either pattern.

Flat-film XRD patterns were developed for sample numbers 292-59, 292-62, and Ryton PPS (polyphenylene sulfide), and Debye-Scherrer powder patterns were made for sample numbers 36-292, 36-292-B, and 59894-47-1. All of these samples showed at least one diffuse diffraction ring.

SECTION III

POLYSACS

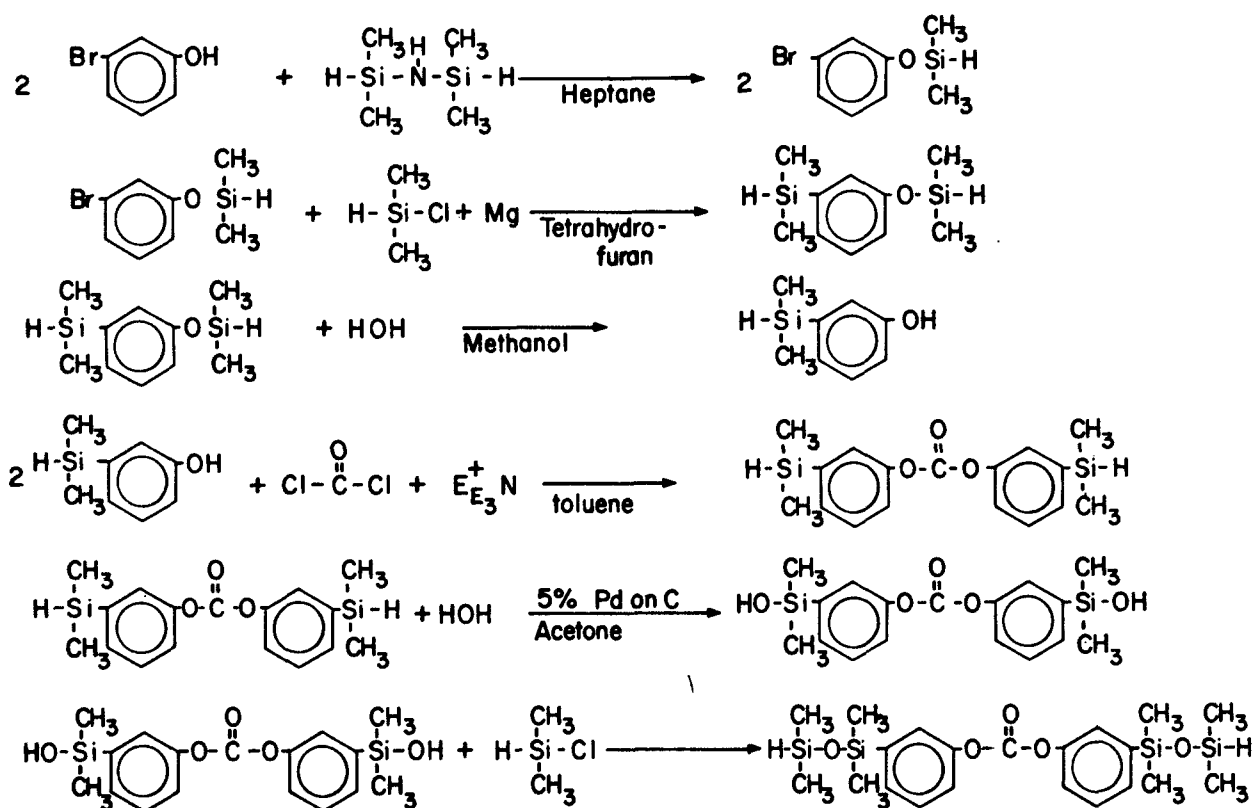
1. INTRODUCTION

This research area of the contract was to provide custom synthesis of very pure intermediates and starting materials. The synthesis of these materials, along with that of SBQ, is discussed in this section.

2. EXPERIMENTAL AND RESULTS

A. Synthesis (W. Price and K. Ngo)

A reaction scheme for the synthesis of Bis (m-1,1,3,3-tetramethyldisiloxanyphenyl) carbonate is:



Synthesis of m-bromophenoxydimethylsilane

A solution of 179.1 g (6.32 oz) [1.04 mole] of m-bromophenol (Eastman Kodak) in 400 ml (24.4 cu. in.) heptane (dried with 4A molecular sieves) is charged to a 4-necked, 1-l (61 cu. in.) flask equipped with a mechanical stirrer, a thermometer, a reflux condenser, and an addition funnel. The addition funnel contains 80 g (2.82 oz) [0.60 mole] of 1,1,3,3-tetramethyldisilazane. With continuous N_2 flow throughout the system, the disilazane is added dropwise over a period of one hour. The HN_3 liberated as the reaction proceeds, is trapped in distilled water with a drop of 1% phenolphthalein (changes to red in presence of NH_3). After the addition is complete, the reaction is stirred for an additional five hours. The heptane is then distilled off under a positive pressure of N_2 . The residue is then distilled under vacuum at a temperature of $47^{\circ}C$ ($116.6^{\circ}F$)/0.10 mm (.0039 in) Hg. The compound obtained was 199.6 g (7.04 oz) [83.8% yield] of m-bromophenoxydimethylsilane.¹⁰

Synthesis of m-dimethylsilyloxyphenyldimethylsilane

A mixture of 26.0 g (.917 oz) [1.07 mole] of activated magnesium turnings, 76.5 g (2.70 oz) [.81 mole] of dimethylchlorosilane (Silar) and 880 ml (53.7 cu in) of tetrahydrofuran (freshly distilled from $LiAlH_4$) is charged to a 4-necked 3-l flask equipped with a mechanical stirrer, a reflux condenser, a thermometer, and an addition funnel. The addition funnel contains a solution of 199.6 (7.04 oz) [.86 mole] of m-bromophenoxydimethylsilane from a previous synthesis, 76.5 g (2.70 oz) [.81 mole] of dimethylchlorasilane (Silar), and 240 g freshly distilled tetrahydrofuran. With continuous N_2 flow throughout the system, the solution in the addition funnel is added at such a rate that the temperature was constant $-38^{\circ}C$ ($100^{\circ}F$). Initially, 20 ml (1.22 cu in) of the silane solution was run in the flask to start the reaction. When the addition is complete (approximately five hours) the reaction is stirred overnight and refluxed

for six hours the next day. After cooling, petroleum ether [BP-30-60°C (86-140°F)] was added to precipitate the MgBr_2 . The solution is filtered under N_2 and washed with 3 x 200 ml (12.2 cu in) of petroleum ether (30-60). The filtrate is filtered again and washed with 2 x 300 ml (18.3 cu in) of petroleum ether (30-60). The filtrate is then concentrated on a rotary evaporator and distilled at room pressure under positive N_2 pressure to remove the solvent. It was then vacuum distilled at 45°C (113°F)/0.30 mm (.0118 in) Hg. The compound obtained was 158.5 g (5.59 oz) [87.6% yield] of the product.¹¹

Synthesis of dimethylsilylphenol

Double distilled water (35.5 ml, 2.17 cu in) was added to a solution of 122.1 g (4.31 oz) [.58 mole] *m*-dimethylsilaxyphenyldimethylsilane in 250 ml (15.3 cu in) of methanol and shaken overnight. Gas chromatography indicates one component. The mixture was put on a rotary evaporator to remove the methanol. Anhydrous MgSO_4 was added and the mixture allowed to sit for two hours. It was then filtered off and washed with 600 ml (36.6 cu in) of toluene. The phenoltoluene solution was then put on a vacuum line overnight to remove the toluene. The compound obtained was 89.85 g (3.17 oz) of the dimethylsilylphenol plus some residual toluene.¹²

Synthesis of Bis(*m*-dimethylsilylphenyl) carbonate

Toluene (1.1 l, 67.2 cu in), dried with 4A molecular sieves, was placed in an ice, rock-salt bath and cooled to -7°C (19.4°F). Phosgene was bubbled through until the weight gain was 64 g (2.26 oz).

A solution of 89.85 g (3.17 oz) [.59 mole] *m*-dimethylsilylphenol, (.64 mole) triethylamine (freshly distilled), and 840 ml (51.3 cu in) of dry toluene was charged to a 4-necked, 3 liter (183 cu in) flask equipped with a mechanical stirrer, addition funnel, a dry ice condenser, and a thermometer. The solution was cooled to -7°C (19.4°F) in an ice, rock-salt bath under continuous N_2 flow. The addition funnel contained 550 ml (33.6 cu in)

of the above phosgene solution [32 g (1.13 oz) phosgene] which was added dropwise over a period of 6 hours. The solution was stirred overnight while warming to room temperature. The triethylamine hydrochloride salts were filtered off and washed with 1 liter (61 cu in) of dry toluene. The filtrate was then concentrated on the rotary evaporator to remove some solvent for ease in handling. The solution was then washed with 5 x 400 ml (24.4 cu in) of saturated NaCl solution. The organic layer was dried with anhydrous MgSO_4 for two hours. The MgSO_4 was then filtered off and washed with 600 ml (36.6 cu in) of toluene. The filtrate was concentrated on a rotary evaporator and then distilled at room pressure to remove the remaining solvent. It was vacuum distilled at 135-139°C (275-282°F)/0.10 mm (.0039 in) Hg to obtain 81 g (2.86 oz) [41% yield] of the product.¹³

Synthesis of Bis(m-hydroxydimethylsilylphenyl) carbonate

A solution of 0.38 g (.013 oz) of 5% palladium on carbon (Englehardt), 71.5 ml (4.36 cu in) of reagent acetone and 14.3 ml (.87 cu in) of double distilled water was charged to a 3-necked, 500 ml (30.5 cu in) flask equipped with a mechanical stirrer, a thermometer and an addition funnel. The addition funnel contained 41.1 g (1.45 oz) [0.12 mole] of bis(m-dimethylsilylphenyl) carbonate and 14.3 ml (.87 cu in) of reagent acetone. The solution was cooled to -7°C (19.4°F) with an ice, rock-salt bath and the dihydride added at such a rate as not to let the temperature rise above 0°C (32°F). Addition time was 2.5 hours. The solution was stirred overnight and allowed to warm to room temperature. The catalyst was filtered off and washed with 200 ml (12.2 cu in) of reagent acetone. The filtrate and washings were concentrated on a rotary evaporator - note: evaporation should be done by vacuum only, or with very little heat, because as the carbonate becomes concentrated, heating will cause the bis-silonal to condense to siloxane. Two hundred ml (12.2 cu in) of toluene was added to redissolve the carbonate. The toluene - carbonate solution was washed with 5 x 400 ml of saturated NaCl

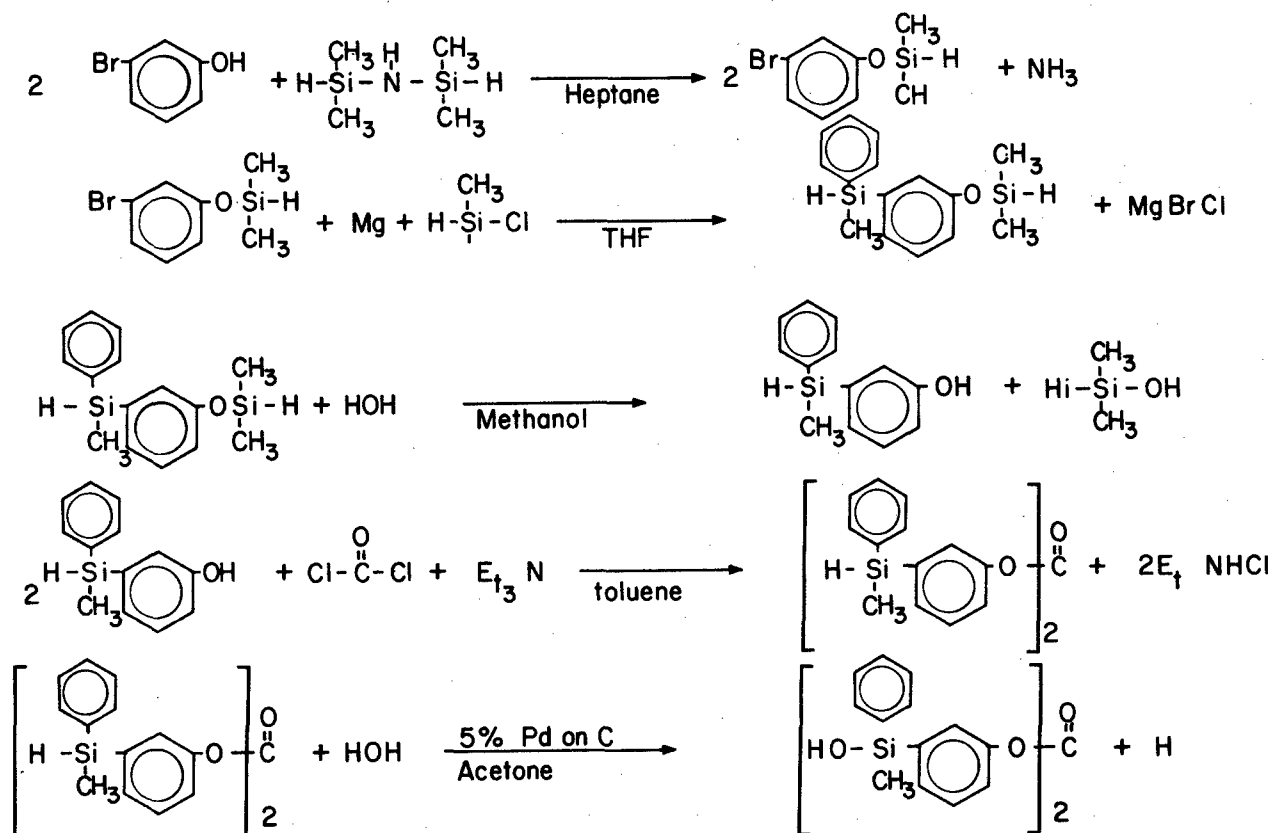
solution. The organic layer was then dried with anhydrous MgSO_4 for two hours. The MgSO_4 was filtered off and washed with 250 ml (15.3 cu in) of toluene. The filtrate and washings were concentrated on a rotary evaporator, using caution not to overheat, to a thick oil. Pentane is added to help in the crystallization. After storing at 5°C (41°F) for one hour, the crystals were filtered and washed with large amounts of pentane. The product was dissolved in 100 ml (6.10 cu in) of boiling toluene and allowed to crystallize at 5°C (41°F) overnight. Pentane was added the next day and the purified crystals were collected and washed with 500 ml (30.5 cu in) of pentane. The white crystals were then dried under vacuum [10 mm (.394 in) Hg] for 16 hours. The compound obtained was 30.9 g (1.09 oz) [75% yield] of melting point $91.0\text{--}91.6^\circ\text{C}$ ($195.8\text{--}196.9$) uncorrected.¹⁴

Synthesis of Bis(m-1,1,3,3 tetramethyldisilazanyphenyl) carbonate

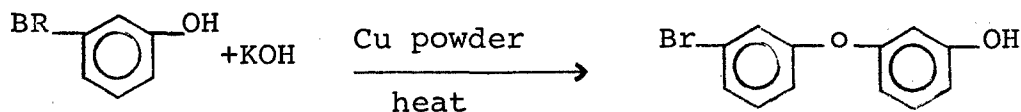
A solution of 36.0 g (1.27 oz) [.10 mole] of Bis(m-hydroxydimethylphenyl) carbonate in 160 ml (9.77 cu in) of toluene (dried with 4A molecarbon sieves) and 110 ml (6.72 cu in) of freshly distilled pyridine was charged to a 4-necked, 500 ml (30.5 cu in) flask equipped with a mechanical stirrer, a thermometer, a condenser, and an addition funnel. The addition funnel contained 35 g (1.23 oz) [.37 mole] of dimethylchlorosilane. The chlorosilane was added slowly to the carbonate solution which had been cooled to -7°C (19.4°F) by an ice, rock-salt bath. After the addition, the reaction was stirred overnight. The pyridine hydrochloride salt was filtered off and washed with 500 ml (30.5 cu in) of toluene. The solution was then washed with 4 x 300 ml (18.3 cu in) of saturated NaCl solution. The organic layer was dried with anhydrous MgSO_4 for two hours and then filtered and washed with 300 ml (18.3 cu in) of toluene. It was concentrated on a rotary evaporator and then distilled at room pressure to remove residual solvent. It was then vacuum distilled at 164°C (327.2°F)/0.10 mm (.0039 in) Hg to give 35.4 g (1.25 oz) [75% yield] of product.

Synthesis of Bis(m-hydroxymethylphenylsilphenyl) carbonate

The following sequence was used for the preparation of the title compound which is analogous to the Bis(m-hydroxydimethylsilylphenyl carbonate synthesis.



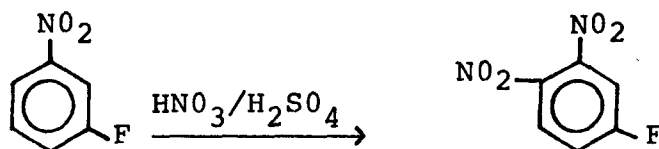
Synthesis of 3-bromo-3'-hydroxydiphenyl ether



A solution 372.8 g (13.15 oz) [2.15 mole] m-bromophenol was introduced to a 4-necked, 500 ml (30.5 cu in) flask equipped with a mechanical stirrer, a team condenser, a thermometer, and a N₂ inlet. The bromophenol was heated to 70°C (158°F) and 27.8 g (.98 oz) [0.47 mole] of powdered 86% KOH and 0.74 g (.026 oz) of Co powder was added. The temperature rose to 110°C (230°F) upon addition. After the initial exotherm the flask was heated to 210°C (410°F). The reaction was monitored by gas chromatography. After four hours of heating, there was 16.9% conversion rate. Next the m-bromophenol and the 2-ring ether was distilled off. This was then vacuum distilled at 149°C (300.2°F)/0.5 mm (.020 in) Hg to yield 48.1 g (1.70 oz) [16.2%] of product.¹⁵

Synthesis of 1,2-dinitro-4-fluorobenzene

This compound was prepared by the nitration of 1-nitro-3-fluorobenzene

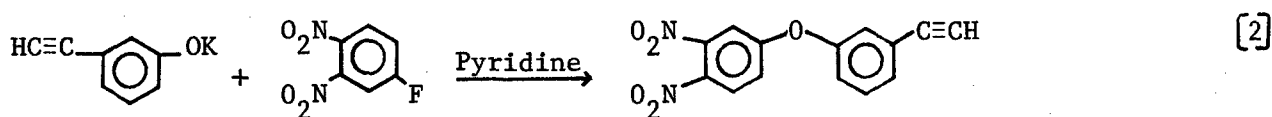
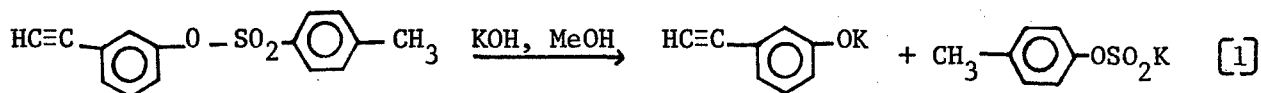


To 433 ml (26.4 oz) of stirred concentrated nitric acid was added, dropwise, 433 ml (26.4 oz) of concentrated sulfuric acid. The temperature of the acid mixture was kept at approximately 20°C (68°F) during mixing. The acid mixture was warmed to 50°C (122°F) and 80.37 g (2.83 oz) [0.57 mole] of 1-nitro-3-fluorobenzene was added dropwise to keep the temperature between 50 (122) and 55°C (131°F). The addition required approximately one hour. The mixture was heated at 50°C (122°F) for an additional hour and then poured into 2.28 Kg (80.4 oz) of cracked ice. The resulting precipitate was collected by filtration and washed with distilled water, with a sodium bicarbonate solution, and again with distilled water. The yellow product was recrystallized from ethanol. It

afforded 52.2 g (1.84 oz) [46.3% yield] of light yellow crystals melting at 51-53°C (123.8-127.4°F). The preceding reaction was prepared according to a known procedure.

Synthesis of 3-(3,4-dinitrophenoxy) phenyl acetylene

These reactions were prepared according to a known procedure



A mixture of 75.9 g (2.68 oz) [0.20 mole] of dry, solid 3-ethynylphenyl (p-toluenesulfonate) 31.2 g (1.10 oz) [0.57 mole] of potassium hydroxide and 500 ml (30.5 cu in) of methanol was charged to a one liter round bottomed flask containing a magnetic footbar stirrer, nitrogen inlet and outlet adapter. The system was thoroughly flamed and purged with nitrogen. The mixture was stirred under nitrogen at room temperature for one hour, at which time a condenser was attached and the flask heated at reflux on a steam bath for an additional hour, the condenser was replaced by a distillation head and methanol distilled from the flask to near dryness, maintaining the pot temperature below 100°C (212°F). Dry benzene (500 ml, 30.5 cu in) was then added and the distillation continued to near dryness. The remaining benzene was removed from the reaction mixture by freeze-drying under vacuum. A dry white residue consisting of a mixture of potassium 3-ethynylphenolate and potassium p-toluene sulfonate [1] was obtained. The reaction flask was again equipped with a nitrogen inlet and outlet adapter and cooled to 0°C (32°F) in an ice bath with rock salt; 500 ml (30.5 cu in) dry pyridine was added; the solution

stirred under nitrogen at 0°C (32°F) for 15 min. and then 5.2 g (.183 oz) [0.29 mole] of solid dry 3,4-dinitrofluorobenzene added at once. The resulting mixture was stirred at 0°C (32°F) for 30 minutes, and the flask was allowed to warm slowly to room temperature over a period of one hour. Finally the flask was heated at 60°C (140°F) for 15 minutes to ensure completion of the reaction. Solvent was then removed. The dark residue was extracted into methylene chloride and filtered. Extracts were washed with two successive portions each of water, 0.1 N sulfuric acid and again with water. The methylene chloride extracts were separated and then filtered through a 610 m x 50.8 mm (2 ft x 2 in) dry column of silica gel, elutriating with methylene chloride. The elutant was evaporated to dryness in vacuum and cooled in an ice bath at 0°C (32°F), causing solidification to occur. The crude product was washed with a small amount of methanol at 0°C (32°F), then filtered, dried, yielding 45 g (1.59 oz) [56% yield] of 3-(3,4-dinitrophenoxy)-phenyl acetylene [2] as pale yellow crystals, melting point 78.5 to 79.5°C (173.3-175.1°F).

Synthesis of 3-ethynylphenol

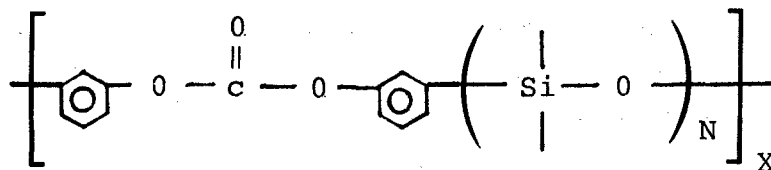
A solution of 20 g (.71 oz) [0.5 mole] sodium hydroxide in 50 ml (3.05 cu in) water was added to a solution of 3-ethynyl p-toluenesulfonate (21.3 g, .75 oz) in 150 ml (9.16 cu in) methanol. The mixture was distilled under nitrogen over a one hour period, during which time 100 ml (6.10 cu in) of distillate was removed. The reaction mixture was then cooled to room temperature, diluted with distilled water and extracted [3 x 50 ml (3.05 cu in)] with hexane. The water layer was poured into a mixture of sulfuric acid [51 ml (3.11 cu in)] and 500 g (17.6 oz) of ice, and extracted with [3 x 50 ml (3.05 cu in)] petroleum ether. The combined ether layers were washed with water [3 x 50 ml (3.05 cu in)] and ether was distilled under nitrogen to give 8 g (.282 oz) [94% yield] of 3-ethynylphenol as a yellow liquid.

Anal. Calcd. for, $C_{22}H_{14}O_3$: C, 81.34; H, 5.12; mol.wt., 118

Found: C, 81.14; H, 5.09; mol.wt. 118 (by mass spectrometry)

B. Thermal Analysis (E. Soloski)

Polysiloxanes were investigated by thermal analysis techniques, i.e., DSC, TMA and isothermal aging. It was shown that as the number of siloxane units in



was increased beyond four, the glass transition temperature was lowered below 18°C (64.4°F). However, the usable range of application is decreased because the upper use temperature [originally 410°C (770°F)] decreases faster than the T_g is lowered. By replacing the meta C_6H_3 with a para C_6H_4 , greater thermal stability was evidenced, but the resulting increased rigidity also resulted in a higher T_g .

Fluorinated aliphatic polysiloxane specimens considered as elastomers, or seals, showed little difference in their T_g 's [all between -91°C (-131.8°F) and -89°C (-128.2°F)] or in their thermal stability [300°C (572°F) to 300°C (626°F)].

SECTION IV

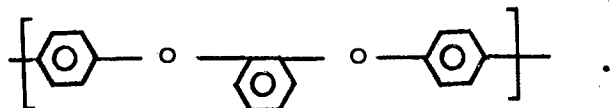
CONCLUSIONS

The contractual effort in preparing intermediates and monomers for the acetylene-resin program is on schedule. The evaluation of various resin systems to determine parameters to guide future synthesis and processing has been very productive. In addition to refining the technique of producing an "ideal" processing window, we have postulated and verified a technique for obtaining a "true" processing window. Both of these techniques are now being applied to the resin systems of current interest to the U. S. Air Force. This aids the processing of test specimens by engineers who are interested in statistical analysis of engineering data. It greatly reduces the quantity of starting material required to perform such an entire engineering analysis.

Specific information relating to the molecular level processing parameters has elucidated an identification of T_g , T_{poly} , etc. in these reactive resin systems. Special attention was given to the mobility of the acetylene groups in relation to observed thermal and mechanical transitions as a function of percent of cure. In the materials studied to date, which have both pendant and terminal acetylene groups, the pendant reactions appear to be faster just due to their accessibility to each other. This reaction brings on vitrification, thus causing the molecules to be less mobile and prevents the terminal acetylene groups from physically being able to unite and react.

In the ordered polymers task of this contractual effort, the introduction of flexible units into the PBO polymer backbone has improved the mechanical properties of cast films. Pure PBO homopolymer cast films were very brittle, as expected, because of the lack of molecular flexibility. Films cast from the flexible unit PBO polymer (articulated PBO) had tensile strengths of 75.8 MPa (11,000 PSI) and modulus 3447 MPa (500,000 PSI).

The best flexible units thus far evaluated were 3'3-biphenyl and



Model compound studies have started to produce enough parameters on a variety of chemical structures to allow preliminary correlation with x-ray diffraction data. This information is being incorporated in the morphology studies on rigid rod - flexible coil (RRFC) blends or molecular level composites. Aggregate size and orientation function techniques, as usually applied to semicrystalline materials, have been determined for these blends.

The recent Ordered Polymers Research review pointed out the necessity of matching the equatorial intensity profile with the computed profile using a model of geometrically packed rods. This yields the aggregate size in terms of the number of rods packed in a parallel fashion (the assumed model). In our blend studies, we have viewed the rigid rod - flexible coil as a biphasic system as evidenced by SEM photographs. Aggregates consisting of a mixture of rigid rod polymer and flexible coil polymer are present in the blend cast films. Because of the presence of these aggregates which are themselves a mixture of rod and coil (53%/47%), no corrections to orientation function parameters as mentioned by Ruland¹⁶ were used in this evaluation.

Precipitated films of ABPBI/PBT blends do show incursions due probably to the heat of reaction between methane sulfonic acid and water. As expected, the cast films would not show this phenomenon. Future morphology studies will involve more small angle x-ray results to help elucidate the blend morphologies. We have been promised deuterated PBT polymer which we plan to blend with different flexible coil polymers to study their compatability. Here we would use small angle neutron scattering (soon available at Oak Ridge National Laboratory). From viewing Zimm plots the compatability of the two polymers can be established.

REFERENCES

1. C. Y.-C. Lee, J. Henes, and T. E. Grossman, "Dynamic Mechanical Measurement of Polysulfone," AFML-TR-79-4062 (1979).
2. C. Y.-C. Lee and I. J. Goldfarb, Polymer Letters (submitted May 1979).
3. C. Y.-C. Lee, I. J. Goldfarb, T. E. Grossman, and J. D. Henes, "Torsion Impregnated Cloth Measurements of Epoxy Cure Behavior," AFML-TR-79- (in preparation, July 1979).
4. I. J. Goldfarb and C. Y.-C. Lee, American Chemical Society-ORPL Preprint (September 1978).
5. D. R. Wiff, Journal of Rheology, 22 (6), 589 (1978).
6. G. Price, "X-ray Diffraction Data of PBO and PBT Fibers," UDR-TR-79-21 (April 1979).
7. G. Price, "X-ray Diffraction Measurements on Molecular Composites. Part I: Study of a Variety of Polymer Blends," UDR-TR-79- (submitted June 1979).
8. C. R. Desper, "Computer Programs for Reduction of X-ray Diffraction Data for Oriented Polycrystalline Specimens," AMMRC-TR-72-34 (November 1972).
9. J. Ball and D. R. Wiff, "Operation Manual for Dynamic Imaging of X-ray Diffraction Patterns," UDRI-TR-76-60 (October 1976).
10. J. L. Speier, J. American Chemical Society, 74, 1003 (1952).
11. R. G. Neville, J. Org. Chem., 25, 1063 (1960).
12. C. A. Pearce, U. S. Patent No. 3,576,032 (April 20, 1971).
13. N. C. Lloyd, C. A. Pearce, and I. Pattison, U. S. Patent No. 3,595,974 (July 27, 1971).
14. Tsu-Tsu Tsai, AFML/MBP, personal communication.
15. G. P. Brown, U. S. Patent No. 3,565,783 (March 2, 1971).
16. W. Ruland and W. Wiegand, J. Polymer Science, Polymer Symposium 58, 43 (1977).